الجمهورية الجزائرية الديمقراطية الشعبية
République Algérienne Démocratique Et Populaire
وزارة التعليم العالي والبحث العلمي
Ministère de L'Enseignement Supérieur et de La Recherche Scientifique
جامعة فرحات عباس- سطيف1
Université Ferhat Abbas - Sétif 1

THÈSE

Présentée à l'Institut d'Optique et Mécanique de Précision pour l'obtention du Diplôme de

DOCTORAT 3ème Cycle LMD

Domaine : Sciences et Techniques
Filière : Optique et Mécanique de Précision
Spécialité: Mécanique Appliquée

Par
FERHAT Hamza

THÈME

Recherche et adaptation des approches d'optimisation pour la conception des systèmes mécaniques

Soutenue, le: 27/02/2021

Devant le jury composé de:

Président du Jury	Semchedine Fouzi	Prof.	UFA Sétif 1
Directeur de thèse	Djeddou Ferhat	Prof.	UFA Sétif 1
Examinateur	Harrag Abdelghani	Prof.	UFA Sétif 1
Examinateur	Zine Ghemari	Prof.	Université de M'Sila
Invité	Dahane Mohammed	HDR.	Université de Lorraine

الجمهورية الجزائرية الديمقراطية الشعبية
People's Democratic Republic of Algeria
وزارة التعليم العالي والبحث العلمي
Ministry of Higher Education and Scientific Research
جامعة فرحات عباس- سطيف1
Ferhat Abbas University – Setif 1

THESIS

Submitted to the Institute of Optics and Precision Mechanics
In Partial Fulfillment of the Requirements for the Award of the Degree of

3rd CYCLE LMD DOCTORATE

Domain: Science and Technology
Field of study: Optics and Precision Mechanics
Specialty: Applied Mechanics

By
FERHAT Hamza

SUBJECT

Research and adaptation of optimization approaches for design of mechanical systems

Submitted: 27/02/2021

Members of the assessment committee:

President	Semchedine Fouzi	Prof.	UFA Sétif 1
Supervisor	Djeddou Ferhat	Prof.	UFA Sétif 1
Examiner	Harrag Abdelghani	Prof.	UFA Sétif 1
Examiner	Zine Ghemari	Prof.	University of M'sila
Guest	Dahane Mohammed	HDR.	University of Lorraine

Acknowledgements

First of all, I express my humility and utmost gratitude to ALLAH (swt) for His guidance and blessings throughout my life. Verily nonsuccess would have been achieved without His grace and mercy. It is a long journey completing this PhD dissertation. From the beginning to end, I am indebted to many individuals for their care and support given to me during this work.

I would like to express profound gratitude to my daily supervisor, Prof. Djeddou Ferhat for his valuable advices and contribution of knowledge, which made this thesis possible. He was the one who inspired and encouraged me to work on this project. His supervision, guidance and encouragement helped me tremendously.

Together with Prof. Djeddou, I would like to give special thanks to Dr. Dahane Mohammed at the National Engineering School of Metz for his invitation to visit his research group. I am very grateful for his help and time, as well as patience of revising this PhD dissertation. I hope our collaboration will go on.

I would also like to express my deepest appreciation to my co-authors: Dr. Hammoudi Abderazek, and Miss Rezki Ines. Thanks for the many fruitful discussions during the completion of this thesis and for the companionship in traveling the bumpy road towards the Ph.D. degree.

Furthermore, I would like to extend the gratitude to the members of my advisory committee, Prof. Semchedine Fouzi at the Department of Optics, Prof. Harrag Abdelghani at the Department of Precision Mechanics, and Prof. Zine Ghemari at the Department of Electrical engineering, University of M'sila.

Last but definitely not least, I would like to thank my family and friends, especially to my mother, for their ceaseless support and encouragement over the years. Thanks to all for the understanding.

Ferhat Hamza **23 June 2020**

Contents

Chapter 2. Synthesis of Cam Mechanisms: A Survey

Chapter 3. Modified Adaptive Differential Evolution Algorithm

List of Figures

List of Tables

List of Symbols

Roman Symbols

A_i	Control points of spline function
b	Length of follower bearing
$B_{i,N}$	B-spline basis function
C	Follower overhang
C_i	Polynomial coefficients
Cr	Crossover rate
d	Vector of deterministic design variables
d_f	Follower diameter
e	Follower offset
E_1	Cam modulus of elasticity
E_2	Follower modulus of elasticity
$f\ (.)$	Objective function
F	Cam force applied on follower
F_e	External load
F_f	Frictional resistance
F_i	Inertia force
F_n	Normal force
F_s	Spring force
F_z	Probability density function
$F_{1,2}$	Mutation factors
FEs	Number of function evaluations
g_i	Inequality constraints
$\mathbf{g}_i$	Approximate deterministic inequality constraints
G_i	Performance functions
h_f	Lift of follower
h_i	Equality constraints
k	Number of inequality constraints
k_s	Constant elasticity of spring
K	Center of cam curvature
L	Length of follower face
$\boldsymbol{L}$	Lower limit of design variables
L_f	Follower length
m	Number of equality constraints

m_n	Normal module
M_f	Follower mass
n	Number of objective functions
nc	Number of control points
N	Order of polynomial function
Np	Population size
Ny	Dimension of the design variables vector
Nz	Dimension of the random vector
O	Cam rotation center
p	Vector of random parameters
P_f	Failure probability
P_n	Penalty function
$\mathrm{Prob}(.)$	Probability function
q	Distance between cam center and follower bearing
Q	Tangency point of curvature radius
r_c	Control parameter of curvature radius
R_b	Base circle radius of the cam
R_e	Elastic limit of follower material
R_i	Structural reliability
R_i^t	Target reliability level
R_r	Roller radius
s	Follower displacement
s'	Follower velocity
s''	Follower acceleration
t	Number of current iteration
t_c	Cam thickness
T_{cam}	Cam input torque
T_{max}	Maximum number of iterations
u_z	Standard normalized vector
$\boldsymbol{U}$	Upper limit of design variables
v	Tolerance allowed for equality constraint violations
v_i^t	Mutated vector
υ_1	Cam Poisson's ratio
υ_2	Follower Poisson's ratio
w_i^t	Trial vector
w_q	Weighting factors
x	Vector of random design variables
$x_{p1,2}$	Profile shift coefficients

y	Vector of design variables
z	Random vector
$\boldsymbol{z}$	Inverse most failure probable point
$z_{1,2}$	Teeth number for pinion and wheel

Greek symbols

α	Direction cosine
a'	Distance of working center
α_n	Normal pressure angle
α_n'	Pressure angle at pitch cylinder
$\beta_{i,}$	Reliability index
β_i^t	Target reliability index
δ_s	Initial deflection of spring
ε_α	Transverse contact ratio
Φ	Standard normal cumulative distribution function
φ	Cam pressure angle
$\gamma_{max1,2}$	Maximum specific sliding coefficients
η	Mechanical efficiency
μ	Friction coefficient of follower / bearing
μ_0	Friction coefficient of cam / follower
μ_P	Mean vector of random parameters
μ_x	Mean vector of random design variables
μ_z	Mean vector of random quantities
θ	Cam rotation angle
ρ	Cam curvature radius
ρ_f	Radius of root curvature
σ	Standard deviation vector
σ_b	Buckling critical limit
$\sigma_{c\,\max}$	Maximum compressive stress
$\sigma_{F1,2}$	Maximum bending stresses
σ_{Hmax}	Hertzian contact stress
σ_{Hp}	Permissible contact stress
ω_c	Cam angular velocity

Introduction

Context and Motivation

Over the past few decades, optimization in mechanical engineering has been still a significant issue for designers and even for researchers due to the often difficulties and the high computational burden. Majority of mechanical design includes an intensive optimization task in which a number of conflicting criteria are concurrently considered, such as cost, performance, strength, and reliability. Therefore, the key challenge in the design process is to define the best compromise between contradictory design requirements. With the increasing development of computing technology during the last fifty years, several theoretical and computational contributions of optimization have been well proposed to handle the complicated design problems in the mechanics area (Gasser and Schuëller 1998; Mastinu et al. 2007; Rao and Savsani 2012).

Conventionally, optimization methods for mechanical systems design are based on the assumption of deterministic models and parameters. This is the so-called Deterministic Design Optimization (DDO) which has been effectively applied to systematically reduce the structure cost and to increase the performance. According to the search procedure, DDO approaches can be divided into two groups, mathematical programming and metaheuristic algorithms (Deb 2012). Most of the first group algorithms are inadequate to resolve the complexities inherent in the mechanical applications, as they substantially rely on the gradient information and usually seek to improve the solution in the neighborhood of a starting point. On the contrary, metaheuristic algorithms are independent of these limiting conditions and can be well suited for practical design problems. They are typically inspired by successful concepts from nature and seek to improve the solution in the whole search space.

Due to the advantages of nature-inspired metaheuristics, such simplicity, flexibility, derivative-free mechanism, and high local optima avoidance, a large number of optimization algorithms have been developed and applied to current mechanical design. Some of the most popular are Genetic Algorithm (GA), Particle Swarm Optimization (PSO), Ant Colony Optimization (ACO), and Differential Evolution (DE). In particular, the DE algorithm introduced by Storn and Price in (1995) has received increased attention from researchers because of its effectiveness and explorative ability. This algorithm can generate high-quality solutions with a good consistency, but however its performance is rather costly in terms of computational resource. Therefore, the adjustments for the DE to balance between the

computational cost and the quality of solutions have recently been one of the more interesting topics in the engineering optimization field (Jia et al. 2013; Ho-Huu et al. 2016; Mohamed 2018; Phat et al. 2020).

In practice, design optimization of mechanical systems is often highly sensitive to uncertainties derived from different sources, like structure sizes, material characteristics, manufacturing tolerances, and operating environments. Any change of these random features may significantly affect the performance of the structure to be optimized and lead to a final design with a high failure. Thus, the uncertainties are inevitable and its impact must be considered during the optimization procedure. In DDO approaches, the propagation of system uncertainties is usually handled by using the well-known safety factors. These factors, in many cases, are inaccurately adopted and cannot guarantee the desired reliability level with the most economical solution (Aoues and Chateauneuf 2010). In this sense, the Reliability-Based Design Optimization (RBDO) is emerged as an alternative and powerful tool to deal with the potential uncertainties. This methodology is capable of offering robust and cost-effective designs, and therefore has gained broad applicability in mechanics and various engineering fields (Yu 2011; Kusano et al. 2014; Ho-Huu et al. 2018; Meng et al. 2020).

Main Aim and Research Contributions

The main aim of this thesis is to contribute new optimization methods that can effectively address the complex problems of mechanical design. The present research passes through three consecutive stages. The first stage introduces an efficient deterministic optimization approach named Modified Adaptive Differential Evolution (MADE). The proposed approach is a new version of the DE algorithm with two improvements. The first improvement is carried out on the mutation and crossover phases, while the second one is executed on the selection process.

The next stage aims to apply the developed MADE for design optimization of complex mechanical systems. In this research, a particular attention has been given to cam-follower mechanism due to its flexibility and versatility in the modern industrial applications. The first problem deals with a multi-objective optimization of a cam mechanism with offset translating roller follower in which more geometric parameters and more design constraints are taken into account. The second problem concerns the size optimization of a cam mechanism with translating flat-face follower in which the influence of the follower motion law is investigated. Additionally, three other recent metaheuristics including Grey Wolf Optimizer

(GWO), Whale Optimization Algorithm (WOA), and Sine-Cosine Algorithm (SCA) are employed to optimize the cam design problems.

The last stage of the thesis attempts to adapt the developed MADE toward reliability based design optimization. In this way, a novel optimization approach is presented to handle the mechanical design problems under highly uncertain manufacturing and operating conditions. The method is based on the integration of the Reliable Design Space (RDS) technique with an optimization algorithm hybridizing the MADE and the Nelder-Mead local search (NM). Consequently, the research presented in this dissertation involves three major contributions summarized as follows:

- ***Contribution 1:***

  An effective optimization method (MADE) is developed for addressing the deterministic mechanical problems with continuous design variables.

- ***Contribution 2:***
  1. *The developed MADE is applied to optimize the cam mechanism design where two types of follower system are studied.*
  2. *The optimization problem of the cam mechanism with offset roller follower translation is developed by considering additional geometric parameters and operating constraints.*
  3. *The optimization problem of the cam mechanism with flat-face follower translation inspects the impact of follower motion by using several types of motion laws.*
  4. *The application of three recently published optimizers (GWO, WOA, and SCA) is extended to the field of cam design optimization.*

- ***Contribution 3:***
  1. *A new reliability-based design optimization method (RDS-MADE-NM) is proposed to deal with the mechanical problems under the impact of uncertainties.*
  2. *The introduced method is able to handle the mixed design variables with continuous, discrete and integer types.*
  3. *To the best of our knowledge, the RBDO formulation for two systems is given in this study for first time and hence, new optimal solutions are presented.*

Thesis Outline

Following the three contributions defined above, the thesis is structured into five chapters as illustrated in Fig. 1.

Chapter 1 gives an overview of the design optimization including the main concerns for DDO and RBDO. The basic formulations corresponding to the two processes are presented and the related methods are reviewed.

Chapter 2 provides a literature survey on the synthesis of cam-follower mechanisms, in which the optimization of cam design and the motion curves of follower are the two interested topics. The principle classifications of these systems are also included in the chapter and the main issues of cam theory are revised.

Chapter 3 presents the variant of the DE algorithm developed in this thesis. The effectiveness of the new deterministic optimization approach is evaluated through solving four real-world engineering benchmarks, and the obtained results are compared with those available in the literature.

Chapter 4 addresses the design optimization of disc cam mechanism with translating roller and flat-face followers. For each type of follower shape, the optimization problem is formulated and an application example is presented to understand and discuss the assumptions adopted in the design process.

Chapter 5 introduces the new probabilistic optimization approach, namely RDS-MADE-NM. To confirm the search performance of this integrated approach, six mechanical design problems and a real challenging application of cylindrical spur gear are studied in the chapter.

Finally, the research findings of the thesis are summarized and recommendations for future research study are proposed.

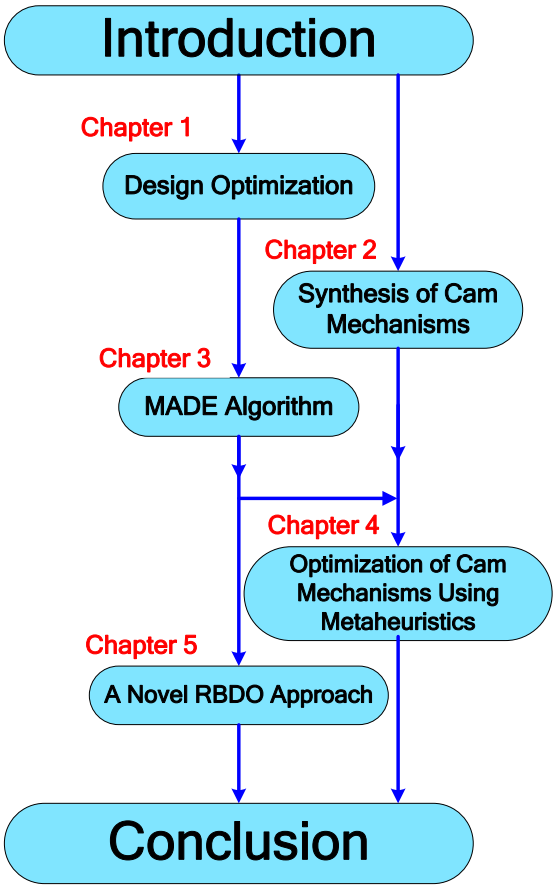

Fig. 1 Overview of the thesis.

Chapter 1

Design Optimization: An Overview

1.1 Introduction

Design optimization of engineering systems involves complex problems with several conflict considerations. The aim of engineers is the search for perfect solutions that achieve the desired objectives while satisfying the prevailing requirements. These solutions can be associated with the minimization of cost functions such as weight and material volume, or maximization of profit functions such as strength and efficiency. Nowadays, optimization takes much importance in almost every aspect of engineering design and its applications can be seen in a number of fields including, for instance, mechanics (Yildiz et al. 2019), automotive (Sun et al. 2018), civil engineering (Bekdaş et al. 2019), architecture (Ding et al. 2018), electronics (Tu et al. 2018), electricity distribution (Tan et al. 2020), and aerospace (Wu 2020; Champasak et al. 2020).

The process of solving an optimization problem is complicated by the inherently random nature of the input data. Traditional deterministic approaches for design optimization assume partial safety factors to accounts for the aleatory uncertainties. But due to the unavailability of approved rules in determining suitable values for these factors, deterministic optimization is usually imprecise and does not necessarily ensure the best balance between the economic cost and required safety (Carter 1997; Libertiny 1997). Over the last two decades, many probabilistic approaches handling uncertainties have been developed and employed to deal with engineering design (Phadke 1995; Melchers 1999; Tsompanakis et al. 2008). The well-known effective methodology is the reliability-based design optimization RBDO which quantifies closely the system uncertainties using probability theories and statistics. According to this, the design results of RBDO are more reliable and less conservative than those obtained using factors of safety concept.

In this context, the present chapter aims at giving an overview of optimization-based design considering both DDO and RBDO processes. The chapter initially deals with DDO which provides the basic knowledge of design optimization. Reliability-based design optimization is then followed in which the various methodologies are reported and the main formulations are discussed. A demonstrative example is studied in the end of this chapter to show the difference between the two processes.

1.2 Deterministic Design Optimization (DDO)

Deterministic optimization per definition refers to the process of finding the best values for design parameters of a given system without modeling the uncertainty. Conventionally, an optimization problem can be described by a vector of design variables, an objective function and a set of constraints. The vector of design variables is the set of decision parameters that have to be determined to acquire the desired structural performance. The objective function or the fitness expresses the objectives that need to be optimized and the constraints are the conditions that must be satisfied to produce the feasible design. Additionally, there are side constraints imposed on the design variables as lower and upper bounds to define the search space. In the deterministic formulation of the design optimization problems, the design variables are assumed to be deterministic and the objective functions as well as the constraints are determined based on their nominal values (Arora 1990).

1.2.1 Optimization Problem Formulation

Typically, a design optimization problem can be defined as the search for the combination of design variable values that either minimize or maximize the objective function value while respecting certain given constraints. The standard form for a deterministic optimization problem can be mathematically given as (Deb 2012):

$$\begin{aligned} &find\{d\} \\ &\min/\max: f(d) \\ &\text{s.t.:} \begin{cases} g_i(d) \geq 0, & i = 1,....,k \\ h_j(d) = 0, & j = 1,...,m \end{cases} \\ &d^L \leq d \leq d^U \end{aligned} \tag{1.1}$$

where d represents the vectors of design variables, $f(.)$ represents the objective function, and $g_i(i = 1,2,....k)$ and $h_j(j = 1,2,....m)$ denote, respectively, the inequality and equality constraints. The search space of design variables vector is bounded by the lower $\boldsymbol{L}$ and upper $\boldsymbol{U}$ limits, referred to as the side constraints. In most practical optimization problems, the fitness and the constraints are often expressed as implicit functions of the design variables and the evaluation of these functions generally involves numerical simulation techniques such as the finite element method (Rao 2019).

1.2.2 Optimization Problem Classifications

From the standard formulation, the problem stated in Eq. 1.1 is called a single-objective, constrained, non-linear optimization problem. In fact, there are many types of design optimization problems which can be classified in several ways:

According to the number of objectives, optimization problems are classified into single-objective and multi-objective problems (Zhou et al. 2011). A single-objective problem has only one objective to be optimized, while a multi-objective problem involves two or more objectives to be optimized concurrently.

Based on the existence of constraints, optimization problems can be classified as constrained and unconstrained problems (Papalambros 1995). A constrained problem is stated with one or more constraints, whereas unconstrained problem is stated without constraints.

Depending on the nature of the equations involved for the objective function and the constraints, optimization problems are classified as linear and nonlinear programming problems (Arora 1990). If both the objective function and the constraints are all linear functions of the design variables, the problem is said to be a linear programming. If, however, either the objective function or the constraints are nonlinear, the problem is said to be a nonlinear programming.

According to the permissible values of design variables, optimization problems may also be classified into continuous and discrete problems (Rao 2019). Design variables of a continuous problem can take their values from within permitted intervals. In contrast, design variables of a discrete problem are restricted to take only discrete (or integer) values.

Another important criterion of classifying optimization problems is based on the type of the design variables to be considered. Accordingly, optimization problems can be distinguished into three categories:

- Sizing optimization problems: design variables of this category are associated with geometrical dimensions such as thickness of cam, module of gear, and length of beam (Haftka and Gurdal 2012; Deb 2012).
- Shape optimization problems: problems of this type include the geometry variables describing the shape of the designed parts (e.g. height of a shell) (Belegundu and Rajan 1988; Masmoudi et al. 1995).

- Topology optimization problems: problems of the last category involve design variables concerning the material distribution and the structural configuration (e.g. truss and frame structure) (Kirsch 1989; Buhl et al. 2000).

1.2.3 Optimization Methodologies

Development and application of optimization methods for engineering design is an intensive topic that has attracted increasing attention in operational research, especially with the great advance of computing technology. In the last fifty or so years, a large variety of optimization algorithms have been developed and adopted to solve various types of problems in different domains. Basically, optimization algorithms can be divided, according the optimum search mode, into two main classes: Local Optimization Algorithms, and Global Optimization Algorithms (Cavazzuti 2012; Boussaïd et al. 2013). A generalized flowchart for describing the classification of optimization methods in the literature is outlined in Fig. 1.1.

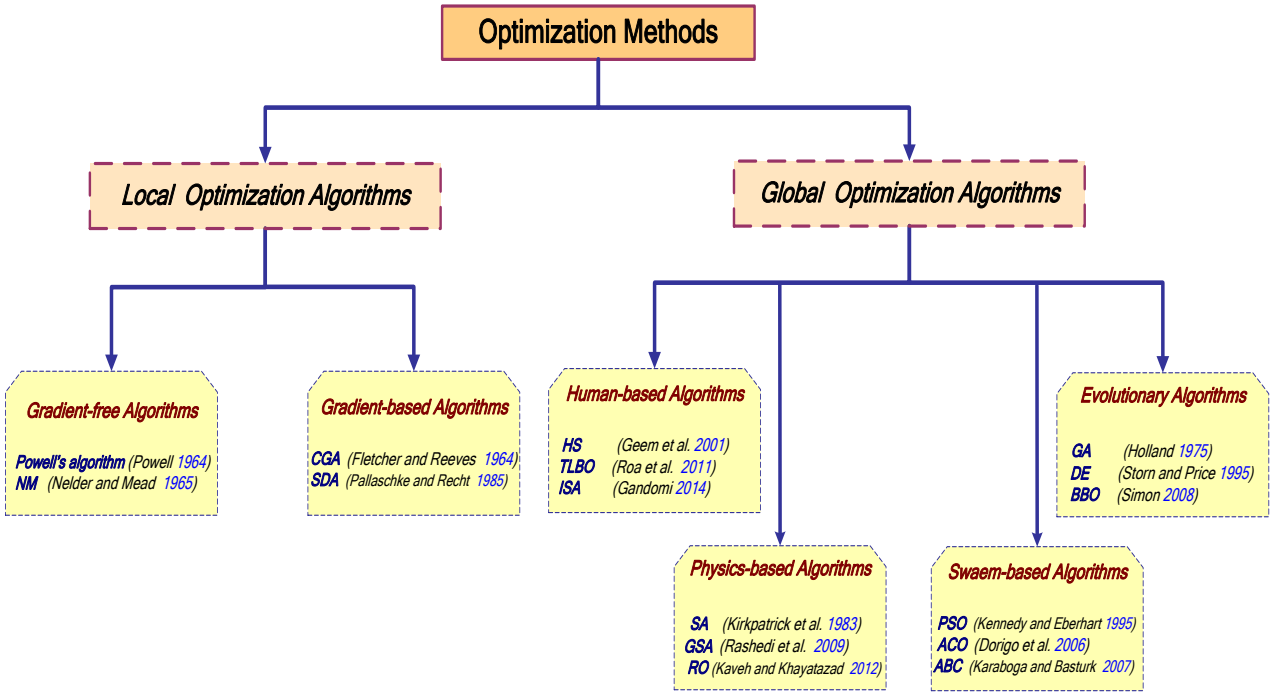

Fig. 1.1 Classification of optimization methods.

1.2.3.1 Local optimization algorithms

As indicated by the name, local optimization algorithms are iterative processes that always search for the optimum in the neighborhood of a starting position. These methods typically start with the selection of an initial point and depend on specific rules for moving from one solution to the other. The objective function is evaluated at each solution and its values are

sequentially improved until the desired convergence is achieved (Ravindran et al. 2006; Wehrens and Buydens 2006).

Local optimization algorithms can be broadly classified into two types: gradient-based algorithms (Arora 1990; Papalambros 1995) and gradient-free or direct algorithms (Parkinson et al. 2013; Rao 2019). Gradient-based algorithms use the gradient information of the objective function and constraints to explore the search space and reach the optimum. They are mainly divided as either first-order or second order methods, depending on whether the first partial derivatives or the second partial derivatives of the functions are required. Popular examples of first-order methods include the Conjugate Gradient Algorithm (CGA) (Fletcher and Reeves 1964) and the Steepest-Descent Algorithm (SDA) (Pallaschke and Recht 1985). For the second-order methods, the well-known quasi-Newton algorithm (Rosen1966) is a good example.

Direct search algorithms, on the other hand, do not require the determination of any derivative during the search process. They are based directly on evaluating the objective function at a sequence of points and comparing their values to find the optimum. Therefore, this type of search methods is generally applicable to problems whose functions are discontinuous and its differentiation is relatively difficult (Onwubiko 2000). The most well-known examples of direct search methods are Powell's algorithm (Powell 1964) and the simplex algorithm of Nelder and Mead (Nelder and Mead 1965). Both algorithms have a high ability to handle nonlinear, unconstrained optimization problems. Powell's algorithm is based on the concept of conjugate directions, while the Nelder–Mead (NM) algorithm depends on a set of simple rules that reflects the worst vertex through the centroid of the simplex.

In general, local optimization algorithms are extensively used for solving optimization problems in engineering. These techniques are popular because they are efficient to attain the optimum, using a reasonable number of function evaluations, and require little problem-specific parameters' setting. However, these algorithms have some deficiencies which include that they often tend to obtain local optimal solutions, they are not suitable for solving discrete and multi-objective optimization problems, as they have difficulty for solving problems involving large number of constraints (Wehrens and Buydens 2006; Venter 2010).

1.2.3.2 Global optimization algorithms

In order to surmount the limitations of the methods presented in the previous section, a new class of global optimization algorithms has been introduced as adequate alternative. These

techniques, often referred to as metaheuristic algorithms, have a great capability to search in the whole design space and can provide solutions near to the global optimum. They are typically based on mechanisms inspired from nature and have the advantage of being successfully applied for complex and real-world optimization problems (Yıldız and Yıldız 2019; Abderazek et al. 2020).

Research worldwide in the metaheuristic field has produced a large number of optimization algorithms which can be classified according to several criteria in the literature (Birattari et al. 2001; Talbi 2009). By far the most common classification of metaheuristics is to take into account their original source of inspiration. In this way, they can be grouped as evolutionary algorithms, swarm-based algorithms, physics-based algorithms, and human-based algorithms. The first group contains the algorithms inspired by natural evolutionary phenomena. The two most popular techniques established here are Genetic Algorithm (GA) (Holland, 1975) and Differential Evolution (DE) (Storn and Price 1995), which simulate biological evolution processes. Other techniques that fall into this group include Evolutionary Programming (EP) (Fogel et al. 1966), Genetic Programming (GP) (Koza 1994), Evolution Strategy (ES) (Beyer and Schwefel 2002), and Biogeography-Based Optimization (BBO) (Simon 2008).

In the second group, swarm-based algorithms mimic the best features of collective behavior of animals and insects in nature. The most common techniques include Particle Swarm Optimization (PSO) (Kennedy and Eberhart 1995), which is inspired by bird flocks behavior, Ant Colony Optimization (ACO) (Dorigo et al. 2006), which is inspired by the behavior of ants in an ant colony, and Artificial Bee Colony (ABC) (Karaboga and Basturk 2007), which is inspired by the honey bee behavior. In the recent decade, many swarm intelligence techniques have been developed such as Bat-inspired Algorithm (BA) (Yang 2010), Fruit fly Optimization Algorithm (FOA) (Pan 2012), Dolphin Echolocation (Kaveh and Farhoudi 2013), Grey Wolf Optimizer (GWO) (Mirjalili et al. 2014), Whale Optimization Algorithm (WOA) (Mirjalili and Lewis 2016), and Grasshopper Optimization Algorithm (GOA) (Saremi et al. 2017).

The third group of metaheuristics includes physics-based algorithms that imitate the physical rules in the universe. Some of the well-known examples for this category are Simulated Annealing (SA) (Kirkpatrick et al. 1983), which simulates the annealing technique used by the metallurgists, Gravitational Search Algorithm (GSA) (Rashedi et al. 2009), which is based on the gravitational force acting between the bodies, and Ray Optimization (RO)

(Kaveh and Khayatazad 2012), which is based the Snell's light refraction law.

In the last group, metaheuristic algorithms are based on the simulations of some human-related concepts. Two of the most popular human-inspired techniques are Harmony Search (HS) (Geem et al. 2001), which works on the principle of music improvisation in music players, and Teaching-Learning-Based Optimization (TLBO) (Roa et al. 2011), which works on the principle of influence of a teacher on its learners. Other popular techniques are Mine Blast Algorithm (MBA) (Sadollah et al. 2013), Social-Based Algorithm (SBA) (Ramezani and Lotfi 2013), Interior Search Algorithm (ISA) (Gandomi 2014), and recently Political Optimizer (PO) (Askari et al. 2020).

1.2.4 Multi-Objective Optimization

The discussion of deterministic optimization would not be sufficient without also mentioning the multi-objective formulation. In the wide variety of problems in engineering, the decision maker aims to optimize a number of objectives simultaneously. The different objectives are usually conflicting where the variables that optimize one objective may be far from optimal for the others. In cam design problems, for instance, minimizing the size of the cam and maximizing its strength are two objectives not compatible. Therefore, it is most necessary to compromise between the two performance criteria by selecting the appropriate values of the cam dimensions.

Formally, a multi-objective optimization problem involves multiple objectives which need to be optimized concurrently. As in single-objective optimization problem, it can contain a number of constraints that must be satisfied at any feasible solution. Since the considered objectives may be either minimized or maximized, the multi-objective optimization problem in the general form can be stated as (Deb 2001):

$$\begin{aligned} &find\{d\} \\ &\min/\max: f_q(d) \quad q=1,....,n \\ &s.t.: \begin{cases} g_i(d) \geq 0 & i=1,....,k \\ h_j(d)=0 & j=1,...,m \end{cases} \\ &d^{\boldsymbol{L}} \leq d \leq d^{\boldsymbol{U}} \end{aligned} \tag{1.2}$$

where n represents here the number of the objective functions. The problem shown above usually does not have a unique optimal solution, but rather a multitude of optimal solutions that provide a potential compromise among the objectives. These solutions are known as

Pareto-optimal solutions or non-dominated solutions (Pareto 1964, 1971).

Several techniques have been made to solve the multi-objective optimization. One of the most intuitively used is the weighted sum method, which was originally proposed by Gass and Saaty (1955). The main idea of this technique is to convert the multiple objective functions into one objective function by associating each objective with a weighting factor. In this manner, the multi-objective problem becomes a single-objective one as follows:

$$\begin{aligned} &find\{d\} \\ &\min/\max: \sum_{q=1}^{n} w_q \times f_q(d) \\ &s.t.: \begin{cases} g_i(d) \geq 0, & i = 1,...,k \\ h_j(d) = 0, & j = 1,...,m \end{cases} \\ &d^{\boldsymbol{L}} \leq d \leq d^{\boldsymbol{U}} \end{aligned} \tag{1.3}$$

The values of the weighting factors w_q are selected by the decision-maker considering the relative importance of each objective. In order to find several Pareto optimal solutions, the optimization problem shown in Eq. 1.3 should be solved repeatedly through modifying the weights in the global objective function (Diwekar 2008).

Another popular alternative technique for solving multi-objective problems is the ε-constraint method, which was initially demonstrated by Haimes (1971). According to this technique, the single most significant objective function f_l is optimized whereas the others are used as constraints bound by some allowed levels ε_q. Thus, the new optimization problem takes the following form:

$$\begin{aligned} &find\{d\} \\ &\min/\max: f_l(d) \\ &s.t.: \begin{cases} f_q(d) \leq \varepsilon_q, & q = 1,...,n, \quad q \neq l \\ g_i(d) \geq 0, & i = 1,...,k \\ h_j(d) = 0, & j = 1,...,m \end{cases} \\ &d^{\boldsymbol{L}} \leq d \leq d^{\boldsymbol{U}} \end{aligned} \tag{1.4}$$

The set of non-dominated solutions can be derived by using multiple different values for ε_q. In this technique, the decision-maker needs to provide the range of the reference objective. In addition, it must be provided the increment for the constraints imposed by the levels ε_q. This increment determines the number of the non-dominated solutions generated (Jaimes et al.

2009).

Apart from the conventional approaches, which turn the original multi-objective optimization into a single-objective optimization by either forming a weighted combination of the different objectives or by treating some of the objectives as constraints, there exist approaches that can solve the multi-objective problems directly, such as evolutionary algorithms (Schaffer 1984). Evolutionary algorithms for multi-objective optimization provide a set of Pareto optimal solutions by one running rather than solve a sequence of single-objective problems. Among the well-known approaches, the Non-dominated Sorting Genetic Algorithm II (NSGA-II) developed by Deb et al. (2002) is widely used due to its high resolving capacity for complex multi-objective combinatorial problems.

1.3 Reliability Based Design Optimization (RBDO)

An optimization process that accounts for feasibility in the presence of uncertainty is commonly referred to as RBDO. RBDO provides an alternative to conventional deterministic optimization and seeks for the adequate balance between cost and safety. The two main components of RBDO structure are reliability analysis and optimization (Ulucenk 2009). Reliability analysis is the inner component that focuses on handling the constraints in probabilistic term to ensure that the required level of safety is satisfied. In this framework, the random quantities involved in the constraints are quantified and their statistical characteristics are defined using apposite probability distributions. On the other side, optimization is the outer component that focuses on searching for the desired performance under the observance of the probabilistic constraints.

1.3.1 RBDO Problem Formulation

A typical RBDO is modelled as a minimization optimization problem where the lowest cost is taken as an objective and the reliability requirements are treated as constraints. In RBDO, three types of quantities are used: deterministic design variables, random design variables and random parameters. The deterministic design variables are computed based on their nominal values with negligible uncertainties, while the random design variables and random parameters are computed based on their mean values with uncertainties property being considered. Mathematically, the basic RBDO formulation can be described as follows (Aoues and Chateauneuf 2010):

$$
\begin{aligned}
&find\ \{d, \mu_x\} \\
&\min: f\left(d, \mu_x, \mu_p\right) \\
&s.t.: \Pr ob\left(g_i\left(d, x, p\right) \geq 0\right) \geq R_i^t, \qquad i = 1, ..., k \\
&d^{\boldsymbol{L}} \leq d \leq d^{\boldsymbol{U}},\ \mu_x{}^{\boldsymbol{L}} \leq \mu_x \leq \mu_x{}^{\boldsymbol{U}}
\end{aligned}
\tag{1.5}
$$

where d and x are, respectively, the vectors of deterministic and random design variables, and p is the vector of random parameters. The symbol (μ) denotes the mean of its corresponding variable, and $\boldsymbol{L}$ and $\boldsymbol{U}$ as in the deterministic formulation refer to the lower and upper bounds, respectively. In addition, $\mathrm{Prob}(.)$ is the probability operator, and R_i^t is the target reliability of the i^{th} constraint satisfaction specified by the designer. Here, only inequality constraints g_i are considered. This is because if an equality constraint involves x or p, there may not exist a solution for any arbitrary desired reliability against failure (Deb et al. 2009).

For convenience of discussion and to avoid confusion in this thesis, we assume that $y = \{d, \mu_x\}$ is the vector of design variables, and $z = \{x, p\}$ is the random vector. Ny and Nz are the dimensions of the vectors y and z, respectively.

-The concern in evaluating the probabilistic constraint is to employ the following integral:

$$
\mathrm{Prob}\left(g_i\left(d, z\right) \geq 0\right) = \int_{g_i(d,z) \geq 0} F_z\left(z\right)\, dz \tag{1.6}
$$

where F_z represents the joint probability density function of the vector z. Theoretically, the exact computation of this integral is very difficult owing to the absence of analytical solvers. Simplest techniques based on stochastic simulations such as Monte Carlo Simulation (MCS) (Mooney 1997) and Subset Simulation (SS) (Au and Beck 2001) are usually used and considered as reference methods. However, the major drawback of these methods lies in the high number of function evaluations. To deal efficiently with the integral in Eq. 1.6, moment techniques such as the first and second-order reliability methods (FORM/SORM) (Hasofer and Lind 1974) (Breitung 1984) can be employed. The idea is to map the constraint function g_i from the original design space (Z space) to the standard normal space (U space), and then establish the linear (or quadratic) approximation of the function at the point of maximum likelihood, known as the most probable failure point (*MPFP*), for estimating the reliability (Madsen et al. 2006). The passage from the Z space to the U space can be achieved based the following transformation (Rosenblatt 1952):

$$\begin{aligned} &\Phi(u_{zj}) = CDF_j(z_j), && j = 1, 2, ..., Nz. \\ &u_{zj} = \Phi^{-1}(CDF_j(z_j)), && z_j = CDF_j^{-1}(\Phi(u_{zj})) \end{aligned} \tag{1.7}$$

where Φ and Φ^{-1} are respectively the standard normal cumulative distribution function and its inverse function. CDF_j and CDF_j^{-1} are the cumulative distribution function and its inverse function of z_j, respectively. u_z denotes the vector z in the standard normal space.

1.3.2 RBDO Methodologies

The main challenge in the resolution of RBDO problem (Eq 1.5) is associated with the evaluation of the probabilistic constraints, as they require high numerical efforts. Many researches have been developed in the past few decades, aiming to overcome this difficult task, which are still the key obstacle for practical engineering applications. According to the strategies used to deal with the probabilistic constraint during the optimization process, RBDO methodologies can be classified basically into three categories: namely double-loop approaches, decoupled approaches, and single-loop approaches, as shown in Fig. 1.2.

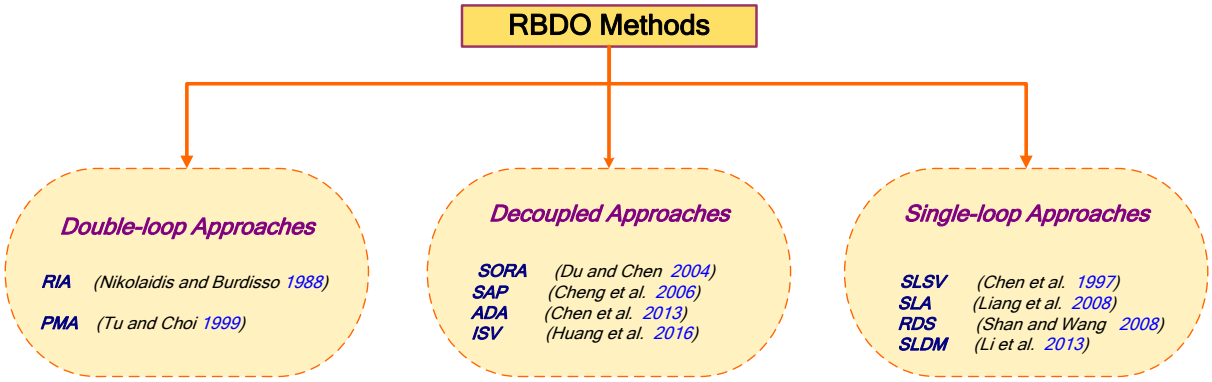

Fig. 1.2 Classification of RBDO methods.

1.3.2.1 Double-loop RBDO Approaches

The basic RBDO methodology employs a double-loop procedure in which the probabilistic constraints evaluation is included in the main optimization loop (Fig. 1.3). This formulation leads to a nested optimization problem where the inner loop concerns the reliability analysis and the outer loop concerns the cost optimization (Wu 1994; Yu et al. 1998; Youn et al. 2003). The two popular techniques encountered in this category are Reliability Index Approach (RIA) and Performance Measure Approach (PMA). RIA technique has been proposed by Nikolaidis and Burdisso (1988) and its principle is to search for the *MPFP* on the limit surface using the reliability index concept. This technique is simple to formulate, but it

requires considerable computational efforts and converges slowly owing to difficulties to compute the constraints reliability (Enevoldsen and Sørensen 1994). To overcome these drawbacks, Tu and Choi (1999) have developed the performance measure approach in which the probability evaluation is converted into a performance measure by solving an inverse reliability problem. The obtained solution of this inverse problem represents the minimum performance point on the target reliability surface, known as the minimum performance target point (*MPTP*).

1.3.2.1.1 Reliability index approach (RIA)

The classical RBDO formulation based on the reliability index approach is expressed as:

$$\begin{aligned} &find\ \{y\} \\ &\min: f(d,\mu_z) \\ &s.t.: \beta_i(d,z) \geq \beta_i^t, \qquad i=1,...,k \\ &y^L \leq y \leq y^U \end{aligned} \tag{1.8}$$

where β_i and β_i^t denote respectively the structural and the target reliability indexes of the i^{th} probabilistic constraint. Through transforming the random vector z to the independent standard normalized vector u_z (using Eq 1.7), the reliability index β_i is calculated by solving the following minimization problem:

$$\begin{aligned} &find\ (u_z) \\ &\min: \beta_i = \sqrt{\sum_{j=1}^{Nz} u_{zj}^2} \\ &s.t:\ G_i(d,u_z) = 0 \end{aligned} \tag{1.9}$$

The optimal solution of this problem is the *MPFP* in the *U* space, and can be obtained using some well-established algorithms such as the HL-RF iterations (Hasofer and Lind 1974; Rackwitz and Fiessler 1978) or the improved HL-RF iterations (iHL-RF) (Madsen et al. 2006). According to FORM approximation (Haldar and Mahadevan 2000), the reliability R_i is given by: $R_i = \Phi(\beta_i)$.

1.3.2.1.2 Performance measure approach (PMA)

The basic idea of the performance measure approach is that optimizing a complex objective function under simple constraints is much easier than optimizing a simple objective function under complex constraints (Aoues and Chateauneuf 2010). Consequently, the RBDO formulation based on the PMA is given as follows:

$$
\begin{aligned}
&find\{y\}\\
&\min: f(d,\mu_z)\\
&s.t.: G_i(d,z)\geq 0, \qquad i=1,...,k\\
&y^{L}\leq y\leq y^{U}
\end{aligned}
\tag{1.10}
$$

where G_i is the i^{th} performance function evaluated by the inverse reliability analysis. Unlike the RIA-based RBDO, which searches for the minimum distance point from the mean values of the vector z to the failure surface subject to null limit state functions, the PMA tries to find the failure point corresponding to the lowest performance that satisfies the target reliability index:

$$
\begin{aligned}
&find(u_z)\\
&\min: G_i(d,u_z)\\
&s.t.: \sqrt{\sum_{j=1}^{Nz} u_{zj}^2}=\beta_i^t
\end{aligned}
\tag{1.11}
$$

The optimal solution of the previous problem is the *MPTP* in the *U* space, and can be obtained using many specific algorithms, such as the Advanced Mean Value (AMV), the Conjugate Mean Value (CMV) and the Hybrid Mean Value (HMV) (Youn et al. 2005). These approaches do not require a line search procedure because the search direction is simply determined by exploring the spherical equality constraint in Eq. 1.11. The accuracy and stability of PMA is demonstrated when compared with RIA in the study of Lee et al. (2002).

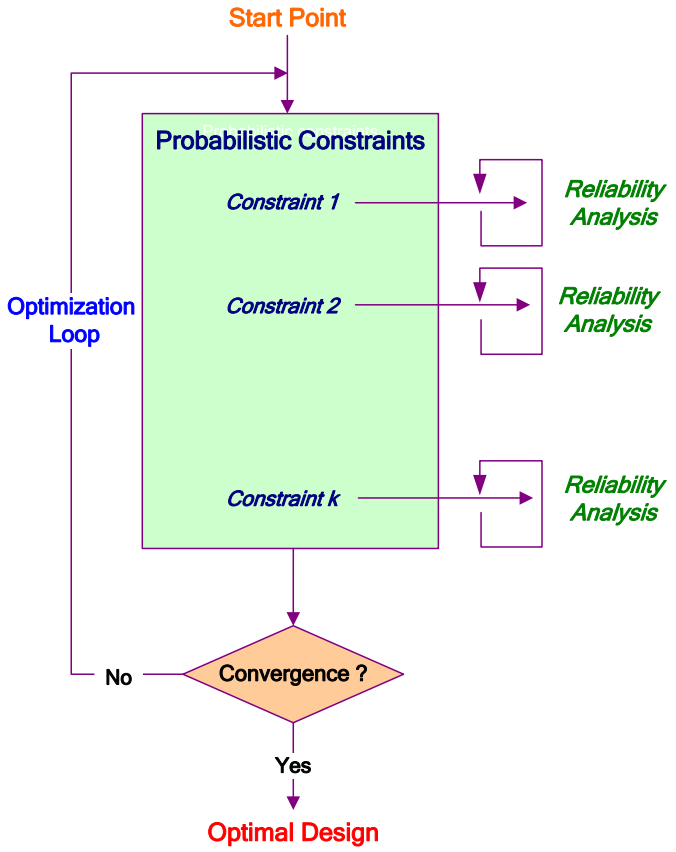

Fig. 1.3 Generalized flowchart of double-loop RBDO, modified from (Yu 2011).

1.3.2.2 Decoupled RBDO Approaches

The RBDO using RIA or PMA requires an expensive computation due to the repeated evaluation and analysis in both reliability and optimization loops. To overcome this difficulty, several researchers have focused on developing more computationally efficient RBDO methodologies, based on either decoupled or single loop procedures. Decoupled techniques have been introduced to separate reliability analysis from optimization process and thus, the evaluation of probabilistic constraints is not carried out within the main optimization loop (see Fig. 1.4). The most common approach in this category is the Sequential Optimization and Reliability Assessment (SORA), developed by Du and Chen (2004). The SORA approach consists in transforming the double loop in RBDO into a sequence of deterministic optimization and reliability analyses where the reliability information obtained from the previous cycle are used to shift the boundaries of the violated deterministic constraints to the feasible region. In this way, the design solution is improved from cycle to cycle until convergence.

There are many other approaches that use the decoupling strategy. For example, Royset et al. (2001) have decoupled the reliability analysis from optimization by using the concept of Semi-Infinite Programming (SIP) (Kirjner-Neto et al. 1998) where the failure probability constraints have been replaced by a parameterized first order approximation. The Sequential Approximate Programming (SAP) approach has been developed by Cheng et al. (2006) where the RBDO has been formulated as a sequence of deterministic sub-programming problems and the probabilistic constraints have been approximated by the first order Taylor series expansion. Authors in (Li et al. 2010) have proposed the Penalty-Based Approach (PBA) using the penalty concept in order to link the reliability requirement to the deterministic optimization. Chen et al. (2013) have introduced the Adaptive Decoupling Approach (ADA) based on the concept of SORA. Furthermore, Huang et al. (2016) have developed another efficient decoupling approach, known as Incremental Shifting Vector (ISV), based on the shifting vector technique.

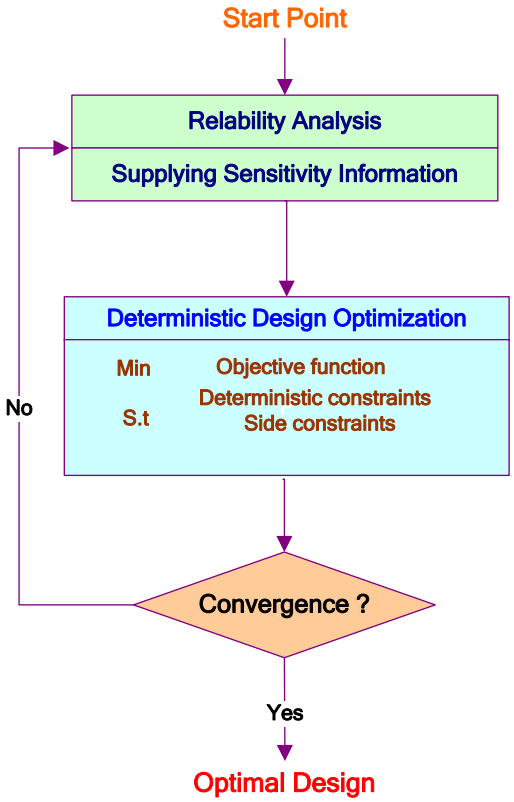

Fig. 1.4 Generalized flowchart of decoupled RBDO, modified from (Yu 2011).

1.3.2.3 Single-loop RBDO Approaches

In addition to double-loop and decoupled approaches, the single-loop techniques have been introduced to convert the nested optimization loops into one loop by eliminating the inner

reliability loops (Fig. 1.5). This type mainly contains iterative single-loop approaches and complete single-loop approaches. The first subgroup of approaches employs an iterative procedure based on the Karush-Kuhn-Tucker (KKT) conditions to remove the reliability analyses, such as the Single Loop Single Vector (SLSV) (Chen et al. 1997) and the Single Loop Approach (SLA) (Liang et al. 2007; Liang et al. 2008). Whereas the second subgroup employs a direct procedure through substituting the probabilistic constraints with approximate deterministic ones in one step. Two approaches have been developed in this context, the Reliable Design Space (RDS) method (Shan and Wang 2008) and the Single-Loop Deterministic Method (SLDM) (Li et al. 2013). Both approaches have the same strategy that uses the partial derivatives at the current design point as an approximation of the derivatives at its corresponding *MPFP*. However, RDS method is derived from RIA while SLDM reaches the formulation based on PMA.

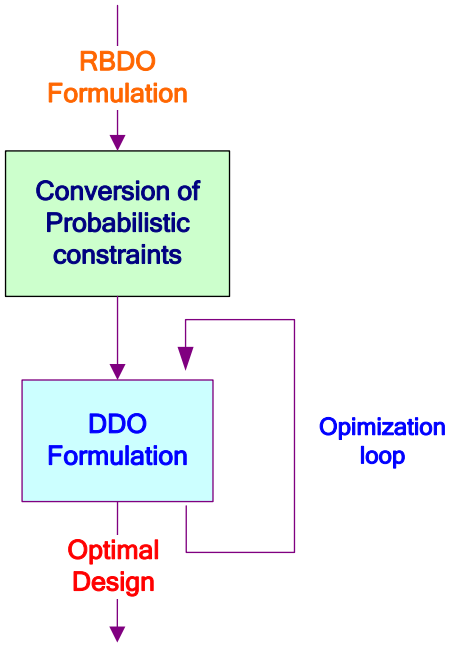

Fig. 1.5 Generalized flowchart of single-loop RBDO, modified from (Shan and Wang 2008).

1.3.3 RBDO with Metaheuristics

In the last few decades, the use of metaheuristic algorithms to solve RBDO problems has rapidly increased, mainly due to the development of sophisticated computing technologies and the extensive applications of the Finite Element Analysis (FEA). Following the double-loop approach, António (2001) has applied the genetic algorithm GA for RBDO of composite structures. The probabilistic constraints have been evaluated by SORM approximation where the reliability index has been computed using the Newton–Raphson iterative procedure and

the arc-length method. Tolson et al. (2004) have employed also the GA for reliability-based optimum design of water distribution systems where the constraints evaluation has been performed based on FORM approximation. In (Yang and Hsieh, 2011), the authors have proposed a modified PSO algorithm, including two new features: auto-tuning and boundary-approaching, to solve the discrete and non-smooth RBDO problem. In their work, the constraints reliability has been evaluated using the subset simulation. Chen et al. (2013) have developed an RBDO approach of composite structures by combining PSO algorithm with FEA. They have used an iterative procedure to estimate the reliability index of the probabilistic constraints. A new RBDO approach that combines PSO algorithm with Support Vector Machine (SVM) has been proposed by Yang and Hsieh. (2013). First, initial solutions have been produced randomly and their satisfaction of the probabilistic constraints has been checked using the subset simulation. The solutions and their feasibility labels have been used by the SVM classifier as the training data set to obtain the decision functions. These functions have been fed to the PSO algorithm to check the feasibility of the generated solutions. After a specific number of generations, the PSO solution has been transferred to the SVM as new training solutions to update the decision functions.

Using the single-loop approach, Papadrakakis and Lagaros (2002) have applied the Evolution Strategy ES for reliability-based optimization of large-scale structural systems. The constraints reliability has been estimated by MCS combined with the importance sampling technique for reducing the sample size. Liao and Ivan (2014) have proposed an efficient RBDO approach based on PSO algorithm. The multi-variable constraint has been transformed into a single variable constraint using exponential polynomial coefficients and the reliability has been then computed by the mean of the adaptive Gauss–Kronrod quadrature. Chakri et al. (2018) have used an improved version of the bat algorithm, namely directional bat algorithm (dBA), for RBDO of engineering systems. By adopting the reliable design space technique, the yielded stochastic problem from the RBDO formulation has been simply converted to a single-loop deterministic optimization problem. Moreover, Ho-Huu et al. (2018) have developed a global single-loop deterministic approach, by integrating the SLDM with Improved DE (IDE) algorithm, for solving RBDO problems of truss structures with continuous and discrete design variables.

Like for the single-objective RBDO problems, metaheuristics have been successfully applied to solve multi-objective RBDO (MO-RBDO) problems. Deb et al. (2009) have proposed a MO-RBDO approach based on NSGA-II where the evaluation of the probabilistic

constraints has been performed using the Fast-PMA (Du and Chen 2001). Mathakari et al. (2007) have employed the multi-objective GA combined with FEA for RBDO of electrical transmission towers. The importance sampling technique has been used to estimate the probabilistic constraints. Kawaji and Kogiso (2013) have applied the multi-objective PSO to solve MO-RBDO problems where the SLSV technique proposed by Chen et al. (1997) has been adopted to deal with the probabilistic constraints. Li and Hu (2014) have provided the PSO approach in combination with principle components analysis for solving many-objective RBDO of wind-excited tall buildings, and they further have extended the framework into the cases with multiple granular failure probabilities (Hu and Li 2014).

1.4 Comparative Study Between DDO and RBDO

The difference between DDO and RBDO is illustrated in this section by studying a well-known mathematical example (Yang and Gu 2004). The simple case study aims at showing the impact of uncertainties related to the structural parameters on the output of optimization. Regarding the RBDO formulation of this problem, there are two normally distributed random design variables (x_1, x_2) and three nonlinear constraints. There are no deterministic design variables or random parameters. The objective function is the sum of the mean of two random variables. The RBDO problem is described as follows:

$$
\begin{aligned}
&find\ \{\mu_{x1}, \mu_{x2}\} \\
&\min: f = \mu_{x1} + \mu_{x2} \\
&s.t.: \mathrm{Prob}\left(g_i(x) \geq 0\right) \geq R_i^t, \quad i = 1,.,3 \\
&g_1 = \frac{x_1^{\,2} x_2}{20} - 1 \\
&g_2 = \frac{(x_1 + x_2 - 5)^2}{30} + \frac{(x_1 - x_2 - 12)^2}{120} - 1 \\
&g_3 = \frac{80}{(x_1^{\,2} + 8x_2 + 5)} - 1 \\
&0 \leq \mu_{x1}, \mu_{x2} \leq 10, \\
&\sigma_1 = \sigma_2 = 0.3, \quad R_i^t = \Phi(3) = 99.87\%
\end{aligned}
\tag{1.12}
$$

where σ_1 and σ_2 are standard deviations of the two random variables. The same target reliability index β_i^t is used for all three constraints. To investigate the difference between the two optimization processes, $x_1$and x_2 are treated as deterministic variables in DDO.

The optimization routine ‘‘fmincon’’ of MATLAB® is used to solve the problem where both processes start with the same initial point $y = (5,5)$. The results obtained by DDO and RBDO are listed in Table 1.1 and shown graphically in Fig. 1.6. It is evident that no matter what optimization problem is considered, only the first two constraints are active. When uncertainty is involved, consideration of the deterministic model to take place of the random model brings sever failure, since the solution of DDO (shown by the blue point) is located at the crossing of the active limit states whereas the RBDO solution (depicted by the green point) falls in the safe region.

Table 1.1 Comparison results of DDO and RBDO for the mathematical example.

Optimization	$f(y)$	y_1	y_2	g_1	g_2	g_3
DDO	5.1765	3.1139	2.0626	00	00	1.5643
RBDO	6.7257	3.4391	3.2866	00	00	0.5000

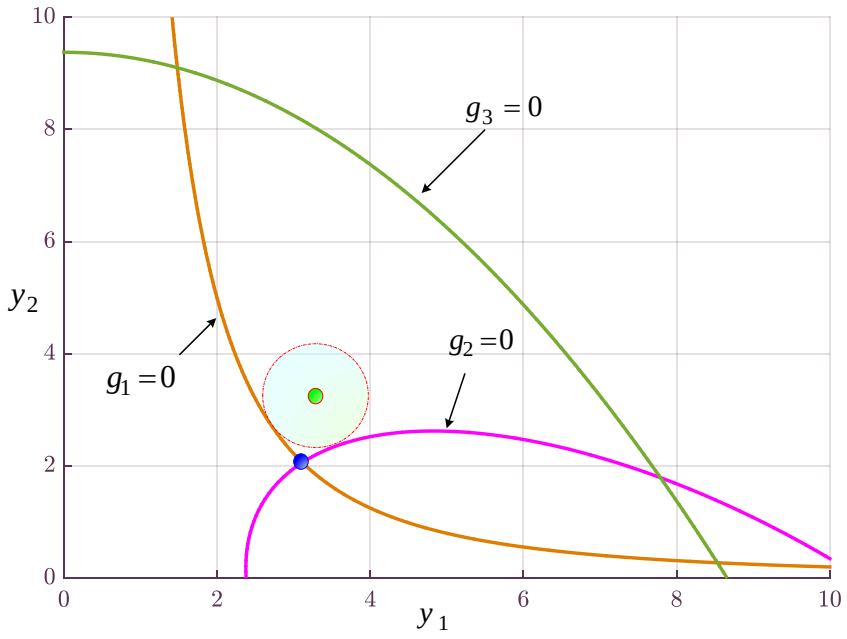

Fig. 1.6 Comparison results of DDO and RBDO processes.

1.5 Conclusion

Design optimization methodologies should account for the stochastic nature of design variables and parameters in engineering systems. In traditional deterministic approaches, the structural uncertainties are handled by using safety factors without direct connection with reliability specifications. These factors are calibrated for average design situations and cannot ensure consistent reliability levels for specific design conditions (Aoues and Chateauneuf

2010). Among the alternative modern tools, reliability-based design optimization is a suitable strategy for finding optimal designs with the careful control of uncertainties propagation. In this sense, the safety factors are optimally defined within the system, compared to deterministic design where they are set before undergoing the optimization process (Tsompanakis et al. 2008).

Through the short overview presented about design optimization in this chapter, the fundamentals and concepts associated with this thesis are introduced. First, the main concerns of DDO have been regarded including the basic formulation, the classifications of problems, and the various methodologies devoted for single and multi-objective optimization. Then, the theoretical basis of RBDO has been described in order to give a clear vision of the links between the classical deterministic approach and reliability-based one. This part has provided a literature survey of the existing methodologies of RBDO, their main formulations as well as their applications with metaheuristics.

Chapter 2

Synthesis of Cam Mechanisms: A Survey

2.1 Introduction

Cam-follower is one of most important and popular mechanisms used in modern machinery when the accuracy is required. The spectrum of engineering applications of this mechanism comprises a wide variety of devices and machines, such as textiles, packaging, printing presses, pumping devices, machine tools, food processing machines, knitting machines, automobile engines, transportation equipment, and control systems.

Conventionally, a cam mechanism consists of three basic members: two moving parts, namely the cam and the follower, and a fixed frame. The cam is the driver member which transmits a specified motion to the driven member (the follower) using predetermined kinematic characteristics. From the practical design point of view, the main drawback of this mechanism is the direct contact between the cam and the follower. This contact induces a load torque on the cam due to friction which causes a loss of energy dissipated as heat in the two parts of contact. Therefore, among the existing solutions in industry, several types of follower systems like roller follower and flat-face follower are employed for reducing the friction and improving the mechanism performance (Chen 1982; Uicker et al. 2003).

The aim of this chapter is to provide a brief introduction to the synthesis of cam mechanisms. The basic classifications and terminology of these systems are firstly included in Section 2.2, and a literature review in the area of cam design optimization is presented in Section 2.3. The kinematic features of follower motion are discussed in Section 2.4, and, in the last section of this chapter, the fundamental concepts of cam design are outlined.

2.2 Classification and Terminology of Cam Mechanisms

Cam mechanisms are among the simplest, versatile, and economical means of producing complex motion with a high level of precision. In the cam synthesis process, the primary concern of the designer is to determine the mechanism structure and select the suitable type of cam-follower combination (Wang and Lin 1989). The mechanism structure is related mainly to the physical form of the cam and the follower, as well as other dimensional considerations such as distance between the cam and the follower bearing, length of the follower bearing, eccentricity of the follower relative to the cam rotation center, and space required to operate the system. The choice of the cam-follower combination is associated with the input-output motion relation of the mechanism.

Generally speaking, the classification of cam systems as described schematically in Fig. 2.1 can be divided according to two basic criteria, depending on the structure of the elements and their type of motion. For the first criteria, the cam mechanisms can be distinguished by referring to the shape of the cam or the follower. For the second one, they are classified in three ways: the input type of motion, output type of motion, and program type of output motion.

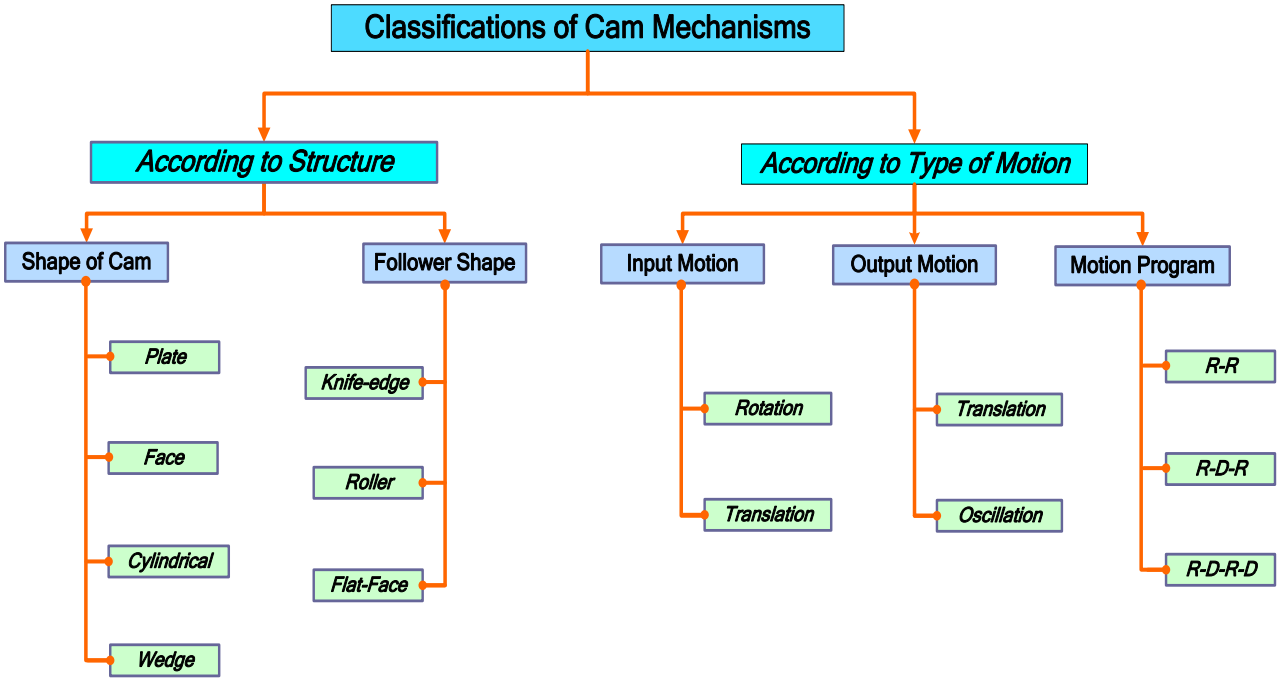

Fig. 2.1 Classifications of cam mechanisms.

2.2.1 Classification According to the Shape of the Cam

The first classification is based on the basic form of the cam disk (Uicker et al. 2003). The common types of cams are plate, face, cylindrical, and wedge, Fig. 2.2a, b, c, and d, respectively. The palate cam is the most extensive due to its compactness and availability in many applications. In this type, the cam axis of rotation is perpendicular to the plane of the follower motion. Unlike the cams of the first three types that have rotational motion, cam of the last type is designed to produce a translational motion. This is the simplest of all cams but its applications are practically limited.

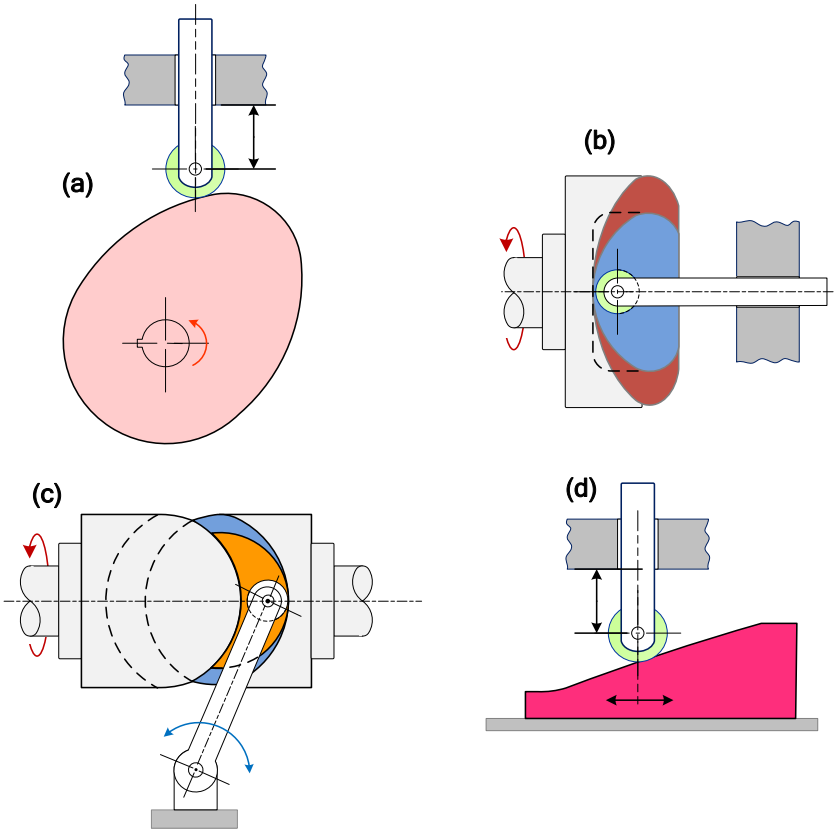

Fig. 2.2 Common types of cams: (a) plate cam, (b) face cam, (c) cylindrical cam, (d) wedge cam, modified from (Uicker et al. 2003).

2.2.2 Classification According to the Shape of the Follower

Cam mechanisms can also be classified through the nature of the follower surface (Angeles and Lopez-Cajún 2012). Fig 2.3 illustrates plat cams action with the well-knew follower shapes, namely, knife-edge, roller, and flat-face followers. The least used of these in machinery is the follower of the first type, shown in Fig 2.3a, because of its need for a sharp edge to contact with the cam surface. This causes a high coefficient of friction when compared with other follower types. By far the most widespread are the roller, and flat-face followers. For the roller follower (Fig 2.3b), the cam rotates in tangent with a cylindrical roller. This latter rolls on the cam surface and produces a pure-rolling relative motion to drive the follower. For the flat-face followers (Fig 2.3c), the cam rotates in tangent with a flat surface to provoke the follower motion.

Another classification of followers is linked to their position with reference to the cam rotation center. This gives radial type, as in Figs. 2.3a, or offset type, as in Fig. 2.3b.

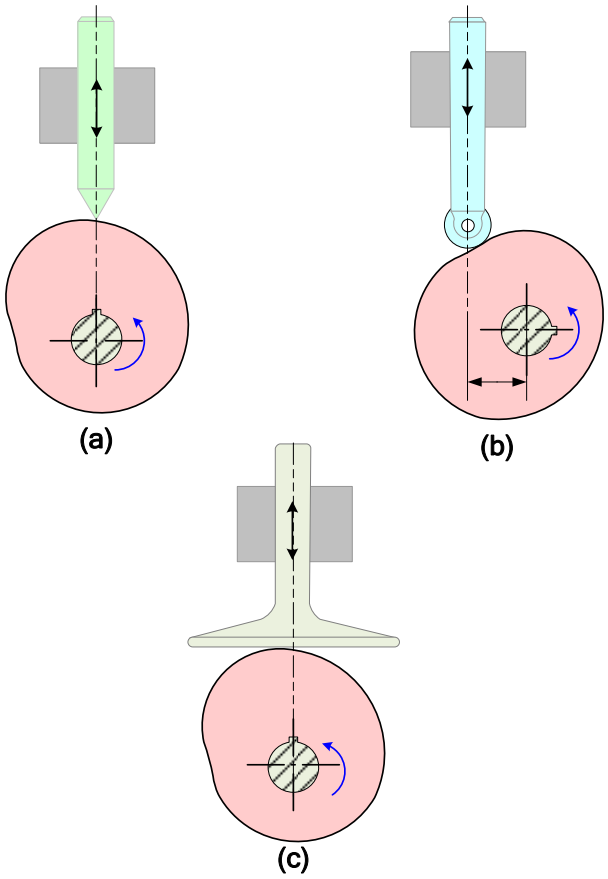

Fig. 2.3 Plat cams action with the common follower shapes: (a) knife-edge, (b) roller, (c) flat-face, modified from (Angeles and Lopez-Cajún 2012).

2.2.3 Classification According to the Input type of Motion

This classification, applicable when the cam motion is considered, comprises two types (Palacios and Angeles 2012):

- *Rotating cams*, as shown in Figs. 2.2a, 2.3. The cam undergoes a periodic rotation.
- *Translating cams*, when the cam undergoes a periodic translation, as shown in Fig. 2.2d.

2.2.4 Classification According to the Output type of Motion

Another method of classifying cam mechanisms is based on the type of follower motion (Rothbart and Klipp 2004), namely,

- *Translating followers*, as shown in Fig. 2.3. The follower pursues a linear motion with respect to the frame. The applicability of this type is very riche in production machinery and automotive field.
- *Oscillating followers*, as shown in Figs. 2.2c. In this case, the follower pursues an

angular motion relative to the frame. Applications of this type are rather infrequent in industries.

2.2.5 Classification According to the Program type of Output Motion

The last classification refers to the working phases of the follower. The periods of the follower motion, which deals with the cam profile determination, includes the rise, return, and dwell. According to the number of dwell periods for a complete cycle of follower motion, there are three scenarios of motion program (Fig. 2.4) (Shakoor 2006):

- *Rise-Return (RR)*, as shown in Fig 2.4a. The follower rises to the upper point and returns directly to its initial position with no dwell. This scenario has very limited applications.
- *Rise-Dwell-Return (RDR)*. The follower remains stationary between the rise and return motion periods, as shown in Fig 2.4b. This scenario is the most common.
- *Rise-Dwell-Return-Dwell (RDRD)*. The last scenario involves a high dwell after the rise of the follower and a lower dwell after the return period, Fig. 2.4c.

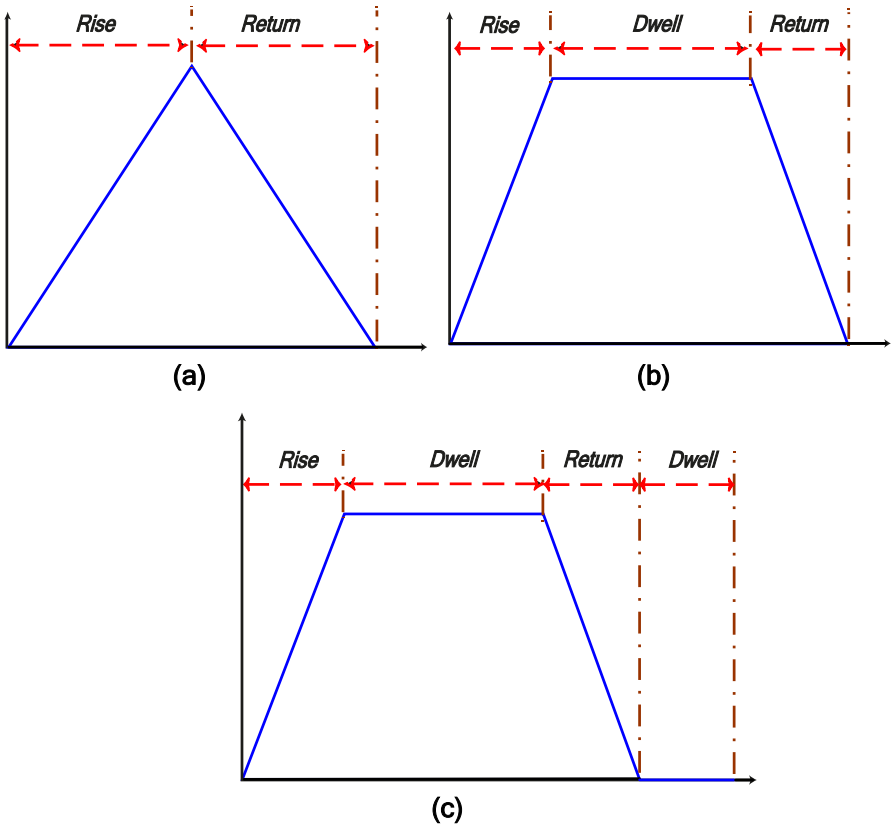

Fig. 2.4 Program types of output motion.

2.3 Review of Cam Design Optimization

Cam design optimization subject is an intensive topic of investigation in the mechanical engineering field. Over the past decades, there has been extensive research focused on the design and analysis of cam mechanisms through considering several aspects and using various optimization methodologies. The optimization approaches used in cam design process can comprise mathematical programming methods such as non-linear programming and gradient optimizers, or metaheuristic methods such as the class of evolutionary algorithms. A literature review on the application of such methods for optimizing cam and follower systems is presented in this section.

2.3.1 Cam Design Optimization Using Mathematical Programming Methods

Requirements for high performance, strength and accuracy of machinery demands efficient methods to deal with the optimization problem of cam design. In the literature, many researches have been published for the cam-follower design using different optimization techniques. For instance, Kwakernaak and Smith (1968) have formulated in their paper an optimization problem for finding cam profiles with limited follower motion kinematics and minimal residual vibrations over a prescribed range of cam speeds. The authors have suggested two numerical approaches to solve the problem, including linear programming and quadratic optimization. Several examples have been carried out in this work, by means of a digital computer, and the results have showed that the presented profiles are better than the well-known cycloidal profile in several respects.

Chew et al. (1983) have developed an optimization procedure for the synthesis of high-speed cam-follower mechanisms by using the optimal control theory formulation. Trade-offs between the characteristics at the cam-follower interface and at the output have been incorporated in this procedure. Although large-scale computations are involved in the numerical integration, the application of optimal-control theory has been shown to be capable of considering both linear and nonlinear relationships between the design variables. Based on iterative numerical methods, Terauchi and El-Shakery (1983) have applied the Regula-Falsi and Newton-Raphson algorithms to minimize the size of plate cam operating a reciprocating roller follower. Many design constraints have been observed in this study such as the maximum contact stress, the follower separation and cam profile undercutting phenomena.

Chew and Chuang (1995) have introduced a direct procedure to the minimization of residual vibrations over a specified range of cam speeds. Two approaches have been taken for

this investigation. The first formulation is based on the generalized Lagrange multiplier technique, and the obtained results are then checked using a nonlinear technique based on the generalized reduced gradient algorithm. Another attempt by (Bouzakis et al. 1997) has presented a non-linear programming approach, with the aid of an integrated computer aided design and manufacturing (CAD-CAM) model, for optimum design of a disk cam mechanism with oscillating roller follower. The objective is to minimize the size of the mechanism given by the maximum radius of the cam profile while considering a number of constructive and functional requirements. For constraint treatment, the exterior penalty function, known as a SUMT algorithm (Kuester and Mize 1973), has been employed in this research.

According to Hwang and Yu (2005), the golden section method has been implemented for optimizing the cam profile of an adjustable knock-out cam-follower mechanism of a bolt former. In order to ensure high quality of the motion, the optimization procedure developed aims to minimize the maximum strike velocity between the knock-out screw and the knock-out pin for all various knock-out strokes. Flores (2013) has presented a comprehensive computational approach for cam size optimization of a cam mechanism with offset or eccentric translating roller follower. The objective function used in his work accounts for the influence of the cam base circle radius, radius of the roller, and offset of the follower as design variables. Furthermore, additional constraints related to the performance of the cam mechanism are considered, namely those associated with the maximum admissible pressure angles and minimum curvature radius of the cam profile. The author has used the fmincon function of MATLAB® toolbox, which is based on the quasi-Newtonian minimization routine, to solve this optimization problem.

In (Kaplan 2014), the Lagrange multipliers method has been adopted for an optimal synthesis of a typical high-speed cam-follower mechanism of an internal combustion engine. The dynamic equation governing the behavior of the system has been simplified using dimensionless analysis method. The resulting model has been then used to find the optimum cam shape to reduce the residual vibrations in the follower part of the system. Further, Ouyang et al. (2017) have applied the sequential quadratic programming for optimal cam profile by integrating a single-objective optimization procedure with a dynamic model of cam-follower mechanism in delivery system of an offset press. In order to improve the kinematic and dynamic characteristics of the mechanism synthetically, an optimization cycle, known as iterative process, has been introduced to implement the procedure of single objective optimization and dynamic simulation alternately. The example illustrated in this

study has demonstrated sufficiently the effectiveness of the proposed methodology.

2.3.2 Cam Design Optimization Using Metaheuristic Methods

Due to the increasing development of computing technology, several studies have proposed to use metaheuristics for design and optimization of cam mechanisms. By using the hierarchical GA, Xiao and Zu (2009) have tackled the cam shape optimization problem for a unique cam mechanism in the cam drive engine. The output torque of the engine is taken as the objective function and the other design specifications, including the contact stress, the pressure angle, and the radius of curvature, are selected as constraints. The same problem has been reformulated as a bi-objective considering the maximum output torque and the minimum Hertzian contact stress (Xiao and Zu 2010). The authors have employed the NSGA-II and a multi-objective optimization algorithm based on Artificial Immune Systems (AIS) for this investigation. The optimization results have demonstrated that the overall engine performance is substantially improved by the evolutionary multi-objective optimization approach compared with the initial design.

Tsiafis et al. (2013) have developed a multi-objective GA to select the optimal design parameters for disk cam mechanism with translating flat-face follower. The design parameters, aimed to be optimized, are the radius of the cam base circle, the follower face width, and the follower offset. The optimization approach has been applied to find the best solutions with respect to the desired performance and to ensure the kinematic requirements. Subsequently, the dynamic analysis of the designed mechanism has been carried out in this study considering the frictional forces. Similarly, the GA approach has been investigated by Jana and Bhattacharjee (2017) for multi-objective optimization of cam-follower mechanism with simple and double harmonic profiles. The kinematic design parameters for this type of mechanism are the cam angle of rotation, maximum lift of the follower, and angle for maximum follower lift. The optimization has been achieved by the development of programs using MATLAB® with GA toolbox applications.

In addition to GA, the application of other metaheuristics can be found in the field of cam-follower optimization. For example, Zhi et al. (2005) have implemented ant colony algorithms to optimize the dynamic performance of distribution cam mechanism in internal combustion engine. An optimization model has been developed for solving this problem and the results have revealed that the behavior of the system is very much enhanced. In (Bravo and Flocker 2011), a new particle swarm optimization algorithm has been proposed for the

optimization of two cam profile problems. The first case is a single-dwell cam in which the magnitude of the negative acceleration is minimized. In the second case, the cam is supposed to have a constant velocity segment where the objective is to reduce the cycle time. The simulation results have proved that PSO technique is robust and well suited for minimizing a wide variety of objective functions applicable to the design of cam-follower systems.

Xuan et al. (2012) in their work have modeled and simulated a multi-objective dynamic optimization technique for reduction of residual vibration in high-speed cam mechanisms by using Non-Uniform Rational B-Spline (NURBS). The Improved Artificial Fish Swarm Algorithm (IAFSA) has been employed to optimize the best cam-follower curve and the results obtained have led to a significant improvement on the design parameters. Authors in (Torrealba and Udelman 2016) have deployed the differential evolution algorithm to define the optimal cam shape of a novel adjustable compliant actuator, called Bidirectional Antagonistic Floating Spring Actuator (BAFSA). According to the optimization procedure, the cam profile is designed for the maximum range of stiffness variability of the system. This research have exhibited that the DE technique is very effective to deal with many aspects of cam design.

Later on, Djeddou et al. (2018) have used an improved variant of the DE algorithm named Adaptive Mixed DE (AMDE) to synthesize a disc cam mechanism with eccentric roller follower translation. The first part of this study performs preliminary deterministic optimization to find the optimum size of the cam system and to ensure its high operating performance. The second part is devoted to the reliability analysis whose probability of system failure is estimated by the approximation methods FORM / SORM and Monte Carlo simulation. Furthermore, Abderazek et al. (2020) have applied seven recent metaheuristics including salp swarm algorithm, moth flame optimization, ant lion optimizer, multi verse optimizer, grey wolf optimizer, evaporation rate water cycle algorithm, and mine blast algorithm to automate the design of cam-roller follower mechanism. The influence of choosing the follower motion law on the optimal design of the mechanism has been investigated in their work. The computational results have indicated that the utilized algorithms are very competitive in structural design optimization.

2.4 Synthesis of Follower Motion Curves

During the process of designing cam mechanisms, one of the most interesting tasks is to select a suitable law of the follower motion that satisfies the constraints of the application. These

constraints mean the relationship of the output positions of the follower to the input motion of the cam (Smith 2001). The choice of the follower motion law plays a key role in relation to the transmission performance of the cam mechanism. The desirable characteristics of the motion law focus on finding an optimum displacement curve for which the velocity, acceleration and jerk to be continuous and their peak values as small as possible. These may not be important when a cam is operating at low speed, but will be crucial at high speeds since they can result in high vibrations and may lead to a short life span for the mechanism (Masood 1999).

The design of the cam profile which determines the kinematic analysis of the follower motion has been a subject of discourse over the past decades. Earlier studies used many mathematical functions which include basic curves, polynomial and Fourier series curves to synthesize the cam (Norton 2002; Angeles and Lopez-Cajún 2012). In recent years, spline curves completely have replaced the use of these conventional curves because of their flexibility and versatile properties. Researcher uses various forms of splines such as basic spline (B-spline), Bezier, and NURBS in cam motion synthesis (Nguyen 2018).

2.4.1 Basic Motion Curves

Traditionally, many basic forms of motion curves have been developed and applied to cam mechanisms including simple trigonometric and modified curves. Some of the most common basic laws of follower motion selected by cam designers are (Chen 1982; Cracks 1992):

- Constant velocity motion.
- Simple Harmonic Motion (SHM).
- Cycloidal motion.
- Modified sine motion.
- Modified Harmonic Motion (MHM).
- Modified Trapezoidal motion.

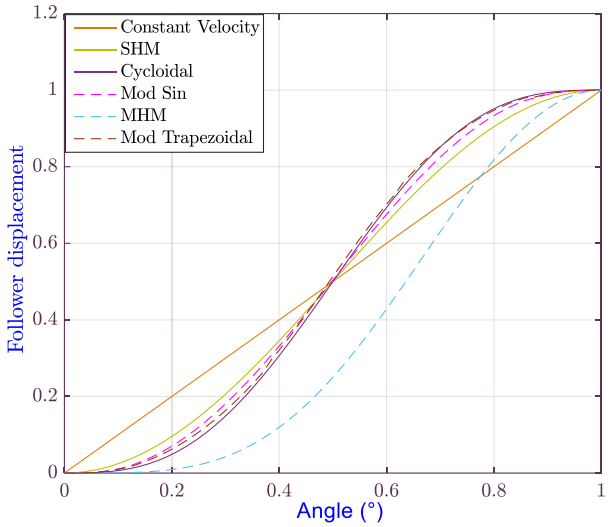

Fig. 2.5 Displacement diagrams for several basic motion laws.

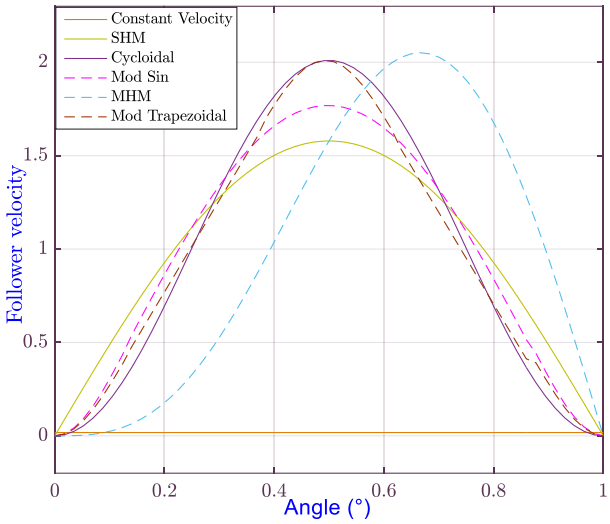

Fig. 2.6 Velocity diagrams for several basic motion laws.

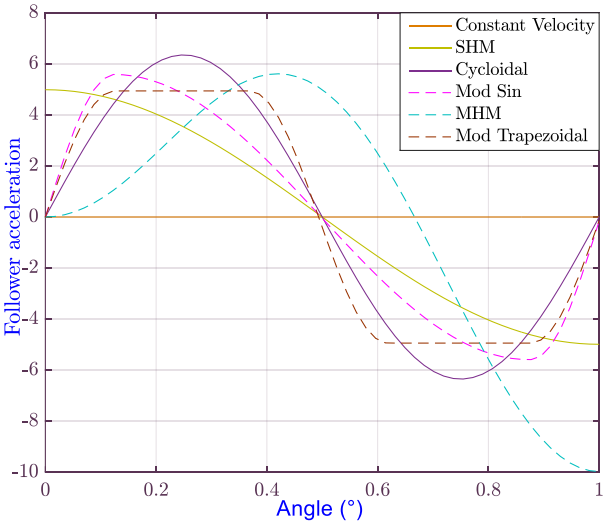

Fig. 2.7 Acceleration diagrams for several basic motion laws.

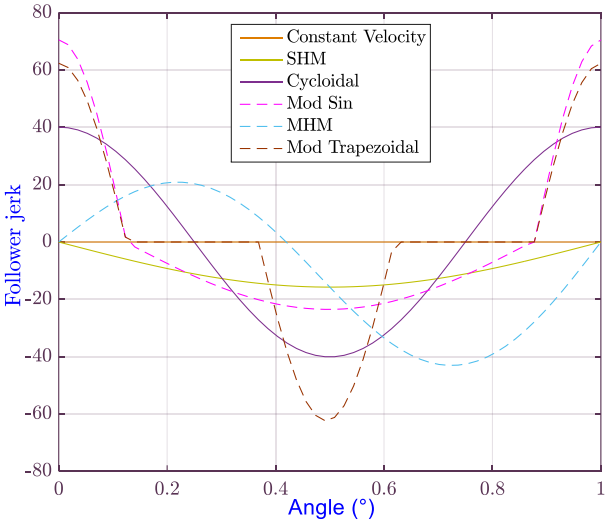

Fig. 2.8 Jerk diagrams for several basic motion laws.

The normalized characteristics of these motion laws including the displacement, velocity, acceleration, and jerk are shown in Figs 2.5 to 2.8, respectively. In constant velocity motion law, the follower velocity during the motion is constant and the acceleration is zero, except at the beginning and end points, where the acceleration reaches infinity instantaneously. Simple harmonic motion has smoothness in velocity and acceleration during the rise of the follower but exhibits a sudden change in acceleration at the ends. Therefore, this curve is suitable only for cams at medium or low speeds. Cycloidal motion is obtained by rolling a circle on a straight line. The length of the line is equal to the circumference of the rolling circle. This law has the smoothest motion among all of the basic laws and therefore, it is suitable for high-speed cams (Sateesh et al. 2009).

Modified sine motion law is a combination of cycloidal and harmonic quadrants occupying different parts of the working period. It has a low maximum velocity and provides excellent characteristics for booth acceleration and jerk. Modified harmonic motion is an improved simple harmonic curve in which every cycle starts from zero acceleration. Its performance is good for medium and high-speed machinery. Modified trapezoidal curve can generate a smooth and acceptable profile that meets the design requirements. It has good acceleration characteristics but accompanied by rough jerk.

The application of basic motion curves for synthesizing cam mechanisms is very extensive in the literature. Zigo (1967) has devised a method based on numerical integration of cam profiles for an arbitrary shape of acceleration curve by means of the trapezoidal rule. Chen (1969) has developed an approximate procedure of calculating the cam contour for a prescribed acceleration characteristic using the reversion of finite differences. The author has extended his previous study to refine the prescribed acceleration data so that it improved the numerical accuracy for the use of finite-difference equation (Chen 1972). On the other hand, he has applied the finite integration technique to synthesize the displacement curve for the same given conditions (Chen 1973).

Dhande et al. (1975) have proposed a unified approach for the analytical design of three-dimensional cam follower systems. The authors have provided generalized expressions for equations of the conjugate profile, the pressure angle, and the locations of the cutter. Lin et al. (1988) have introduced a methodology by which cam drawings and NC codes can be automatically created after specifying the cam motion function. This approach has been developed based on the combined curves fitting method. Chan and Sim (1998) have developed a CAD tool for optimum plate cam design using an exploratory search process called the Monte Carlo method. The CAD system which is an integration of the design calculations and an optimization algorithm allows providing an optimal solution, a graphical diagram, and a simulation of cam movement for different programs of follower motion.

A new approach using universal motion curves has been synthesized in a generalized model by Cheng (2002). These curves are designed using sine curves and constants on an acceleration basis. This approach establishes generalized design equations based on a generalized model of the motion curves. The curve shape on each varying-acceleration interval may be represented by trigonometric, polynomial, exponential or other functions and the motion curve may be symmetric or asymmetric. Modified trapezoidal cam profile with an adjustable forward and backward acceleration has been investigated in (Flocker 2009).

Through this study, the profile is suitable for single-dwell cam and follower applications, and can give an easy way to adjust the maximum forward or backward acceleration to prevent vibration problems.

Using the cycloidal motion and ramp curves, Kapucu et al. (2010) have presented an efficient approach to eliminate the residual vibration of shedding system and the associated mechanism that connects the heddle shafts with the cam mechanisms. Their work uses a simplified dynamic model of the shedding cam-linkage mechanism to create the equation of motion for the system. Simple harmonic motion has been used to describe the rise and return of the follower for disk cam with translating flat-face follower mechanism (Moise et al. 2011). In this work, the minimum size of the mechanism has been determined by considering the base radius of the cam profile. Recently, Tamboli et al. (2016) have used many standard basic curves such as cycloidal motion, parabolic motion, uniform motion, and constant acceleration for dynamic analysis of high speed cam and follower systems. The first part of this study deals with the combined static and inertial analysis of the systems. In the second part, the cam follower system is analyzed for the jump speed using well known Johnson method for determining the follower response.

2.4.2 Polynomial Motion Curves

Polynomial functions are successfully utilized to design cam profiles due to their smoothness properties. This class of motion curves is highly versatile in high speed applications and can be tailored to many design specifications. The general form of a polynomial function can be expressed as follows (Norton 2004):

$$s(\theta) = C_0 + C_1\theta + C_2\theta^2 + C_3\theta^3 .....C_N\theta^N \tag{2.1}$$

where s is the follower displacement, θ is the cam angular position, and C_i are constant coefficients determined on the basis of the boundary conditions imposed. By properly choosing the boundary conditions and the order of the polynomial function N, the suitable motion can usually be developed.

The normalized motion curves using 2-3, 3-4-5 and 4-5-6-7 polynomial functions are depicted in Figs 2.9 to 2.12. The 2-3 polynomial curve with a degree of three is cubic in nature and requires four boundary conditions of displacement and velocity at the ends of the rise and return stroke. The acceleration has discontinuities at the end points while the jerk values are infinitive at these points. The 3-4-5 polynomial curve with a degree of five uses six boundary conditions of displacement, velocity, and acceleration at the end points. This motion

curve has an extended control as it provides zero acceleration at the ends but no control over the follower jerks. In the case of 4-5-6-7 polynomial function, eight boundary conditions are needed to be specified for finding all the polynomial coefficients. This polynomial curve extends the control feature producing zero jerks at the ends (Rothbart and Klipp 2004).

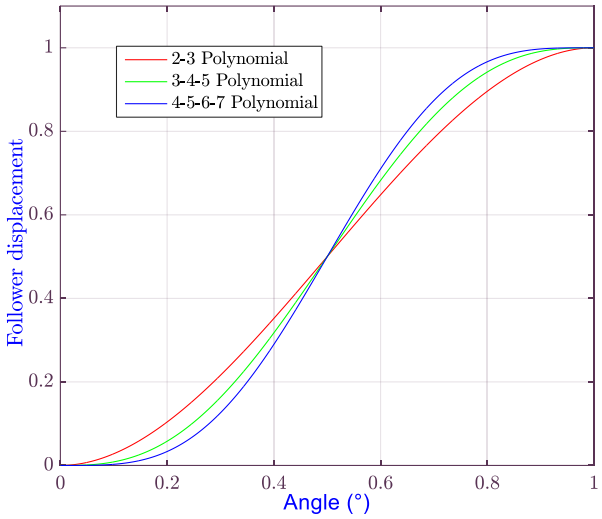

Fig. 2.9 Displacement diagrams with different polynomial motion curves.

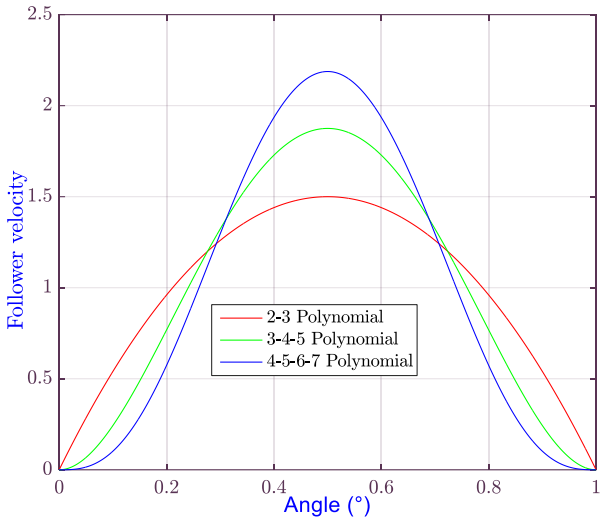

Fig. 2.10 Velocity diagrams with different polynomial motion curves.

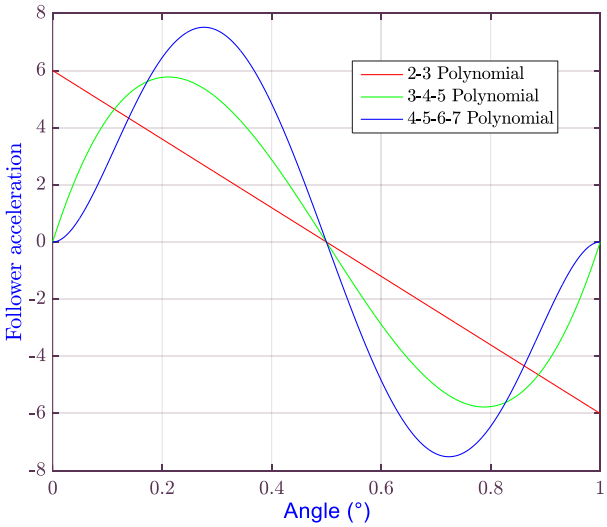

Fig. 2.11 Acceleration diagrams with different polynomial motion curves.

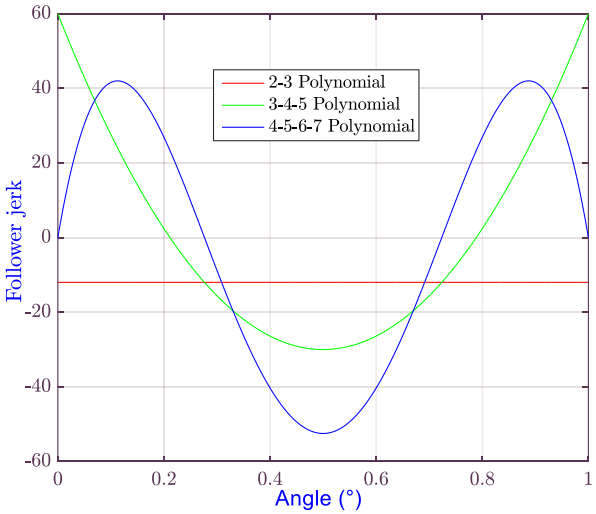

Fig. 2.12 Jerk diagrams with different polynomial motion curves.

The application of algebraic polynomials for cam synthesis has been developed by Dudley (1948), in which the differential equations of motion are solved using polynomial follower motion equations. This is the first method ever proposed that designs the cam profile to provide the desired follower action. Stoddart (1953) further have showed an application of these polynomial equations and proposed that vibration of the follower of Polydyne cam will be close to zero as long as there is sufficient spring force to keep it in contact. The cam profile

is designed such that the follower position curve matches an appropriate polynomial equation giving the desired characteristics of the cam mechanism. This method has been apparently tried by many of the car companies but has not been adopted by any one because it uses an incomplete polynomial to specify the profile.

Kanzaki and Itao (1972) have developed a cam design method for type head positioning in high-speed tele printers. They have determined the polynomial equations for the follower motion by considering certain boundary conditions and the characteristics of the residual vibrations over a wide range of rise times. Berzak (1982) has proposed a general method for obtaining the optimum design of a cam-follower mechanism using polynomial output motions. This method deals with both the kinematic and dynamic properties of the system. Phan et al. (1989) have investigated an indirect repetitive control theory for linear discrete multivariable systems using the polynomial functions. A suitable family of polynomial output motions are selected to obtain optimum design using a linear sum of the weighted performance coefficients. Proposed theory is described by numerical examples for third degree polynomial curves.

Sadek and Daadbin (1990) have presented a method of smoothing the specified profile curve by using polynomial curve fitting. The designed cam profile produces less vibration than the original profile and minimizes the tendencies to bounce. Fabien et al. (1994) have used linear quadratic optimal control theory to design high speed cams. They have designed such cam profiles at a fixed operating speed as well as over a range of speeds. Also, they have used trajectory sensitivity minimization to design a cam profile which is insensitive to speed variations. All these problems are solved by using an efficient numerical procedure. Chang (1996) has developed a repetitive control system for high speed cam mechanism. His study has used third degree polynomial curve for cam lift trajectory and five degree polynomial as desired output trajectory.

An alternative method called input shaping has been developed for generating automated motion commands to reduce the residual vibration in cam systems (Pridgen and Singhose 2010). This method compares the reduction of vibration between 3-4-5 and 4-5-6-7 polynomials, and takes them as smooth reference commands in single degree of freedom. Shala and Likaj (2013) have presented an analytical method of geometrical and kinematical syntheses for the exact design of cam profile. In this research, the polynomial function used to specify the motion can be obtained by converting the problem of cam design into a problem of solving the equations system of unknown coefficients. Later attempt by (Yang et al. 2014) has used the polynomial motion curve to analyze the reciprocating roller follower of a cam

system. The cam design approach presented in this study is applied for transient and heavy loads in the operating system of a large hydraulic press.

2.4.3 Spline Motion Curves

Although the basic and polynomial curves are usually adequate, they certainly do not represent an exhaustive list of motions which might be used in cam design. Another common approach in designing cams is to synthesize suitable motion curves with splines functions. The term "spline" refers to a smooth curve drawn through a set of plotted control points. Such curves can be described mathematically as piecewise approximations of cubic polynomial functions having all orders of continuity (Schumaker 2007). In the past few decades, spline curves have been widely used to develop cam profiles because of their versatility, flexibility, and ease of application. The research activities on this family of motion curves include B-spline, Bezier, and NURBS.

The class of B-spline curves is the more popular which not only interpolates a set of given control points, but can also allow localized modifications to be made easily without greatly affecting other parts of the curve (Loprencipe and Ranzo 2001). A particular property of B-spline is that any number of control points can be specified by a designer without increasing the degree of the curve. A cubic curve could then be used for many different curves shapes, without the need to piece curve segments together. Any number of control points can be added or modified to manipulate the curve shape. The general expression for a B-spline function that can be applied to the problem of interpolating nc constraints is written as follows (Zeid 1991):

$$s(\theta) = \sum_{i=1}^{nc} A_i B_{i,N}(\theta) \tag{2.2}$$

where A_i are the control points, $B_{i,N}$ is the B-spline basis function for the N^{th} order polynomial representation. The B-spline curve is determined by selecting values for the control points and the knot sequence.

Many researchers have used the properties of B-spline curve for cam and follower motion synthesis. Tsay and Huey (1988) have applied B-spline functions for general synthesis of cam motion programs. The proposed approach allows the designer to refine locally the motion curve with satisfying the discrete constraints on follower displacements, velocities, and accelerations. Yoon and Rao (1993) have presented a design procedure for representing the follower displacement using piecewise cubic spline functions. They have found that cubic

splines are more convenient and simpler to use compared to general spline functions and also result in smaller peak acceleration and jerk due to the application of the minimum norm principle.

Masood (1999) has developed a CAD-CAM system which graphically generates the cam profile on the cylindrical drum using a B-spline representation of follower curves. Eight different types of follower motion are considered in his research and the kinematic performance is based on the criteria of achieving the lowest levels of velocity and acceleration for each curve. An optimal synthesis for cam motion with non-constant angular velocity has been presented based on the dynamic model of a complete spring-actuated cam system (Kim et al. 2002). In order to satisfy asymmetric constraints and guarantee continuous contact at the cam-follower interface, the follower motion, which is dependent on the requirements during the closing period of a vacuum circuit breaker, has been optimized using a cubic spline. The optimized cam has been compared with a cam having constant angular velocity and with a polynomial cam. Simulation results have revealed that the dynamic behaviors of the optimized cam are superior to those of the original and polynomial cams.

Qiu et al. (2005) have proposed a universal optimal approach to cam curve design. The approach consists of four issues that include a cam curve description using uniform B-splines, an objective function in a universal weighting form to integrate the design requirements, an automatic adjusting technique for weighting coefficient values, and an improved complex search algorithm to optimize the control points of B-splines. With this approach, it is possible to deal simultaneously with multiple objectives for either kinematical or dynamic optimization. Sateesh et al. (2009) have generated a new follower velocity curve using cubic B-spline with six control points for optimizing the cam follower motion. They have developed a CAD-CAM tool which provides graphical and numerical representation of follower motion curves, i.e. displacement, velocity, acceleration, and jerk. It also provides cam profile coordinates to manufacture a cam on computer numerical control machines.

Jamkhande et al. (2012) have discussed the impact of various cam profile options designed using Polydyne, N-Harmonic and B-Spline methodologies on a field problem of cam wear for high speed engine application. According to simulation and experimental results, the cam profile design using B-spline method has showed the smoothest follower response compared to the two other methods. In recent work, Sahu et al. (2016) have proposed a novel design method of cam motion that approximates the basic cycloidal velocity curve using higher order B-spline. The motion characteristics of the desired smooth cam profile have been

generated by using a developed five degree B-spline free form curve with eight control points. The designed cam-follower system has been efficient and provided better continuity with uniform acceleration as compared to the basic cycloidal motion curve.

2.5 Basic Concepts of Cam Design

Once the follower motion is specified to synthesize the cam profile, a series of analyses regarding the cam mechanism performance should be performed to test the design. In such analyses, the following design concepts are considered (Chen 1982; Norton 2002):

- Cam Pressure angle.
- Cam radius of curvature.
- Force and torque analyses.
- Contact stress.

The aim of this section is to present in review manner the fundamental kinematic and dynamic aspects of cam design, in order to better understand the main issues investigated later throughout this study. The description adopted here is interested only with translating roller and flat-face follower cam mechanisms.

2.5.1 Pressure Angle Analysis

The pressure angle φ is defined as the angle formed between the line of the follower motion and the normal direction to the cam profile at the cam-follower contact point, as displayed in Fig. 2.13. This angle measures the efficiency of the force transmission between the cam and the follower (Rothbart and Klipp 2004). Only the component of force along the direction of the follower motion is useful in overcoming the output load. Therefore, the perpendicular component should be kept as low as possible to reduce sliding friction between the follower and its guide way. Cam pressure angles of 30º are about the largest that can be used without causing serious mechanical problems. The expression that allows the evolution of pressure angle is given as follows (Arthur et al. 2001):

$$\varphi = \tan^{-1}\left(\frac{s' - e}{s + a}\right) \tag{2.3}$$

For a roller follower, the α parameter is calculated as:

$$\alpha = \sqrt{\left(R_b + R_r\right)^2 - e^2} \tag{2.4}$$

For a flat-face follower, α is replaced by the following equation:

$$\alpha = \sqrt{R_b^{\,2} - e^2} \tag{2.5}$$

where s' is the follower velocity with respect to the cam angle, R_b is the base circle radius of the cam, R_r is the roller radius, and e is the offset of the follower.

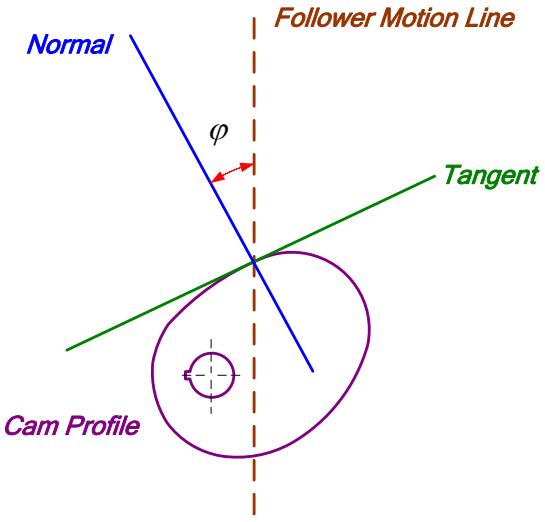

Fig. 2.13 Visualization of the cam pressure angle.

2.5.2 Radius of Curvature Analysis

The radius of curvature ρ is another factor that plays a vital role in the design of cam mechanisms, since it measures the rapidity at which the cam surface changes its direction (Chen 1982). As shown in Fig. 2.14, the radius of curvature at a point of the cam profile is the radius of a circle tangent at that point to the cam profile. This radius is positive if the center of the circle K is located between the cam rotation center O and the point of tangency Q; otherwise, this radius is negative. For a roller follower, the cam curvature radius can be expressed as follows (Wilson and Salder 2013):

$$\rho = \frac{\sqrt{\left(\left(R_b + R_r + s\right)^2 + s'\right)^3}}{\left(R_b + R_r + s\right)^2 + 2s' - \left(R_b + R_r + s\right)s''} \tag{2.6}$$

In this case, the minimum curvature radius ρ_{min} should be too greater than the roller radius R_r to prevent the undercutting phenomenon. For a flat-face follower, the curvature radius is written as the following (Wang and Lin 1989):

$$\rho = R_b + s + s'' \tag{2.7}$$

where s'' is the follower acceleration with respect to the cam angle.

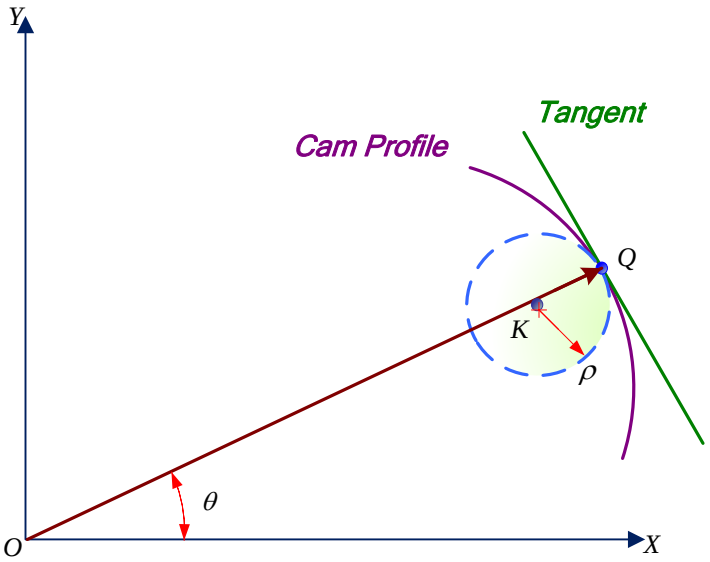

Fig. 2.14 Visualization of the cam curvature radius.

2.5.3 Force and Torque Analyses

There are various forces associated with the motion of the cam and follower. In cam design process, the magnitude, the direction and the line of forces action should be identified and evaluated to select the suitable dimensions the cam mechanism elements. Generally, the forces acting on the cam-follower system include inertia forces, spring forces, frictional resistances, and other external loads (Shakoor 2006).

The inertia force F_i caused by the necessity of moving the follower mass M_f is formulated as follows:

$$F_i = M_f \times s'' \times \omega_c^2 \tag{2.8}$$

The spring force F_s, which should always be large enough to ensure the permanent contact between the cam and follower, is proportional to the follower displacement:

$$F_s = k_s (s + \delta_s) \tag{2.9}$$

For the frictional resistances, the horizontal and vertical components concern the follower motion relative to its bearing:

$$F_f = \mu (N_1 + N_2) \tag{2.10}$$

where ω_c is the cam angular velocity, k_s is the constant elasticity of the spring, δ_s is its initial deflection, and μ is the coefficient of friction between the follower stem and its bearing.

In addition, an important part of the cam-follower system design is the determination of the torque, which is continually changing through the performance of any machine. From the torque information, the designer is able to determine the camshaft loads, the power required to

drive the follower, and thus the driving motor size. The input torque T_{cam} created in cam-follower mechanisms can be expressed as (Norton 2002):

$$T_{cam} = F \times s' \tag{2.11}$$

where F is the force of the cam acting on the follower. For a roller follower, F is calculated as follows:

$$F = \frac{F_i + F_s + F_e}{\left(1 - \mu\left(\frac{2C+b}{b}\right)\tan(\varphi)\right)} \tag{2.12}$$

For a flat-face follower, the required cam force to move the follower is given by the following equation:

$$F = \frac{F_i + F_s + F_e}{\left(1 + \mu\left(\frac{\mu_0(2C+b) - 2s'}{b}\right)\right)} \tag{2.13}$$

where F_e is the external applied load, C is the follower overhang, b is the length of follower bearing, and μ_0 is the coefficient of friction between the cam and follower.

2.5.4 Contact Stress Analysis

The contact stress is a significant design specification that must be considered for evaluating the durability of the cam mechanism. The exact determination of contact stresses for complicated surfaces is a difficult process. It depends strongly on the geometry and the size of the contacting zone. According to the theory of Hertz (1881), the contact stress problem between the cam and follower is simplified by assuming two parallel bodies in a linear contact. For cam mechanisms with translating roller followers, the Hertzian contact stress σ_{Hmax} developed at the contact area can be computed as (Chen 1982):

$$\sigma_{Hmax} = 0.564\sqrt{\frac{F \times (R_b + R_r)}{t_c \times (R_b \times R_r) \times \left[(1-\upsilon_1^2)/E_1 + (1-\upsilon_2^2)/E_2\right] \times \cos(\varphi)}} \tag{2.14}$$

For a flat-face follower shape, σ_{Hmax} is evaluated as follows:

$$\sigma_{Hmax} = 0.564\sqrt{\frac{F}{t_c \times \rho \times \left[(1-\upsilon_1^2)/E_1 + (1-\upsilon_2^2)/E_2\right]}} \tag{2.15}$$

where t_c is the cam thickness, υ_1, υ_2 are Poisson coefficients, and E_1, E_2 are the elasticity modulus of the material for the cam and follower respectively.

2.6 Conclusion

Cam-follower mechanism is preferred over a wide variety of machines because of its simple structure and high accuracy. The design of this mechanism is a complicated process which involves substantial work knowledge and several activities. The initial decision to be made is to identify the shape of the mechanism elements and select an appropriate combination of cam and follower. The next decision concerns the determination of follower motion and dimensional synthesis of the cam profile. After that, a number of analyses considering the kinematical and dynamical requirements should be studied to ensure the proper operating conditions.

The object in writing this chapter is to present a typical survey on the synthesis of cam mechanisms. First, the common classifications and terminology used in cam design have been presented. Second, the different optimization approaches applied in the field of cam-follower design have been displayed. Third, the design of cam profile which determines the characteristics of follower motion has been discussed. In the sequel of this chapter, the theoretical foundation of the main issues associated with the cam synthesis and analysis has been reviewed.

Chapter 3

Modified Adaptive Differential Evolution Algorithm

3.1 Introduction

Deterministic optimization of mechanical engineering structures is well known as a hard problem with many difficulties like nonlinearity, dimensionality and differentiability. Therefore, to deal with such problems effectively, it is highly needed to use powerful optimization algorithms that compromise between the accuracy of the solutions and the computational cost. In the present chapter, a novel differential evolution algorithm is proposed to solve the deterministic mechanical optimization problems. The proposed approach, named Modified Adaptive Differential Evolution (MADE), is a new version of the DE with two improvements. Firstly, the self-adaptive mechanism is employed in order to automate the tuning of mutation and crossover parameters instead of the manual mode as in the conventional DE. Secondly, the superiority of feasible points technique is applied to the selection phase instead of basic selection.

Originally, the MADE algorithm has been developed by Hamza et al. (2018) for solving the design optimization problem of cam system with eccentric translating roller follower, as well discussed in the next chapter. To demonstrate the efficiency and applicability of the proposed algorithm, four engineering optimization problems are investigated and the results obtained are compared with those reported recently in the literature using several methods. Thus, the organization of the remaining chapter is as follows. The basic concepts of the standard DE are firstly provided in Section 3.2. Then, the developed MADE is described in Section 3.3 and validated in Section 3.4. Finally, some conclusions are given in Section 3.5.

3.2 Basics of Differential Evolution

The differential evolution DE is one of the most popular and effective evolutionary algorithms, initially was introduced by Storn and Price (1995). Thanks to its attractive features, compact structure, fewer number of control parameters, and ease of implementation, the DE algorithm has been widely addressing to solve many problems in various areas of engineering during the past two decades. We find several studies in chemical science (Dragoi and Curteanu 2016), gas oil and petroleum industry (Nobakhti and Wang 2006), defense (Starkey 2005), signal processing (Lobato et al. 2012), image registration (Jiang et al. 2013), power system transfer capability assessment (Wong and Dong 2005), optimal power flow (Biswas et al. 2018), mechanical precision engineering (Abderazek et al. 2015; Abderazek et al. 2017; Redjechta et al. 2019), machining applications (Yildiz 2013a; Yildiz 2013b) and structural design optimization (Ho-Huu et al. 2015; Ho-Huu et al. 2018).

Typically, the basic operators in classical DE involve four principal phases as briefly summarized in Fig. 3.1. The inputs parameters associated with these operators are the population size Np, the maximum number of iterations T_{max}, the scale factor F, and the crossover rate Cr (Fan and Lampinen 2003).

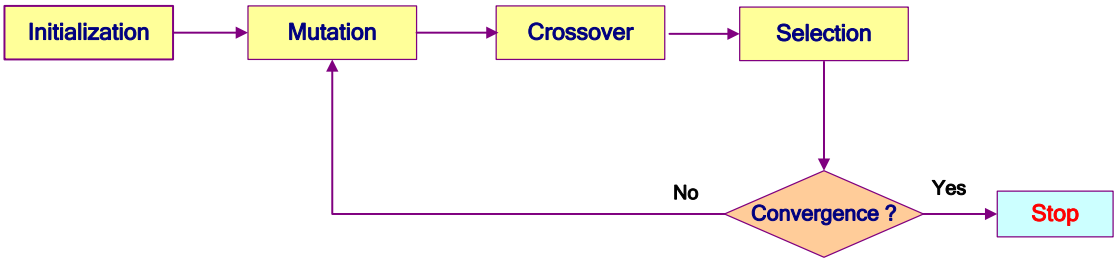

Fig. 3.1 Flowchart of the basic DE algorithm, modified from (Ho-Huu et al. 2018).

- ***Phase 1: Initialization***

Similar to the population-based evolutionary algorithms, the DE starts the search with an initial population containing Np individuals within the search space of the design variables. The individuals for the first population are generated randomly using the following equation:

$$y_{i,j}^{t=0} = y_i^L + rand_{i,j}\{0,1\} \times \left(y_i^U - y_i^L\right), \quad i = 1,...,Ny \text{ and } j = 1,...,Np \tag{3.1}$$

where i corresponds to the design variable index, j corresponds to the individual index, and $rand$ generates a random value uniformly distributed in the range [0,1]. In this chapter, the vector $y = \{d\}$ is assumed to contain only deterministic design variables. After the initialization phase, the fitness of each solution is evaluated and the best individual $y_{i,best}$ is selected (Storn and Price 1995).

- ***Phase 2: Mutation***

The mutation operator serves to create a new mutated vector $v_{i,j}^{t+1}$ for each target vector $y_{i,j}^t$ in the current population. The most extensively utilized mutation strategies in the basic DE are (Vitaliy 2006):

DE/rand/1: $$v_{i,j}^{t+1} = y_{i,r1}^{t} + F \times \left\{y_{i,r2}^{t} - y_{i,r3}^{t}\right\} \tag{3.2}$$

DE/best/1: $$v_{i,j}^{t+1} = y_{i,best}^{t} + F \times \left\{y_{i,r1}^{t} - y_{i,r2}^{t}\right\} \tag{3.3}$$

DE/rand to best/1: $$v_{i,j}^{t+1} = y_{i,r1}^{t} + F_1 \times \left\{y_{i,best}^{t} - y_{i,r2}^{t}\right\} + F_2 \times \left\{y_{i,r3}^{t} - y_{i,r4}^{t}\right\} \tag{3.4}$$

DE/rand/2: $$v_{i,j}^{t+1} = y_{i,r1}^{t} + F_1 \times \left\{y_{i,r2}^{t} - y_{i,r3}^{t}\right\} + F_2 \times \left\{y_{i,r4}^{t} - y_{i,r5}^{t}\right\} \tag{3.5}$$

DE/best/2: $$v_{i,j}^{t+1} = y_{i,best}^{t} + F_1 \times \left\{ y_{i,r1}^{t} - y_{i,r2}^{t} \right\} + F_2 \times \left\{ y_{i,r3}^{t} - y_{i,r4}^{t} \right\} \quad (3.6)$$

where t denotes the number of the current iteration, $r_1, r_2, r_3, r_4,$ and r_5 are integer indices chosen randomly within [1,…, *Np*], different from each other as well as different form the index j, and F_1 and F_2 are the mutation factors. In this study, the fourth strategy DE/rand/2 is selected to generate the mutated vector. It usually converges slowly but exhibits powerful exploration ability (Xu et al. 2018).

- ***Phase 3: Crossover***

The crossover operator is implemented to increase the diversity of the population in the next generation. The two common crossover types are binomial and exponential (Jia et al. 2013). However, the binomial crossover is the most often used where the trial vector $w_{i,j}^{t+1}$ is obtained by mixing the target vector $y_{i,j}^{t}$ with the mutated vector $v_{i,j}^{t+1}$ according to the following rule (Lieu et al. 2018):

$$w_{i,j}^{t+1} = \begin{cases} v_{i,j}^{t+1} \ if \left(rand_{i,j} \{0,1\} \le Cr \right) \vee \left(i == pr \right) \\ y_{i,j}^{t} \ \text{otherwise} \end{cases} \quad (3.7)$$

where pr is an integer number chosen randomly within $[1, \ldots, Ny]$.

- ***Phase 4: Selection***

In this phase, the target vector $y_{i,j}^{t}$ is compared with the trial vector $w_{i,j}^{t+1}$ in terms of the fineness value and the better one will survive to the next generation. The selection scheme for a minimization optimization problem is implemented as follows (Das and Suganthan 2010):

$$y_{i,j}^{t+1} = \begin{cases} w_{i,j}^{t+1} \ if \quad f\left(w_{i,j}^{t+1} \right) \le f\left(y_{i,j}^{t} \right) \\ y_{i,j}^{t} \quad \text{otherwise} \end{cases} \quad (3.8)$$

The optimization process including mutation, crossover, and selection is repeated until the stopping criterion (like the maximum number of iterations) is reached.

3.3 Modified Adaptive Differential Evolution (MADE)

Generally, the performance of any optimization approach is evaluated by three main factors: the accuracy of the best obtained solution, the stability when executing several runs, and the convergence rate to the final result. It is well known that the standard DE is a successful evolutionary algorithm that has been proven to be efficient and robust for global optimization. However, there are still some limitations and there is room for more improvements (Civicioglu and Besdok 2013). In this section, a new version of the DE is proposed to reinforce its search capability and accelerate convergence speed (Hamza et al. 2018). The novel version called MADE is effectively applied for solving the deterministic mechanical optimization problems with continuous design variables. The first improvement is carried out on the mutation and crossover phases, while the second one is performed on the selection phase. In addition, the reflection technique is used in MADE to control the boundary of the search space, during the mutation phase, and the exterior penalty method is applied to handle the design constraints. The details of these points are presented in the following subsections.

3.3.1 Improvement on the Mutation and Crossover Phases

The mutation and crossover operators play a key role in exploring the whole search space and converging faster to the optimum. As seen in the second and third phases, the specific factors for these two strategies are randomly chosen without primary information. This may lead the DE to be poor at searching ability and hence slowly converge to a global optimal solution (Semenov and Terkel 2003). In fact, the DE algorithm requires an exact configuration of its control parameters for efficiently searching progress. Therefore, the MADE proposed throughout this study uses the self-adaptive jDE technique introduced by Brest et al. (2006) to avoid the manual tuning of the mutation and crossover parameters (F_1, F_2 and Cr).

In the jDE technique, the initial values of scaling factors and the crossover rate are firstly specified based on the trial and error method. After that, their values are adjusted using the jDE mechanism for each target vector from the current population. Thus, the new values influence directly the mutation, crossover and selection operations of the new individual. The control parameters for the DE/rand/2/bin scheme are updated at each generation according to the following expressions:

$$F_{1,j}^{t+1} = \begin{cases} F_l + rand\{0,1\} \times F_u & if \ \ \delta_1 < \tau_1 \\ F_{1,j}^{t} & \text{otherwise} \end{cases} \tag{3.9}$$

$$F_{2,j}^{t+1} = \begin{cases} F_l + rand\{0,1\} \times F_u & if \ \ \delta_2 < \tau_2 \\ F_{2,j}^t & \text{otherwise} \end{cases} \tag{3.10}$$

$$Cr_j^{t+1} = \begin{cases} rand\{0,1\} & if \ \ \delta_3 < \tau_3 \\ Cr_j^t & \text{otherwise} \end{cases} \tag{3.11}$$

where F_l= 0.1, F_u= 0.9, δ_q (q=1,..3) are uniform random values within [0, 1], and τ_q (q=1,..3) represent the probabilities to adapt the parameters F_1, F_2 and Cr, respectively.

For further clarification, the self-adaptive jDE procedure is described schematically in the flowchart given in Fig. 3.2. It should be noted that this technique is conducted with the same manner for other mutation schemes.

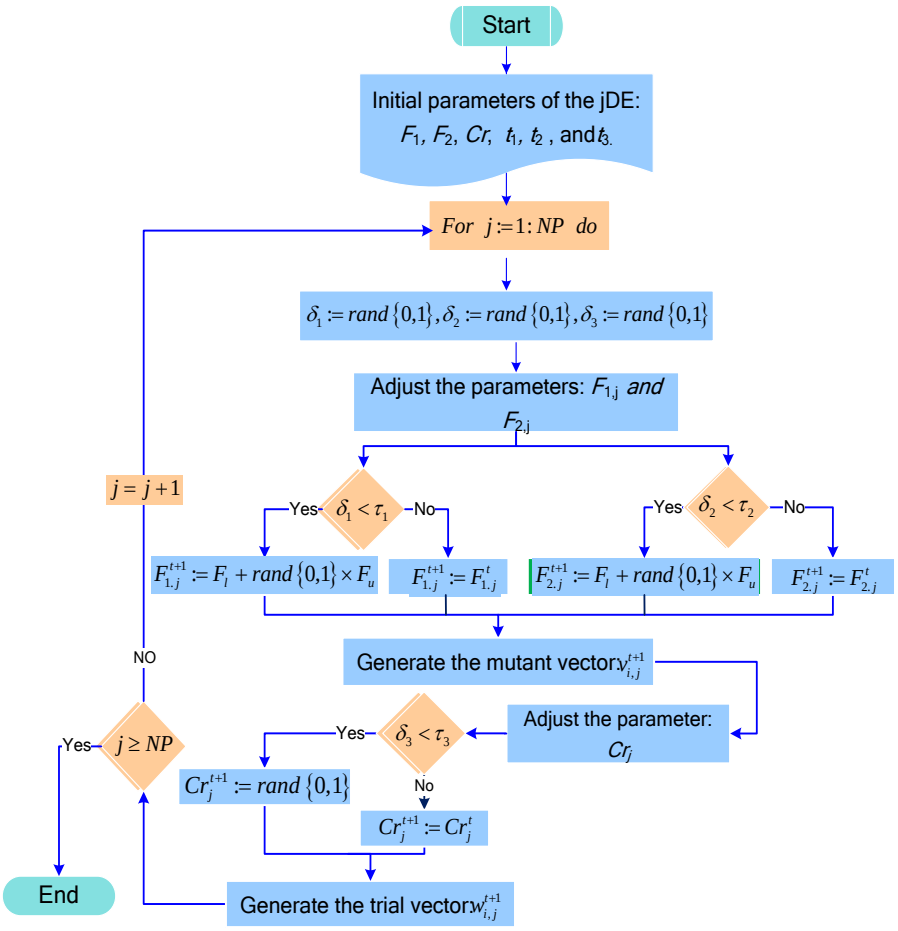

Fig. 3.2 Flowchart of jDE technique.

3.3.2 Improvement on the Selection Phase

The selection operator aims at comparing the trial vector created by crossover progress with the target vector and selecting the better one for the next generation. The idea of competing two solutions only in terms of the fitness value is usually inaccurate and does not necessarily

ensure the survival of the competent individuals. To overcome this deficiency, the MADE variant replaces the basic selection of the conventional DE by the superiority of feasible points technique proposed by Deb (2000).

According to this approach, the comparison between the trial and target vectors are based on three priorities: the feasibility of the individual, the best fitness value, and the lowest rate of the constraint violations. This involves three possible selection scenarios as explicated as follows: (1) when the two compared solutions are in the feasible region, the one with better fitness value is selected, (2) when one solution is feasible and the other is infeasible, the feasible one is chosen directly, and (3) when the two solutions are infeasible, the one with the smaller constraint violations is preferred. For more details, the feasibility rules procedure, in case of minimization problem, is illustrated in the flowchart presented in Fig. 3.3.

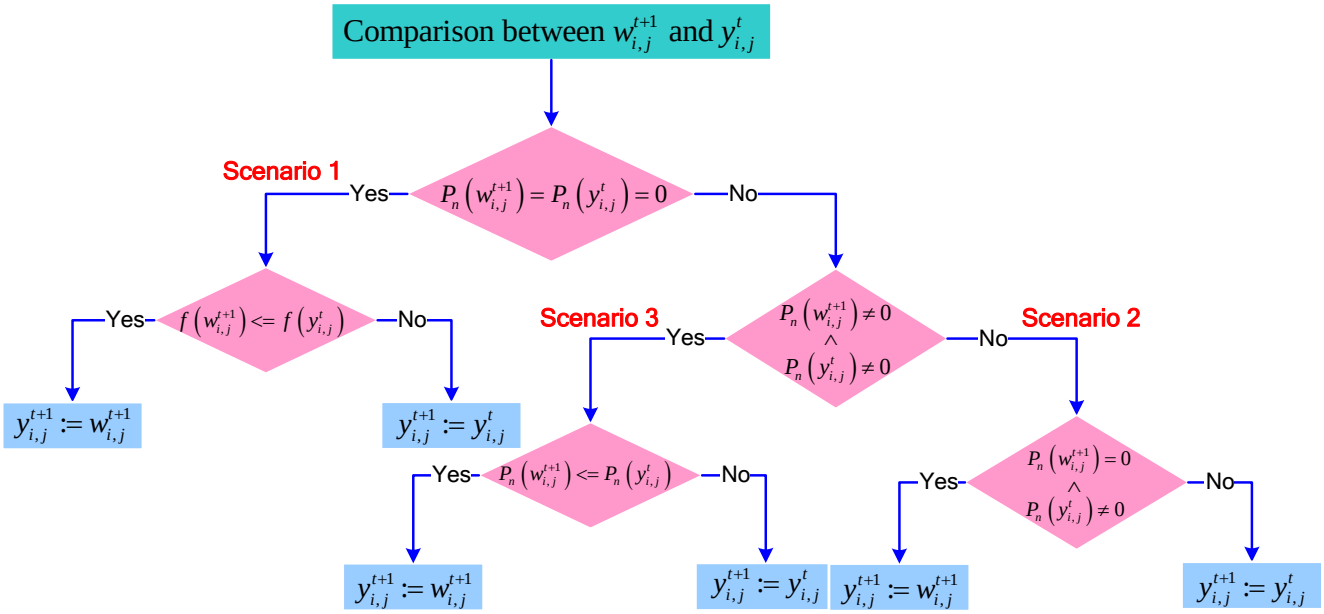

Fig. 3.3 Flowchart of feasibility rules technique.

3.3.3 Constraints Handling

3.3.3.1 Boundary constraints

In the second phase, the mutation operator may generate individuals whose components violate the boundary of the search space. Therefore, in such cases, a correction procedure is necessary employed to check and repair the infeasible components of the individual. There are various correction strategies to handle the boundary constraints (Kukkonen and Lampinen 2006; Wang et al. 2011). In this study, the well-known reflection method is employed and executed as follows (Juárez-Castillo et al. 2019):

$$v_{i,j}^{t+1} = \begin{cases} 2 \times y_i^{\boldsymbol{L}} - v_{i,j} & if \ v_{i,j}^{t+1} < y_i^{\boldsymbol{L}} \\ 2 \times y_i^{\boldsymbol{U}} - v_{i,j} & if \ v_{i,j}^{t+1} > y_i^{\boldsymbol{U}} \\ v_{i,j} & \text{otherwise} \end{cases} \tag{3.12}$$

3.3.3.2 Constraints functions

Constraint handling to solve real-world optimization problems is one of the challenging tasks when using metaheuristic algorithms. For this reason, many researches have been focused on developing effective methods to deal with the constraints functions. These methods can be simply classified into four groups (Mezura-Montes and Coello 2011): penalty functions, decoders, special operators, and separation of objective function and constraints. The methods of the first group are the most frequently used in evolutionary algorithms due to its simplicity of application. They are based on the idea of transforming a constrained optimization problem into an unconstrained one by defining a new extended objective function (Mezura-Montes 2009). Examples of penalty functions in the literature comprise exterior penalty, annealing penalty, adaptive co-evolutionary penalty, dynamic penalty, and death penalty (Kramer 2010). For further theoretical details about these methods, the interesting readers are encouraged to refer to the specialized literature such as (Coello 2002).

In MADE, the exterior penalty technique adjusted by Abderazek et al. (2017) is considered to treat the constraints. The mathematical model of this technique is expressed as follows:

$$P_n(y) = \begin{cases} \sum_{i=1}^{k} \min\left(0,\ g_i(y)\right)^2 \\ \sum_{j=1}^{m} \max\left(0,\ \left|h_j(y)\right| - \upsilon\right) \end{cases} \tag{3.13}$$

where P_n is the penalty function used to compute constraint violations, and ν is a very small value.

By integrating two above mentioned improvements into the DE, a so-called modified adaptive differential evolution MADE algorithm is developed for solving the continuous optimization problems. The pseudocode of the proposed MADE is shown in Algorithm 3.1.

Algorithm 3.1: MADE optimization algorithm

Input: $Np,\ T_{max}, F_1,\ F_2, Cr$ and $\tau_1,\ \tau_2,\ \tau_3$.

Initialize the population Eq. 3.1.
Evaluate the fitness for all individuals and select the best initial solution y_{best}^1.
while $t < T_{max}$ **do**
  for $j \coloneqq 1\ to\ Np$ **do**
    Mutation Phase
    Update the parameters $F_{1,j},\ F_{2,j}$ and Cr_j Eqs. 3.9, 3.10, and 3.11.
    Generate the mutant vector $v_{i,j}^{t+1}$ Eq. 3.5.
    Handle boundary constraints Eq. 3.12.
    Crossover Phase
    Randomly chose an integer number pr within $[1, Ny]$.
    for $i \coloneqq 1\ to\ Ny$ **do**
      if $\left(rand_{i,j}\{0,1\} \le Cr_j \right) \vee (i = pr)$ **then**
        $w_{i,j}^{t+1} \coloneqq v_{i,j}^{t+1}$
      else
        $w_{i,j}^{t+1} \coloneqq y_{i,j}^{t}$
      end
    end
    Selection Phase
    Compare between $w_{i,j}^{t+1}$ and $y_{i,j}^{t}$ by following the flowchart of feasibility rules (Fig. 3.3).
  end
  $t = t + 1$
end

Output: The best found solution y_{best} with the corresponding fitness value f_{best}.

3.4 Evaluation of MADE

In order to demonstrate the performance of the new proposed algorithm, four real-world optimization problems from the structural engineering field are studied, namely, three bar truss, tension spring, welded beam, and hydrostatic thrust bearing. All the mentioned problems have continuous nature of design variables. The initial parameters of MADE for the problems are set as follows: $F_1 = 0.8, F_2 = 0.5,\ Cr = 0.5,\ \tau_1 = 0.5,\ \tau_2 = 0.2$ and $\tau_3 = 0.1$. The population size and the maximum number of function evaluations (FEs) are listed in Table 3.1. Moreover, for each problem, 50 independent runs are performed and the MADE statistical results are compared with other recent algorithms including the best, mean, worst solutions, and standard deviation (SD). The MADE is implemented in MATLAB® and the optimization runs are executed on a PC i5 with a 2.2 GHz and 4 GB of RAM memory.

The best values of objective function, design variables and constraints obtained by MADE in each optimization problem are presented in Table 3.2. In addition, the statistical results are summarized in Table 3.3. Commonly, it is remarked from the two tables that the developed approach can acquire the feasible global optimal solution for all problems with

small function evaluations number, lesser than 20,000 in case of the three bar truss and welded beam. This indicates that the proposed MADE is perfectly adapted for solving the considered problems in terms of solution quality, convergence speed, and robustness.

Table 3.1 *Np* size and FEs number of the MADE for each optimization problems.

Problem	***Np***	**FEs**
Three bar truss design	10	4,000
Tension spring	40	20,000
Welded beam	40	18,000
Hydrostatic thrust bearing	50	40,000

Table 3.2 Optimal results obtained by MADE for the four engineering design problems.

Variables	**Three bar truss**	**Tension spring**	**Welded beam**	**Hydrostatic thrust**
d_1	0.788675136255	0.051689060739	0.20572963978	5.9557806
d_2	0.408248285767	0.356717731547	3.47048866562	5.3890131
d_3	–	11.28896623541	9.03662391035	5.3587E-06
d_4	–	–	0.20572963978	2.26965688
$g_1(d)$	0	0	1.8189894E-12	0.033765361542
$g_2(d)$	1.4641016204770	0	0	0.000102761472
$g_3(d)$	0.5358983795229	4.0537856140377	0	0.000108170138
$g_4(d)$	–	0.7277288051420	3.43298420860	0.000324364889
$g_5(d)$	–	–	0.08072963978	0.566768002669
$g_6(d)$	–	–	0.23554032258	0.000996361382
$g_7(d)$	–	–	2.7284841E-12	0.004303914875
$f(d)$	263.8958433764	0.012665232788	1.72485230859	1625.44281765801

Table 3.3 Statistical results obtained by MADE for the four engineering design problems.

Problem	**Best**	**Mean**	**Worst**	**SD**
Three bar truss	263.8958433764684	263.8958433764685	263.895843376468	2.7005E-13
Tension spring	0.012665232788319	0.012665232788320	0.01266523278823	5.8876E-16
Welded beam	1.724852308597364	1.724852308597365	1.72485230859736	9.6318 E-16
Hydrostatic thrust	1625.442817658010	1625.450964132840	1625.58794200080	2.1550E-02

3.4.1 Three Bar Truss

The first problem deals with the design of a three-bar truss structure (Nowacki 1973) in which the weight is to be minimized and subjected to stress, deflection, and buckling constraints. The design variables come from the cross-sectional areas of the two members d_1 and d_2, as shown in Fig. 3.4. This optimization problem is formulated as follows:

$$
\begin{aligned}
&find\ \{d_1, d_2\} \\
&\min: f(d) = \left(2\sqrt{2}d_1 + d_2\right) \times l \\
&s.t.: g_i(d) \geq 0, \quad i = 1,.,3 \\
&g_1 = \sigma - \frac{\sqrt{2}d_1 + d_2}{\sqrt{2}d_1^2 + 2d_1 d_2} P \\
&g_2 = \sigma - \frac{d_2}{\sqrt{2}d_1^2 + 2d_1 d_2} P \\
&g_3 = \sigma - \frac{1}{\sqrt{2}d_2 + d_1} P \\
&0 \leq d_1, d_2 \leq 1
\end{aligned}
\tag{3.14}
$$

where l=*100cm*, P=2*KN*, and σ=2*KN/ cm.*^{2}

The above problem has been recently solved using several approaches like Dynamic Stochastic ranking based DE (DSS-MDE) (Zhang et al. 2008), DE with Level Comparison (DELC) (Wang and Li 2010), Constrained Optimization based on a Modified DE (COMDE) (Mohamed and Sabry 2012), Water Cycle Algorithm (WCA) (Eskandar et al. 2012), rank-iMDDE (Gong et al. 2014), ε-constrained DE algorithm with a novel Local Search operator (εDE-LS) (Yi et al. 2016), and Adaptive Mixed DE (AMDE) (Abderazek et al. 2017). The results of these algorithms are collected in Table 3.4, a result in boldface means a better solution obtained. In terms of the standard deviation, rank-iMDDE is the better, followed by εDE-LS, DELC, MADE, AMDE and COMDE. However, MADE and AMDE exhibit superiority in terms of FEs among the compared algorithms. The convergence of MADE to the best solution is given in Fig. 3.5.

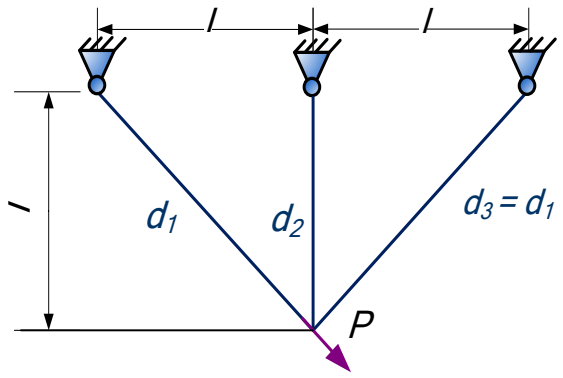

Fig. 3.4 Three bar truss design.

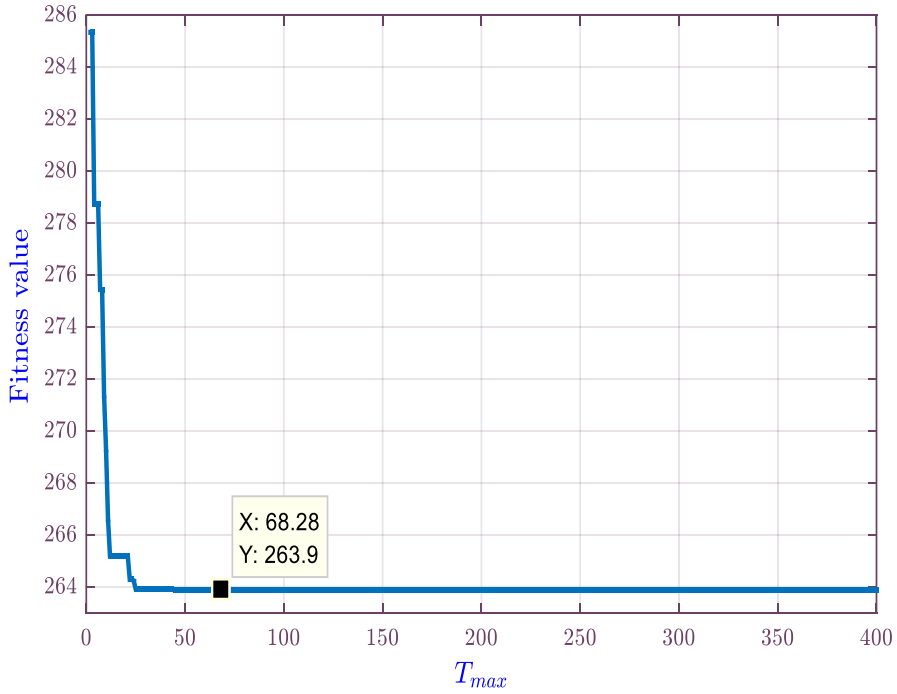

Fig. 3.5 Convergence diagram of MADE for the three bar truss problem.

Table 3.4 Comparison of MADE statistical results with literature for the three bar truss problem.

Algorithm	Best	Mean	Worst	SD	FEs
MADE	263.8958433764684	263.8958433764685	263.8958433764686	2.7005E-13	**4,000**
DSS-MDE	263.8958433	263.8958436	263.8958498	9.70E−07	15,000
DELC	263.8958434	263.8958434	263.8958434	4.34E−14	10,000
COMDE	263.8958434	263.8958434	263.8958434	5.34E−13	7000
WCA	263.895843	263.895843	263.895843	8.71E−05	5,250
Rank-iMDDE	263.89584340	263.8958434	263.8958434	**0.00E+00**	4,920
εDE-LS	263.895843376468	263.895843376468	263.895843376468	2.3206E−14	15,000
AMDE	263.8958433764684	263.8958433764685	263.8958433764686	2.7441E-13	**4,000**

3.4.2 Tension Spring

The aim of this problem is the volume minimization of a tension spring (Arora 2004), under constraints on shear stress, surge frequency, minimum deflection, and limits on outside diameter of design variables. There are three design variables consisting of the wire diameter d_1, the mean coil diameter d_2, and the number of active coils d_3, as illustrated in Fig. 3.6. The mathematical formulation of the optimization problem can be described in the following form:

$$
\begin{aligned}
&find\{d_1, d_2, d_3\}\\
&\min: f(d) = (d_3 + 2) d_2 d_1^2\\
&s.t.: g_i(d) \geq 0, \quad i = 1,., 4\\
&g_1 = \frac{d_2^3 d_3}{71785 d_1^4} - 1\\
&g_2 = \frac{d_1 d_2 - 4 d_2^2}{12566\left(d_2 d_1^3 - d_1^4\right)} - \frac{1}{5.108 d_1^2}\\
&g_3 = \frac{140.45 d_1}{d_2^2 d_3} - 1\\
&g_4 = 1 - \frac{d_2 + d_1}{1.5}\\
&0.05 \leq d_1 \leq 2, \quad 0.25 \leq d_2 \leq 1.3, \quad 2 \leq d_3 \leq 15
\end{aligned}
\tag{3.15}
$$

The convergence of MADE to the best fitness value for this problem is plotted in Fig. 3.7. The optimal results obtained by MADE and other algorithms, including Ideal Gas Molecular Movement (IGMM) (Varaee and Ghasemi 2017), modified Backtracking Search Optimization Algorithm (SSBSA) (Wang et al. 2019), rank-iMDDE, COMDE, DSS-MDE, WCA, DELC and εDE-LS are reported in Table 3.5. As it can be seen from the table, the best solution found for this example is 0.01266523. Further, among the compared algorithms, it is observed that MADE is more robust in solving this problem with a standard deviation value of 5.8876E− 16. In addition, the proposed variant gains the best results compared with the other eight approaches regarding the values of best, mean, and worst solutions.

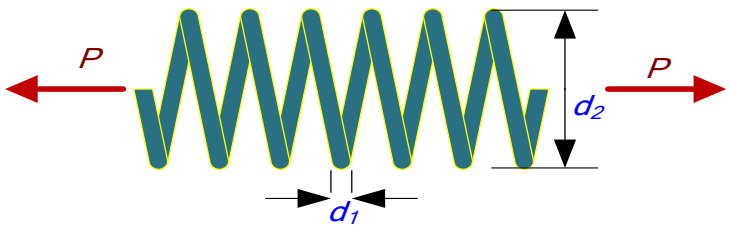

Fig. 3.6 Tension spring design.

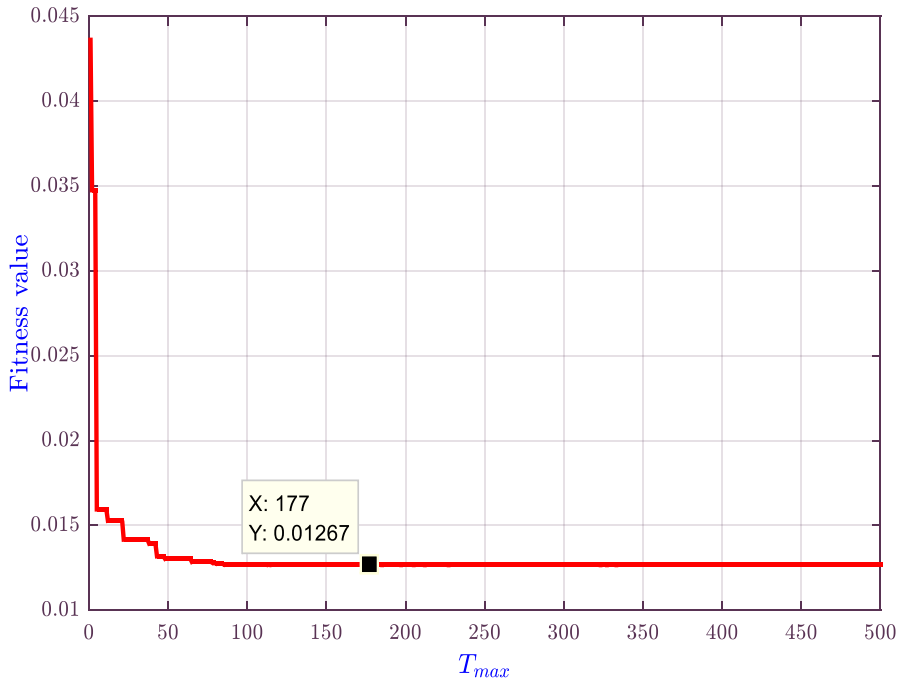

Fig. 3.7 Convergence diagram of MADE for the tension spring problem.

Table 3.5 Comparison of MADE statistical results with literature for the tension spring problem.

Algorithm	Best	Mean	Worst	SD	FEs
MADE	**0.012665232788319**	**0.012665232788320**	**0.012665232788323**	**5.8876E-16**	20,000
IGMM	0.0126653	0.0128657	0.0135125	2.56E−04	**4,000**
SSBSA	0.012665	0.012749	0.013300	1.31E-04	36,030
Rank-iMDDE	0.012665233	0.012665264	0.01266765	2.45E−07	19,565
COMDE	0.012665233	0.012665233	0.012665233	3.09E−06	24,000
DSS-MDE	0.012665233	0.012669366	0.012738262	1.25E−05	24,000
WCA	0.012665	0.012746	00.012952	8.06E−05	11,750
DELC	0.012665233	0.012665267	0.012665575	1.30E−07	20,000
εDE-LS	0.012665233	0.012665233	0.012665233	5.0075E−14	20,000

3.4.3 Welded Beam

This optimization problem has been initially formulated by Rao (2019) where the goal is to minimize the manufacturing cost of a welded beam (Fig. 3.8). This example involves four design variables and seven constraints which are related to mechanical quantities, such as shear stress, bending stress, buckling and displacement. The problem can be expressed as:

$$
\begin{aligned}
&find\ \{d_1, d_2, d_3, d_4\}\\
&\min: f(d) = 1.10471 d_1^2 d_2 + 0.04811 d_3 d_4 (14.0 + d_2)\\
&s.t.: g_i(d) \geq 0, \quad i = 1,.,7\\
&g_1 = 13600 - \tau(d)\\
&g_2 = 30 d_3^2 d_4 - 504\\
&g_3 = d_4 - d_1\\
&g_4 = 5 - 0.1047 d_1^2 - 0.04811 d_3 d_4 (14 + d_2)\\
&g_5 = d_1 - 0.125\\
&g_6 = 0.25 d_3^2 d_4 - 3.293\\
&g_7 = 0.10237\sqrt{d_3^2 d_4^2}\,(1 - 0.028235 d_3)\\
&0.1 \leq d_1, d_4 \leq 2, \quad 0.1 \leq d_2, d_3 \leq 10,
\end{aligned}
\tag{3.16}
$$

where

$$
\begin{aligned}
&\tau(d) = \sqrt{(\tau')^2 + (\tau'')^2 + 2\tau'\tau''\frac{d_2}{2R}}, \quad \tau' = \frac{6000}{\sqrt{2} d_1 d_2}, \quad \tau'' = \frac{MR}{J}, \quad M = 6000\left(14 + \frac{d_2}{2}\right),\\
&R = \sqrt{\frac{d_2^2 + (d_1 + d_3)^2}{4}}, \quad J = 2\sqrt{2} d_1 d_2 \left(\frac{d_2^2}{4} + \frac{(d_1 + d_3)^2}{2}\right)
\end{aligned}
\tag{3.17}
$$

The convergence diagram of MADE for the welded beam optimization problem is demonstrated in Fig. 3.9. In this case, MADE is compared with Multiple trial vector-based DE (MDDE) (Mezura-Montes et al. 2007), Social-Spider Algorithm (SSO-C) (Cuevas and Cienfuegos 2014), SSBSA, rank-iMDDE, COMDE, DELC, and WCA. The comparison results listed in Table 3.6 show that all the mentioned algorithms are able to find the global optimal solution. MADE and rank-iMDDE outperform the others with the lower standard deviation value. Besides, with the smallest Fes number, MADE is considered the most efficient among here tackled algorithms.

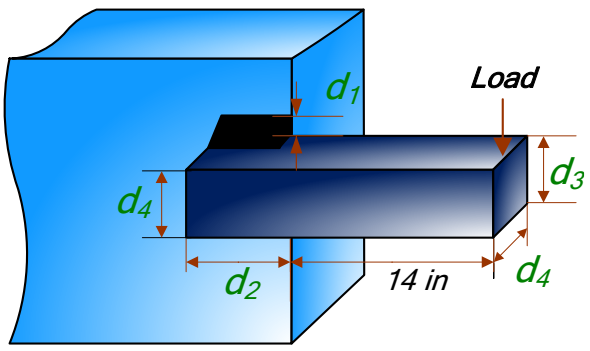

Fig. 3.8 Welded beam design.

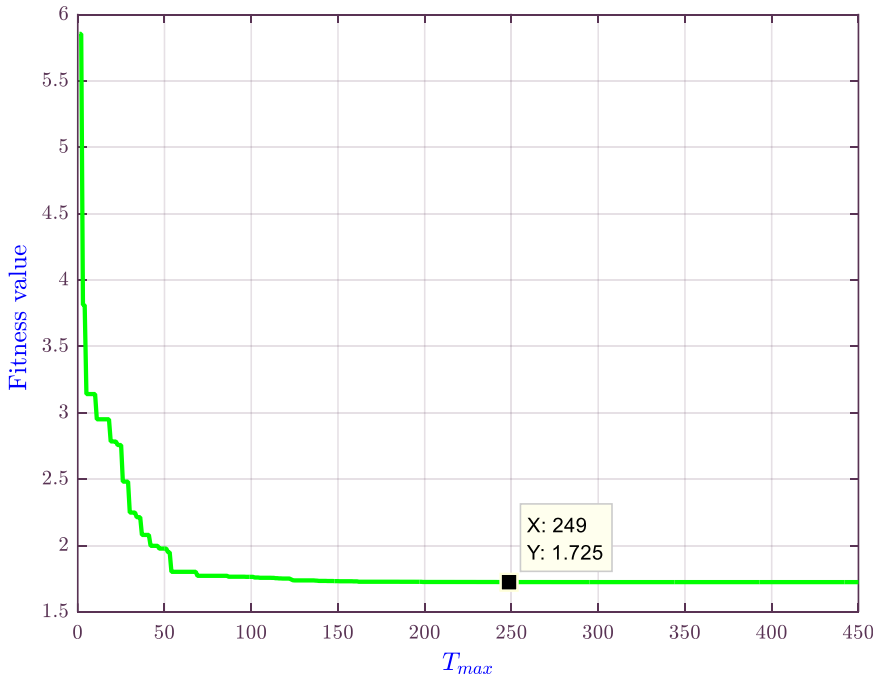

Fig. 3.9 Convergence diagram of MADE for the welded beam problem.

Table 3.6 Comparison of MADE statistical results with literature for the welded beam problem.

Algorithm	**Best**	**Mean**	**Worst**	**SD**	**FEs**
MADE	1.724852308597364	1.724852308597365	1.724852308597366	**9.6318 E-16**	**18,000**
MDDE	1.725	1.725	1.725	1.00E−15	24,000
SSO-C	1.7248523085	1.746461619	1.799331766	2.57E−02	25,000
SSBSA	1.724851	1.910178	2.217041	0.154774	34,340
Rank-iMDDE	1.724852309	1.724852309	1.724852309	**9.06E-16**	19,830
COMDE	1.724852	1.724852	1.724852	1.60E−12	20,000
DELC	1.724852	1.724852	1.724852	4.10E−13	20,000
WCA	1.724856	1.726427	1.744697	4.29E−03	46,450

3.4.4 Hydrostatic Thrust Bearing

In this problem, the power loss during the operation of a hydrostatic thrust bearing (see Fig. 3.10) is minimized (Coello 2000). Optimization constraints are on load carrying capacity, inlet oil pressure, oil temperature rise, oil film thickness, and physical restrictions. There are four design variables including the bearing step radius d_1, the recess radius d_2, the oil viscosity d_3, and the flow rate d_4. The formulation of the optimization problem is given as follows:

$$
\begin{aligned}
&find\left\{d_1, d_2, d_3, d_4\right\}\\
&\min: f\left(d\right)=\frac{d_4 P_o}{0.7}+E_f\\
&s.t.: g_i\left(d\right)\geq 0, \quad i=1,.,7\\
&g_1=W-101000\\
&g_2=1000-P_o\\
&g_3=50-\Delta T\\
&g_4=h-0.001\\
&g_5=d_1-d_2\\
&g_6=0.001-\frac{0.0307}{386.4P_o}\left(\frac{d_4}{2\pi d_1 h}\right)\\
&g_7=5000-\frac{W}{\pi\left(d_1^{\,2}-d_2^2\right)}\\
&1\leq d_1, d_2, d_4\leq 16, \quad 1e-6\leq d_3\leq 16e-6
\end{aligned}
\tag{3.18}
$$

where

$$
\begin{aligned}
&W=\frac{\pi P_o}{2}\frac{\left(d_1^{\,2}-d_2^2\right)}{\ln\left(\frac{d_1}{d_2}\right)},\ P_o=\frac{6d_3 d_4}{\pi h^3}\ln\left(\frac{d_1}{d_2}\right),\ E_f=143.3076 d_4\Delta T,\ \ \Delta T=2\left(10^P-560\right)\\
&P=\frac{10.04-\log_{10}\log_{10}\left(8.122e6d_3+0.8\right)}{3.55},\ \ h=\left(\frac{1500\pi}{60}\right)^2\left(\frac{2\pi d_3}{E_f}\right)\left(\frac{d_1^{\,4}}{4}-\frac{d_2^4}{4}\right)
\end{aligned}
\tag{3.19}
$$

Hydrostatic thrust bearing optimization problem has been previously solved using TLBO (Rao et al. 2011), ABC (Rao et al. 2011), Novel Differential Evolution (NDE) (Mohamed 2018), rank-iMDDE and MMDE. The statistical results of the six competitive algorithms are tabulated in Table 3.7. Although ABC shows slight superiority in terms of the best solution, MADE can produce better results with respect to the mean and worst solutions. Furthermore, MADE is the most stable among the compared algorithms in solving the problem based on the lowest value of standard deviation (2.1550E-02). The convergence history of MADE for this problem is depicted in Fig. 3.11.

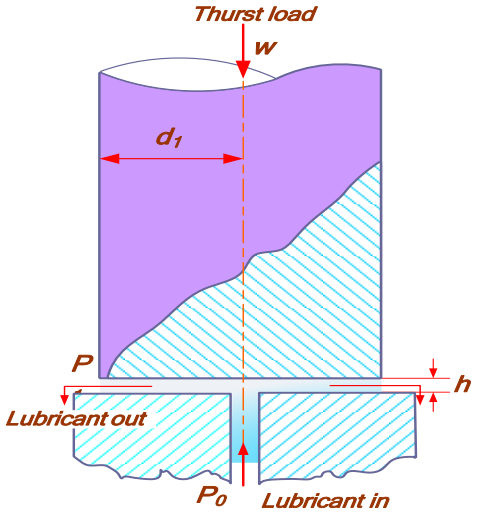

Fig. 3.10 Hydrostatic thrust bearing design.

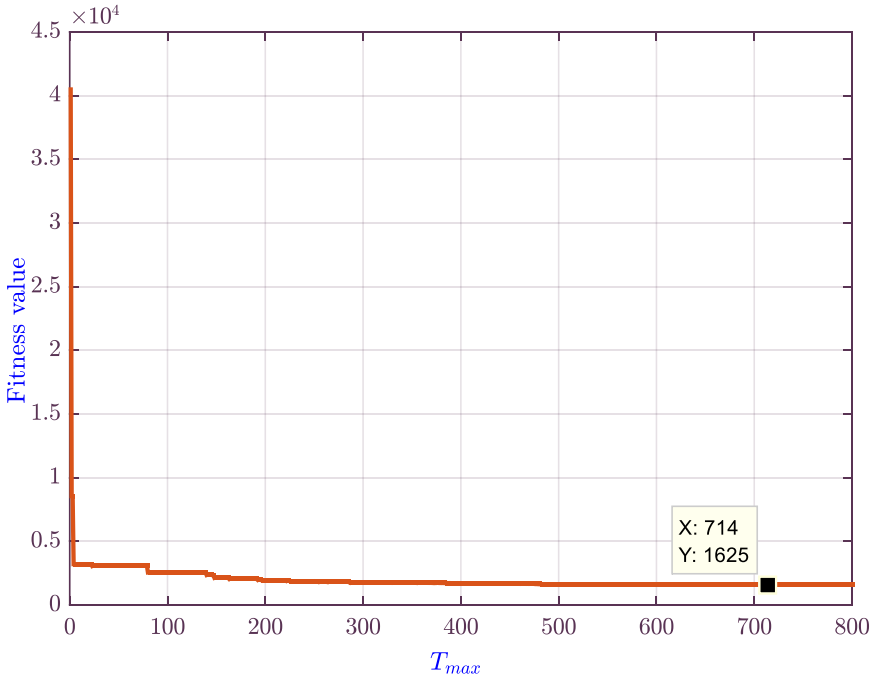

Fig. 3.11 Convergence diagram of MADE for the hydrostatic bearing problem.

Table 3.7 Comparison of MADE statistical results with literature for the hydrostatic bearing problem.

Algorithm	**Best**	**Mean**	**Worst**	**SD**	**FEs**
MADE	1625.44281765801	**1625.45096413284**	**1625.58794200080**	**2.1550E-02**	40,000
NDE	1625. 44276496	1692. 67262344	1789. 233019362	53 .7568525	**24,000**
TLBO	1625.443000	1797.707980	2096.801270	–	25,000
ABC	**1625.442760**	1861.554000	2144.836000	–	25,000
Rank-iMDDE	1625.460142	1724.727935	1894.734127	–	25,000
MMDE	1638.403234	1759.103885	2553.358476	–	25,000

3.5 Conclusion

This chapter presents a new version of the DE algorithm called MADE for solving the deterministic mechanical optimization problems with continuous design variables. The proposed MADE is based on two improvements including the self-adaptive mechanism to update the values of mutation and crossover parameters, and the feasibility rules for the selection step. This helps the developed approach increase the search capability of the basic DE and acquire a better convergence rate.

The performance of MADE has been verified through four engineering examples. As shown in Tables 3.2 and 3.3, the MADE is successfully adapted to optimize the several design problems with high-quality solutions and robustness. According to the statistical analysis illustrated in Tables 3.4 to 3.7, it is concluded that the MADE is a very competitive approach when compared with other recently published optimizers such as DSS-MDE, DELC, COMDE, WCA, rank-iMDDE, εDE-LS, AMDE, IGMM, SSBSA, MDDE, SSO-C, TLBO, ABC, and NDE. In addition, from the convergence histories shown in Figs 3.5, 3.7, 3.9 and 3.11, it can be easily seen that MADE have detected best solutions for the four optimization problems in early generations. This demonstrates that with two proper improvements, the developed MADE is efficient, robust, and can be considered as a competent optimization tool to deal with the challenging problems in the real mechanical engineering applications. In the next chapter, the MADE is extended to optimize the design of disc cam mechanism where two popular types of follower system are investigated.

Chapter 4

Optimization of Cam Mechanisms Using Metaheuristics

4.1 Introduction

The problem of cam design optimization, as pertaining to cam mechanisms with translating roller and flat-face followers, is handled in this chapter. The problem addressed here is solved using the developed MADE and three other metaheuristics, namely, Grey Wolf Optimizer (GWO) (Mirjalili et al. 2014), Whale Optimization Algorithm (WOA) (Mirjalili and Lewis 2016), and Sine-Cosine Algorithm (SCA) (Mirjalili 2016).

In the first application, the optimal design of disc cam mechanism with eccentric roller follower translation is performed. The optimization procedure is developed for three objectives: minimizing the cam size, maximizing the mechanism efficiency, and maximizing the cam mechanical resistance. To enhance the design quality of the mechanism in the optimization process, more geometric parameters and more design constraints are included in the problem formulation.

The second application deals with the optimization of disc cam mechanism with flat-face follower translation considering several laws of the follower motion. According to the optimization process, the objective is to minimize the size of the mechanism under a number of constraints regarding the performance requirements as well as geometric restrictions. A demonstrative example evaluating the proposed design methodology and showing the applicability of the algorithms is presented for each type of mechanism.

4.2 Metaheuristics Description

The first section of this chapter provides a short description of the algorithms employed to optimize the cam design problems, GWO, WOA, and SCA. For full details about these methods, interested readers can refer to their corresponding literature.

4.2.1 Grey Wolf Optimizer (GWO)

The GWO algorithm has been developed by Mirjalili et al. (2014) based on emulating the social hierarchy and hunting behavior of grey wolves in nature. Like other metaheuristics, this algorithm starts the search process by creating a set of random candidate solutions. During the optimization, the three best candidate solutions are saved and considered as alpha, beta, and delta wolves, who take the lead toward to promising regions of the search space. The rest of grey wolves are assumed as omega and required to encircle alpha, beta, and delta with the aim to find better solutions. The grey wolf hunting comprises three phases (Muro et al. 2011): (1) tracking, chasing and approaching the prey, (2) pursuing, encircling and harassing the prey

until it stops moving, and (3) attacking the prey.

4.2.2 Whale Optimization Algorithm (WOA)

The WOA is one of the recent swarm intelligence techniques introduced by Mirjalili and Lewis (2016) to optimize engineering design problems. This algorithm mimics the hunting strategy of humpback whales in sea. The humpback whales prefer to hunt school of krill or small fishes near the surface. This foraging is accomplished by swimming around the prey within a shrinking circle and creating distinctive bubbles along a circle or '9'-shaped path. In addition to the initialization phase, the WOA involves the following: (1) encircling prey, (2) spiral bubble-net attacking method, and (3) search for prey.

4.2.3 Sine-Cosine Algorithm (SCA)

This is another recent metaheuristic proposed by Mirjalili (2016) for solving constrained optimization problems. The basic idea is to simulate the mathematical behaviors of trigonometric sine and cosine functions. The SCA algorithm starts the search process by generating several random solutions. Then, the algorithm stores the better solution obtained so far, denotes it as the destination point, and updates the other solutions to create new ones according to sine and cosine functions. Finally, the optimization procedure is stopped when the maximum number of iterations is satisfied.

4.3 Optimum Design of Cam-Roller Follower Mechanism

A schematic representation of a disc cam mechanism with offset translating roller follower is shown in Fig. 4.1. The cam is supposed to rotate with a constant angular velocity ω_c. The translating roller follower consists of a follower, constrained to move in a straight line, with a roller attached to its extremity by means of a pin. Thus, as the cam rotates, the roller rolls on the cam surface and causes the follower to translate. The spring is assumed to have a constant elastic ratio k_s with an initial compression δ_s to ensure the return motion of the follower. The cam profile is determined here considering the kinematical and dynamical requirements of the system.

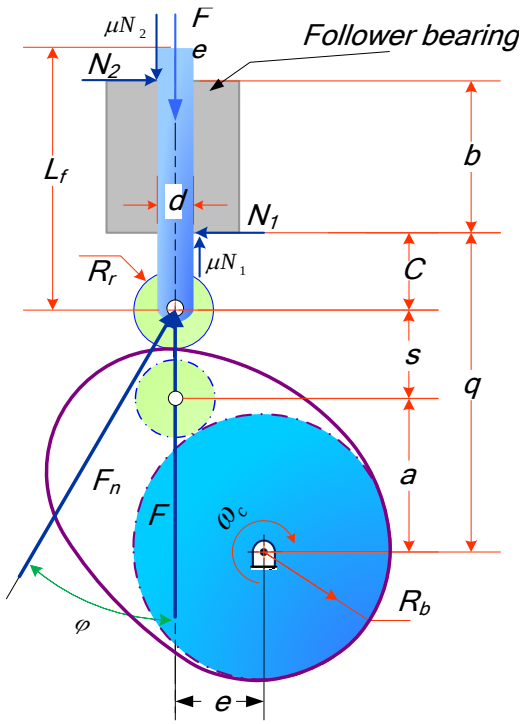

Fig. 4.1 Cam mechanism with offset translating roller follower.

4.3.1 Design Optimization Procedure

The optimization of cam-roller follower mechanism has been extensively reported in the literature. According to previous studies (Yu and Lee 1998; Tsiafis et al. 2009; Flores 2013), the optimum design of this mechanism can be achieved by considering three major parameters that affect the cam design process, namely the base circle radius of the cam R_b, the roller radius R_r and the offset of the follower e. However, it is of great importance to consider other parameters that may improve the system performance. Particularly, those associated with the geometric elements of the mechanism such as the cam thickness, the distance between the cam center and the follower bearing, and the length of follower bearing.

Consequently, the main task is to propose a global optimization procedure by taking into account additional geometric parameters that influence the design quality of the cam mechanism. The optimization problem is formulated as a multi-objective while observing several design constraints. In the following, the objective functions, constraints and design variables will be detailed.

4.3.1.1 Objective functions

The optimization problem is simultaneously investigated for three objectives among them minimum congestion, maximum efficiency, and maximum strength resistance of the cam.

The first goal is the cam size minimization, which is defined according to the base circle radius R_b and thickness of the cam t_c.

$$f_1 = R_b + t_c \tag{4.1}$$

The second objective is to reduce the maximum input torque required to drive the cam T_{cam}, which is directly decreasing the cost of performance.

$$f_2 = T_{cam} = F \times s' \tag{4.2}$$

The last objective is to minimize the maximum contact stress σ_{Hmax} between the cam and the roller follower, which is directly decreasing the cost of maintenance.

$$f_3 = \sigma_{Hmax} = 0.564\sqrt{\frac{F_n \times (R_b + R_r)}{t_c \times (R_b . R_r) \times \left[(1-\upsilon_1{}^2)/E_1 + (1-\upsilon_2{}^2)/E_2\right]}} \tag{4.3}$$

4.3.1.2 Constraints

The above objective functions are subjected to ten design constraints. In this subsection, each constraint is given in detail.

- To simplify the mechanism assembly, the first two constraints are specified by the following constructive conditions (Fig. 4.1):

$$g_1 = e - R_r \geq 0 \tag{4.4}$$

$$g_2 = R_b - e \geq 0 \tag{4.5}$$

- To ensure that the mechanism is operated correctly, during the high dwell of the follower, the roller must not touch the follower bearing (Fig. 4.1). So, the following constraint should be added to avoid the contact:

$$g_3 = q - \alpha - h_f - R_r \geq 0 \tag{4.6}$$

- On the other hand, during the low dwell, the follower level should not be lower than the level of bearing to avoid any contact between the external mass and this latter. Mathematically, the constraint can be formulated as (Hamza et al. 2018):

$$g_4 = L_f - (q - \alpha) - b \geq 0 \tag{4.7}$$

where h_f is the lift of follower, and L_f is its length.

- In order to guarantee the proper operation of the mechanism, two constraints are imposed

on the pressure angle. These are the maximum allowed values for the rise and return periods (Flores 2013):

$$g_5 = 30° - \max\left|\varphi_{Rise}\right| \geq 0 \tag{4.8}$$

$$g_6 = 45° - \max\left|\varphi_{Return}\right| \geq 0 \tag{4.9}$$

- To avoid undercutting as well as to ensure the desired movement of the mechanism, two other constraints are imposed on the curvature radius of the pitch curve ρ. When the cam is on the convex part, the minimum positive radius of curvature ρ_{min} should be greater or equal to the roller radius R_r (Chen 1982). When the cam is on the concave part, the absolute value of the minimum curvature radius $|\rho_{min}|$ should be too greater than R_r. (Norton 2002). Thus, the two constraints are written as the following:

  For $\rho > 0$

$$g_7 = \rho_{\min} - R_r \geq 0 \tag{4.10}$$

  For $\rho < 0$

$$g_8 = \left|\rho_{\min}\right| - R_r - r_c \geq 0 \tag{4.11}$$

where r_c is a positive constant to control the variation of the curvature radius for the concave part of the cam.

- To ensure the mechanical resistance of the cam, the maximum contact stress $\sigma_{H\max}$ should be less or equal to the permissible value σ_{Hp}. Mathematically, the constraint is expressed as:

$$g_9 = \sigma_{Hp} - \sigma_{H\max} \geq 0 \tag{4.12}$$

- Regarding the mechanical efficiency of the system η, the power transmission from the cam to the follower should be done with a minimum loss of energy, mainly due to friction and pressure angle. Thereby, the constraint on the minimal limit of energy loss is established as follows:

$$g_{10} = \eta_{\min} - 0.90 \geq 0 \tag{4.13}$$

4.3.1.3 Design variables

From the problem formulation, it is clear that the design optimization of the cam mechanism is affected by the geometric parameters proposed previously, which are conflicting with each other. When the cam thickness t_c is increased, the resistance of the cam is improved (third objective) due to the direct reducing in the contact stress. But at the same time, the cam size

becomes greater which does not serve the first objective. It is then necessary to select an optimum value of this parameter. Also, the reduction of the distance q allows the decrease of the input torque T_{cam} by increasing the mechanical efficiency η. It means that we play on the second objective, but at the same time the constraint g_3 should be respected. On the other hand, the length of the follower bearing b has a certain influence on the input torque and on the constraint g_4. In addition, the two latter parameters have a direct influence on the normal force F_n and thus affecting the contact stress $\sigma_{H\max}$ (third objective).

Based on the above analysis, the final optimization model of the cam mechanism design is developed for six variables. They are the cam base circle radius R_b, roller radius R_r, follower offset e, cam thickness t_c, distance between the cam center and the follower bearing q, and follower bearing length b. All the design variables are continuous.

Thus, to conclude, the resulting mathematical formulation of the optimization problem can be summarized as:

$$\textit{Find} \quad y = \{R_b,\ R_r,\ e,\ t_c,\ q,\ b\}$$

$$\textit{Minimize} \quad \begin{cases} f_1(y) = R_b + t_c \\ f_2(y) = F \times s' \\ f_3(y) = \sigma_{H\max} \end{cases} \tag{4.14}$$

$$\textit{Subject to:} \quad \begin{cases} g_1(y) = e - R_r \geq 0 \\ g_2(y) = R_b - e \geq 0 \\ g_3(y) = q - \alpha - h_f - R_g \geq 0 \\ g_4(y) = L_f - (q - \alpha) - b \geq 0 \\ g_5(y) = 30° - \max|\varphi_{Rise}| \geq 0 \\ g_6(y) = 45° - \max|\varphi_{Return}| \geq 0 \\ \textit{For} \quad \rho \geq 0 \quad g_7(y) = \rho_{\min} - R_r \geq 0 \\ \textit{For} \quad \rho < 0 \quad g_8(y) = |\rho_{\min}| - R_r - r_c \geq 0 \\ g_9(y) = \sigma_{Hp} - \sigma_{H\max} \geq 0 \\ g_{10}(y) = \eta_{\min} - 0.90 \geq 0 \end{cases} \tag{4.15}$$

4.3.2 A Practical Design Example

The introduced design methodology is applied and evaluated by providing a demonstrative application example. Initially, the length of the follower L_f, its diameter d_f and its mass M_f are defined under the resistance conditions which must be verified to the following compressive and buckling solicitations:

$$\begin{cases} \sigma_{c\max} \le R_e \\ R_e \le \sigma_b \end{cases} \tag{4.16}$$

where $\sigma_{c\max}$ is the maximum compressive stress, σ_b is the buckling critical limit, and R_e is the elastic limit of the follower material.

The input data for the follower and the parameters of case study example are presented in Table 4.1 and Table 4.2, respectively. In addition, by following the same methodology as in (Halicioglu et al. 2017; Halicioglu et al. 2018; Pedrammehr et al. 2018), the kinematic analyses of the follower motion such as displacement, velocity, and acceleration are presented in Figs. 4.2, 4.3, and 4.4 respectively. Moreover, the dynamic analysis including the external force, inertial force, spring force and total force acting on the follower is given in Fig. 4.5. Assuming the simple harmonic motion SHM of the type rise-dwell-return-dwell RDRD, the motion kinematics are given by Eqs. 4.17, 4.18, and 4.19 (Rothbart and Klipp 2004):

$$s = \frac{h}{2}\left(1-\cos\left(\pi\frac{\theta}{\theta_{Rise}}\right)\right) \tag{4.17}$$

$$s' = \left(\frac{h}{2}\cdot\frac{\pi}{\theta_{Rise}}\right)\cdot\left(\sin\left(\pi\frac{\theta}{\theta_{Rise}}\right)\right) \tag{4.18}$$

$$s'' = \left(\frac{h}{2}\cdot\frac{\pi^2}{\theta_{Rise}^2}\right)\cdot\left(\cos\left(\pi\frac{\theta}{\theta_{Rise}}\right)\right) \tag{4.19}$$

where θ is the cam rotation angle and θ_{Rise} is the rise period angle. The follower characteristics are calculated for 60° rise, 130° high dwell, 140° returns, 30° low dwell, follower lift h_f = 20 mm, and cam speed ω_c = 2 rad/sec.

From Figs. 4.3 and 4.4, it is observed that the dwell periods have always zero velocity and zero acceleration. During the rise and the return periods, the follower velocity follows a sine function and its peak values are respectively 60 mm/sec and 25.72 mm/sec. The follower acceleration follows a cosine function and its peak values are respectively 360 mm/sec^2 and

66.12 mm/sec^2. It can then be deduced that the motion law considered in this study provides an acceleration curve with finite values at the rise and the return periods, which leads to reduce the amplitude of the inertia force applied on the follower, as can be seen in Fig. 4.5. On the other hand, the spring force, which is directly related to the follower displacement, has the major contribution on the total force.

Table 4.1 Input data of the follower.

Input data	**Values**
Material density (Kg/m^3)	8027
Material elastic limit R_e(Mpa)	170
Inertial moment (mm^4)	$\pi . d^4/64$
Diameter d_f (mm)	10
Length L_f (mm)	80
Mass M_f(Kg)	50.183×10^{-3}

Table 4.2 Input parameters of the case study example.

Input data	**Values**
Cam module of elasticity E_1 (Mpa)	2.1×10^5
Follower module of elasticity E_2 (Mpa)	2×10^5
Cam Poisson's ratio υ_1	0.28
Follower Poisson's ratio υ_2	0.265
Permissible contact stress σ_{Hp}(Mpa)	235
Friction coefficient of follower /bearing μ	0.1
Spring rate k_s (N/mm)	1.2
Spring initial deflection δ_s (mm)	8
Curvature radius constant r_c (mm)	10
External force F_e(N)	30

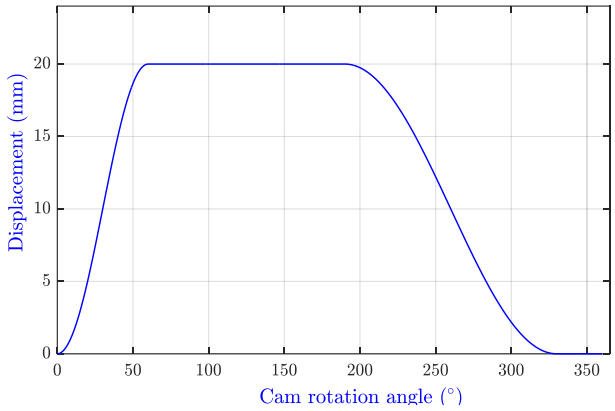

Fig. 4.2 Displacement diagram of the follower motion.

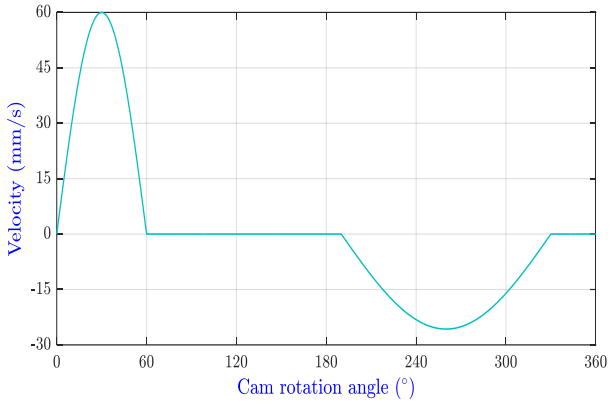

Fig. 4.3 Velocity diagram of the follower motion.

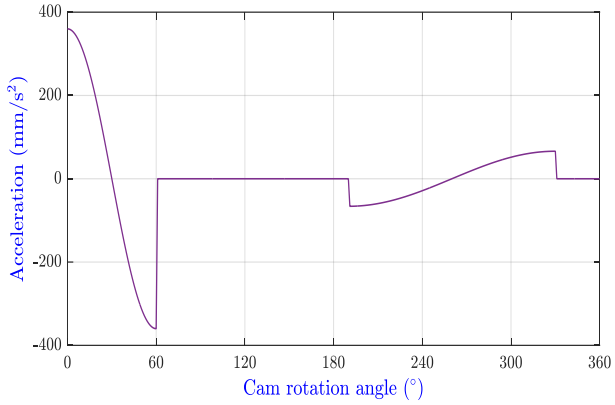

Fig. 4.4 Acceleration diagram of the follower motion.

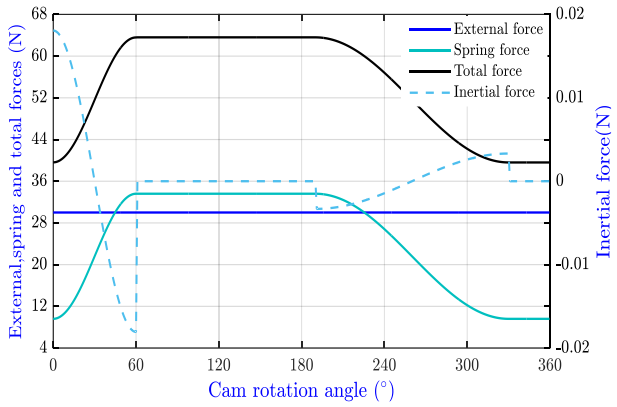

Fig. 4.5 Evolution of external, inertial, spring, and total forces respect to cam rotation angle.

4.3.2.1 Results and discussions

The cam mechanism with offset roller follower translation must be designed for minimum congestion, maximum efficiency, and maximum strength resistance of the cam. The above multi-objective optimization problem involves six continuous design variables and ten inequalities constraints, two linear and eight nonlinear. The complexity of the problem arises from the non-linear interactions of the six design variables in the objective functions and the constraints. The upper and the lower variables limits are: $20 \le R_b \le 60,\ \ 0 \le R_r \le 20,\ \ 0 \le e \le 20,\ \ 0 \le t_c \le 20,\ \ 50 \le q \le 130,\ \ 25 \le b \le 55.$

In order to handle this multi-objective problem, we use firstly the weighted sum method presented in Chapter 1; the multi-objective formulation is converted into a single-objective one by using the weighting factors. After several tests, the factors are chosen in the present example as, w_1=0.8, w_2=0.1, and w_3=0.1. Hence, the objective function, has to be minimized, is established as follows:

$$f(y) = w_1 \left(R_b + t_c \right) + w_2 \cdot T_{cam} + w_3 \cdot \sigma_{H\max} \tag{4.20}$$

Four recent algorithms are used for solving the optimization problem including MADE, WOA, GWO, and SCA. For the specific parameters of WOA, GWO, and SCA, we conserve the similar values suggested by the authors as in the original versions. For the specific parameters of MADE version, please refer to our article (Hamza et al. 2018). In order to assess the quality of the results and the robustness of the utilized algorithms, the whole metaheuristics are run 25 independent times with Np = 20 and T_{max}= 600.

The best optimal solutions of the problem obtained by the compared algorithms are given in Table 4.3. The statistical results including the best, mean, and worst solutions as well as the standard deviation are also tabulated in Table 4.4. As it can be observed from Table 4.3, the four optimizers can reach the feasible solutions for all runs. By providing the lower fitness value of 217.70907431, MADE performed better than other here utilized algorithms. The best solution given by MADE is {28.633568856151, 9.3006758804433, 9.3006758804458, 9.8395981706191, 67.0770861444, 48.6993241195}. WOA can reach good results compared with GWO, it is slightly worse than MADE. In contrast, the SCA approach is not able to find the near optimal solution, where its best solution is about 0.80 % greater than those obtained by the other algorithms.

According to the statistical analysis presented in Table 4.4, MADE is the best algorithm because of the lowest values of mean, worst, and SD. Whereas SCA is the weakest algorithm in optimizing the cam design problem with the highest solutions of the mean (227.5906), worst (236.5448), and SD (6.4421E+00). GWO with lower mean, worst, and SD values of 217.8324, 218.0257, and 8.0349E-02, respectively, shows more uniform performance rather than WOA.

Moreover, the convergence graphs of the best fitness value for the four algorithms are given in Fig. 4.6. From the figure, it is visible that WOA can converge to the global solution faster than the compared algorithms where its best value is reached in average of 215 iterations. MADE started converging to the final result after about 250 iterations. Fig. 4.6 demonstrates also that GWO achieved the best solution at the end of iterations (580 iterations), while the SCA failed in solving the cam optimization problem and converged to a local optimal solution.

The optimal values of the design parameters obtained by MADE approach are used to plot the evolution of pressure angle, radius of curvature, efficiency, input torque, and contact

stress in function of the cam rotational angle, as shown in Figs. 4.7 to 4.11 respectively. According to Fig. 4.7, it is clear that both values of φ_{Rise} and φ_{Return} are well below the allowable limits 30° and 45° respectively. This is due to the fact of second term of the objective function which indicates that reducing the input torque leads to an increase in the efficiency and a reduction of pressure angles, thereby confirming the desired performance of the mechanism. Fig. 4.8 shows that the minimum values of the curvature radius for convex and concave parts of the optimized cam profile are satisfied (constraints g_7 and g_8 respectively in Table 4.3). Following the same logic, we can deduce from Fig. 4.11 that the large gap between the maximum contact stress applied on the cam and its allowable limit is due to the influence of third term of the objective function, which indicates a good strength of the cam (g_9).

In addition, the risk of the contact between the roller and the follower bearing during the high dwell of the follower is avoided with a safety distance equal to 1.00 mm, (constraint g_3 of Table 4.3). For cons, the value found for the constraint g_4 presents the safety height between the follower and its bearing during the low dwell. Finally, the obtained optimal cam profile is given in Fig. 4.12.

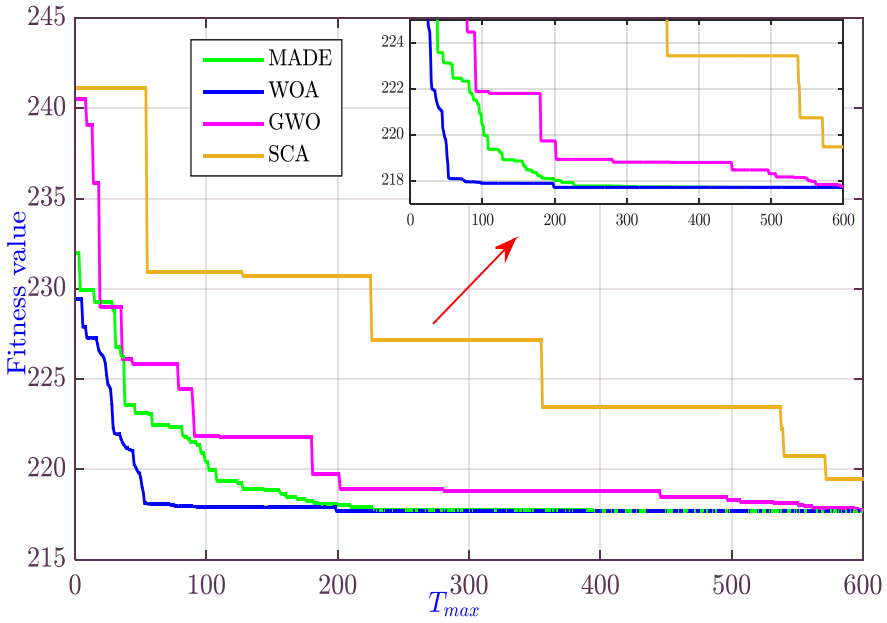

Fig. 4.6 Convergence diagrams of the four algorithms for the cam design example.

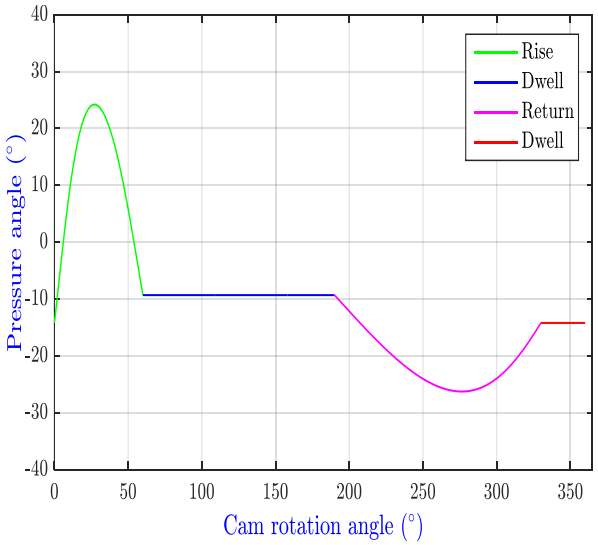

Fig. 4.7 Evolution of the pressure angle.

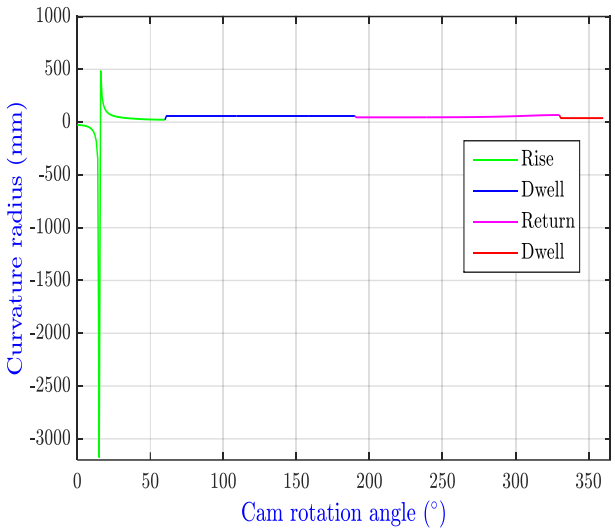

Fig. 4.8 Evolution of the curvature radius.

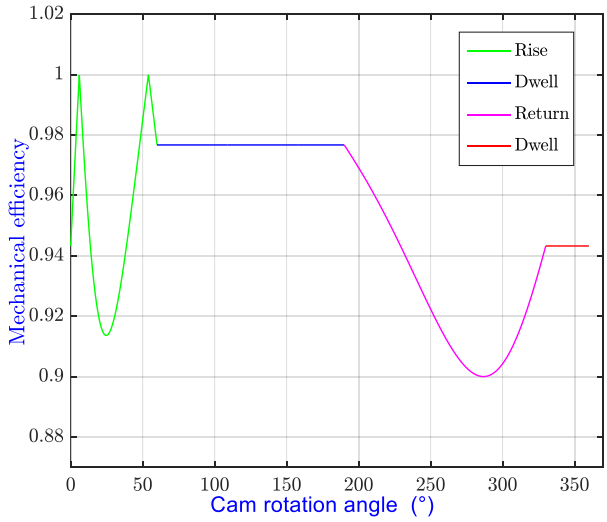

Fig. 4.9 Evolution of the mechanical efficiency.

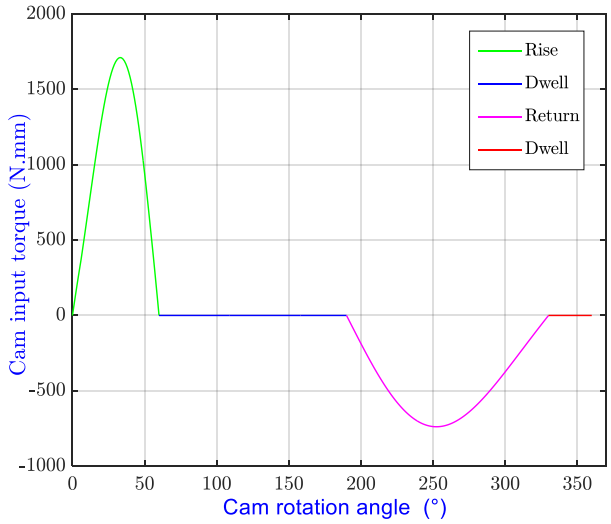

Fig. 4.10 Evolution of the cam input torque.

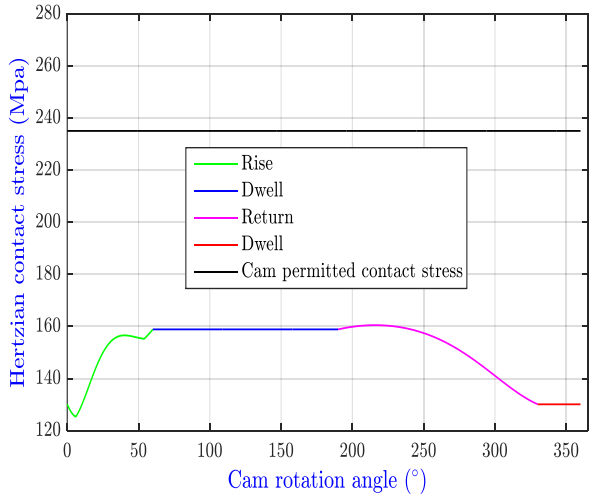

Fig. 4.11 Evolution of the Hertzian contact stress.

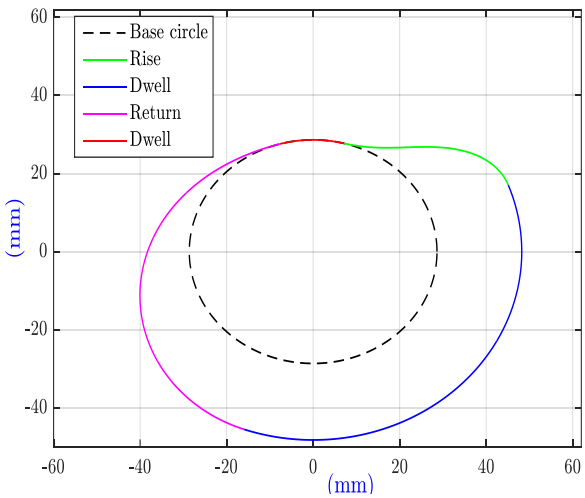

Fig. 4.12 Optimized cam profile.

Table 4.3 Global optimal results of the cam-roller follower mechanism.

Variables	MADE	WOA	GWO	SCA
R_b (mm)	28.633568	28.822083	29.179371	33.091260
R_r (mm)	9.3006758	9.3767281	9.4875717	9.9269133
e (mm)	9.3006758	9.3767282	9.5149594	10.297035
t_c (mm)	9.8395981	9.6887704	67.970099	73.039466
q (mm)	67.077086	67.406800	48.481906	45.170925
b (mm)	48.699324	48.621652	9.7468829	10.524811
g_1	2.4797E-12	9.8946E-08	6.3408e+00	8.9329e+00
g_2	1.9332E+01	1.9445E+01	1.8885e+01	2.0162e+01
g_3	1.0000E+00	1.0002E+00	8.9333e-06	6.3792e-04
g_4	1.0003E+00	1.0022E+00	7.8335e+01	8.9085e+01
g_5	5.7885E+00	5.9881E+00	4.5605e-03	3.4493e-01
g_6	1.8746E+01	1.8799E+01	2.5961e-02	2.5572e+00
g_7	1.3387E+01	1.3478E+01	3.6636e+00	6.0261e+00
g_8	8.3376E+00	3.4784E+00	1.3664e+01	1.6026e+01
g_9	7.7566E+01	7.6949E+01	2.7388e-02	3.7012e-01
g_{10}	2.0761E-14	9.7436E-09	1.9664e+01	2.2794e+01
f_{min}	**217.70907**	217.71152	217.74125	219.47174

Table 4.4 Statistical results of the four algorithms for the cam design example.

Algorithm	Best	Mean	Worst	SD
AMDE	**217.70907431416**	**217.709074327487**	**217.709074371881**	**1.0809E-08**
WOA	217.71152132005	218.15852504050	219.75563069304	4.5165E-01
GWO	217.74125905577	**217.83240028686**	**218.02570172087**	**8.0349E-02**
SCA	219.47174900595	227.59061893368	236.54489741682	6.4421E+00

The second method used to solve this multi-objective problem is the Pareto optimization technique. The well-known NSGA-II (Deb et al. 2002) is employed with a population size of 100 and a maximum iterations number of 300. Fig. 4.13 displays the non-dominated solutions obtained from the optimization procedure. Some of the Paretian points and the corresponding objective functions values are presented in Table 4.5. As it can be seen from the table, the values of the six design variables are varied according to the contribution of each objective. This provides multitude solutions and thus the designer can closely analyze the appropriate decisions for the comparison and the choice.

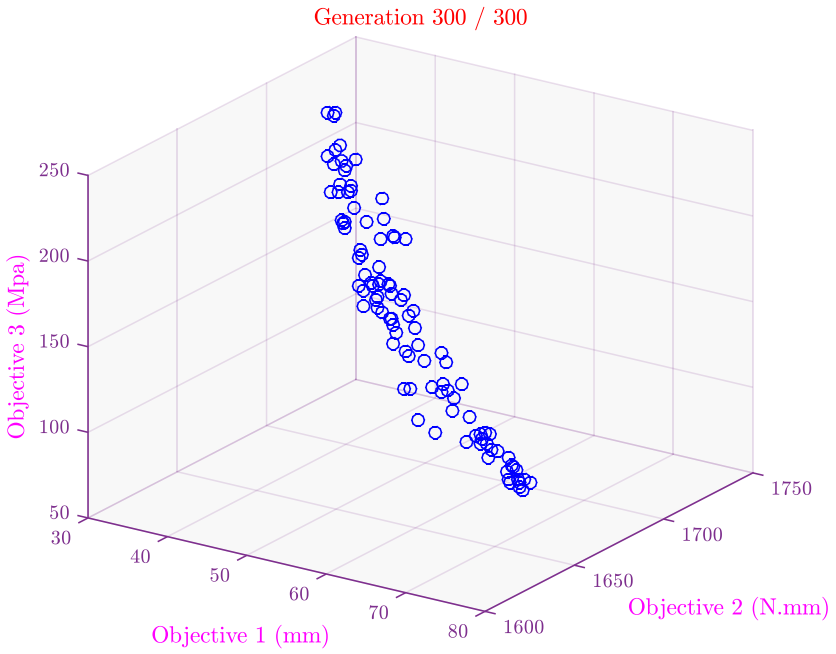

Fig. 4.13 Non-dominated solutions obtained by NSGA-II for the cam design example.

Table 4.5 Some of the Pareto optimal solutions for the cam design example.

Variables	**Solution 1**	**Solution 2**	**Solution 3**	**Solution 4**	**Solution 5**
R_b (mm)	25.0752	46.8010	36.7350	56.6534	39.1237
R_r (mm)	07.7768	13.5756	12.2634	13.0410	09.1789
e (mm)	07.7768	15.9022	12.2634	20.0000	13.9578
t_c (mm)	06.0540	16.5936	12.9015	18.7434	06.3758
q (mm)	60.6951	92.8204	80.7023	100.8042	76.4209
b (mm)	50.2232	44.4244	45.7366	44.9590	48.8211
f_1 (mm)	31.1291	63.3946	49.6365	75.3968	45.4995
f_2 (N.mm)	1.7311E+03	1.6508E+03	1.6809E+03	1.6254E+03	1.6640E+03
f_3 (Mpa)	2.1794E+02	9.9561E+01	1.2041E+02	9.3717E+01	1.9127E+02

4.4 Optimum Design of Cam Flat-Faced Follower Mechanism

The design optimization problem of cam mechanism with translating flat-face follower is investigated in this section. The schematic view of the mechanism is presented in Fig. 4.14. The cam's position, characterized by the angle of rotation θ, is defined as the input motion of the system while the position of the follower, given by the straight line $s(\theta)$, is the output motion. The contact between the cam and the follower is shown theoretically by a linear contact, along the face of the follower, but practically is a surface contact.

In the cam synthesis procedure, the suitable choice of the law to describe the follower motion is an influential factor on the design quality. The present design method is introduced to optimize the size of the mechanism by properly selecting the type of follower motion. There are four motion laws considered in this study including two basic curves and two polynomial functions. The proposed approach considers the main geometric parameters of the mechanism as design variables and is based on satisfying multiple constraints like cam pressure angle, curvature radius and other geometric restrictions. The mathematical formulation of the optimization problem is detailed bellow. It should be noted that the problem is developed at the kinematics design level only.

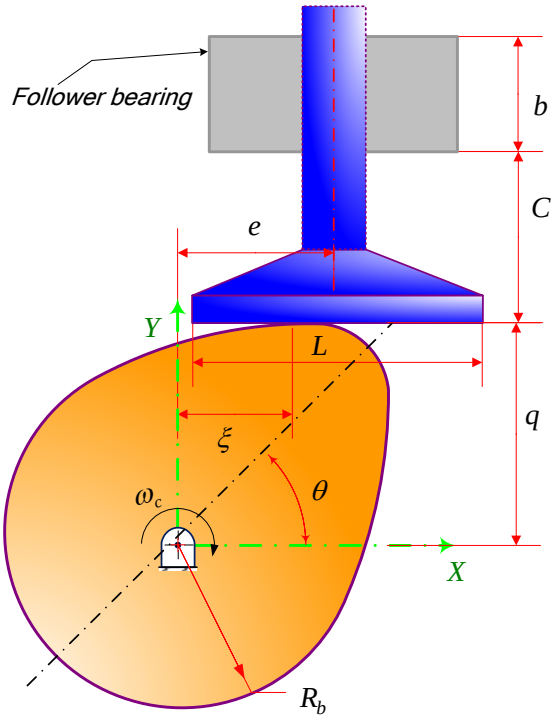

Fig. 4.14 Cam mechanism with translating flat-face follower.

4.4.1 Design Optimization Procedure

The objective function established in the current section considers the size minimization of the mechanism shown in Fig 4.14. It is known that the size of this system can be varied by the base circle radius of the cam R_b according to the axis Y and the length of the follower face L according to the axis X. Therefore, the objective function can be written mathematically as:

$$f(y) = (R_b + L) \tag{4.21}$$

The design parameters, aimed to be optimized, include the base circle radius of the cam R_b, length of the follower face L, and the follower eccentricity e as shown in Fig. 4.14. The following functional constraints are included during the optimization:

- To prevent jamming in the guide, the maximum pressure angle on the cam profile should be less than the permissible value (Tsiafis et al. 2013):

$$g_1 = 30° - \max|\varphi| \geq 0 \tag{4.22}$$

- The radius of curvature is an important factor that affects the cam mechanism size. To ensure that the mechanism is operated without undercutting and cusp, the minimum curvature radius should always be positive (Rothbart and Klipp 2004):

$$g_2 = \rho_{\min} \geq 0 \tag{4.23}$$

- To ensure good working conditions of the system, the following geometric constraints must be respected (Chen 1982):

$$g_3 = b + \mu\mu_0(b + 2C) - 2\mu\xi \geq 0 \tag{4.24}$$

$$g_4 = \frac{L}{2} - \xi \geq 0 \tag{4.25}$$

$$g_5 = \frac{L}{2} - e \geq 0 \tag{4.26}$$

The distance ξ as shown in Fig. 4.14 is calculated with the following relation (Tsiafis et al. 2013):

$$\xi = \sqrt{(x'^2 + y'^2) - (R_b + s)^2} \tag{4.27}$$

where $x'(\theta)$ and $y'(\theta)$ are the coordinates of the cam profile.

As a result, the optimization procedure presented above leads to a problem that can be summarized as follows:

$$\begin{aligned} &\textit{Find} && y=\{R_b,\ L,\ e\} \\ &\textit{Minimize} && f(y)=(R_b+L) \end{aligned} \tag{4.28}$$

$$\textit{Subject to:} \quad \begin{cases} g_1(y)=30^\circ-\max|\varphi|\geq 0 \\ g_2(y)=\rho_{\min}\geq 0 \\ g_3(y)=b+\mu\mu_0(b+2C)-2\mu\xi\geq 0 \\ g_4(y)=L/2-\xi\geq 0 \\ g_5(y)=L/2-e\geq 0 \end{cases} \tag{4.29}$$

4.4.2 A Practical Design Example

An application example is presented and used to demonstrate the optimization approach of the cam mechanism. The follower eccentricity is set in this example equal to zero ($e = 0$ mm) and hence, the last constraint g_5 is not enforced. The follower motion laws under the optimization are cycloidal, modified sinusoidal acceleration (modified sine), 3-4-5 polynomial, and 4-5-6-7 polynomial. For each motion curve, the above optimization problem is solved and the results are discussed and compared.

The input data for the present design example are given in Table 4.6. The cam angular velocity is supposed to be equal to 1 rad/sec (ω_c= 1 rad/sec). The follower describes a rise of 8 mm during the cam rotation from 0 to 60°. Then, it remains stationary for amplitude of cam rotation angle equal to 130°. The follower returns to its initial position during cam rotation angle equal to 100°. Recently, it remains stationary during the remaining cam rotation. According to the follower characteristics, the kinematic analyses of the four motion laws including the displacement, velocity, acceleration, and jerk are illustrated during the rise period in Figs. 4.15 to 4.18, respectively. For more mathematical details about these types of motion, please refer to the specialized literature such as (Lin et al. 1988; Norton 2004; Rothbart and Klipp 2004).

Table 4.6 Input parameters of the case study example.

Input data	**Values**
Total follower rise h_f (mm)	8
Rise angle: θ_{Rise} (°)	60
High dwell angle: $\theta_{\text{Dwell-H}}$ (°)	130
Return angle: θ_{Return} (°)	100
Low dwell angle: $\theta_{\text{Dwell-L}}$ (°)	70
Guide length: b(mm)	40
Distance q(mm)	70
Friction coefficient of follower/bearing μ	0.1
Friction coefficient of cam/ follower μ_0	0.15

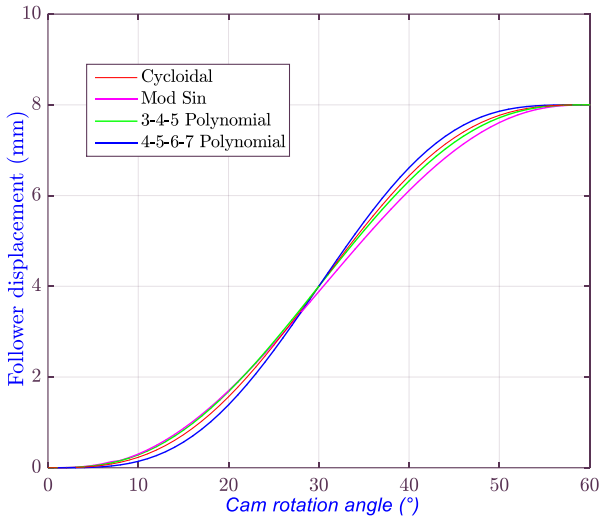

Fig. 4.15 Follower displacement with different motion laws.

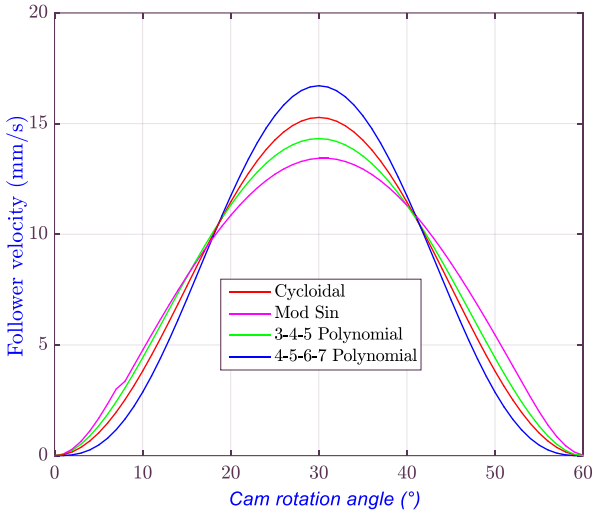

Fig. 4.16 Follower velocity with different motion laws.

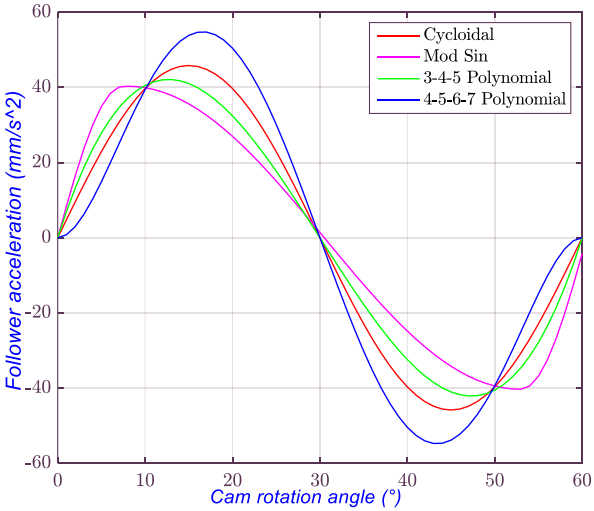

Fig. 4.17 Follower acceleration with different motion laws.

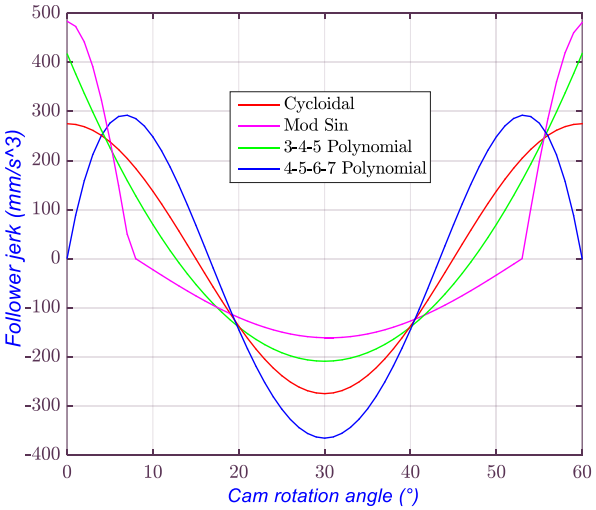

Fig. 4.18 Follower jerk with different motion laws.

4.4.2.1 Results and discussions

The algorithms applied in the first section for optimizing the cam mechanism with roller-follower are now extended to flat-face follower. The parameters' setting of the different algorithms as well as the FEs number are the same as those used in the previous example. The best values of objective function, design variables and constraints for the four motion laws are listed in Table 4.7. Table 4.8 summarizes the statistical results in the form of the best, mean, worst, and SD values. In addition, the convergence plots of the utilized algorithms for the four investigated cases are displayed in Figs. 4.19 to 4.22, respectively.

A. Case 1: Cycloidal motion law

The results obtained in the first case implied that MADE is the best algorithm because of the lower objective value of 71.326916 mm. Moreover, MADE with SD value of 1.450E-14 is the more consistent in solving the cam design optimization problem. GWO by achieving the lowest values of the best (71.327708 mm), mean (71.333626 mm), worst (71.340716 mm), and SD (0.0027433) reached good results when compared with WOA and SCA.

Furthermore, the convergence graphs of the best results shown in Fig. 4.19 demonstrate that WOA and MADE converged to the best solution from the initial iterations, while SCA and GWO did not converge to the final results until the latest iterations.

B. Case 2: Modified sine motion law

In the case of the modified sine motion curve, MADE version is the most effective and robust among the four algorithms based on the lowest values for the best (61.5859074 mm) and SD (7.2519E-15). WOA by the best fitness value of 61.5865665 mm performed better than GWO and SCA, but produced worst results in terms of the mean, worst and SD values.

On the other hand, Fig. 4.20 exhibits that WOA and MADE get close to the final solution faster than the others from the initial iterations. SCA reached its best value in average of 450 iterations, while GWO achieved the near optimal value at the end of iterations.

C. Case 3: 3-4-5 Polynomial motion law

According to the results reported in the third case, MADE and WOA can get the lowest design of 65.5338 mm. However, MADE with the lower SD value of 4.3512E-14 proves more stability than WOA with 0.45465239. GWO by providing the lower value of the mean, worst, and SD is better than WOA and SCA.

The convergence rate plot in Fig. 4.21 is a clear evidence of a fast convergence of MADE rather than other used algorithms. In this case, WOA started converging to the final solution after 160 iterations.

D. Case 4: 4-5-6-7 Polynomial motion law

Concerning the last case, the results collected in Tables 4.7 and 4.8 show that MADE and WOA reached the lowest objective value of 83.2029 mm. Further, MADE by achieving the very small value of SD displayed an excellent performance in terms of robustness. As in the first three cases, SCA performed the weakest record with the highest values of best (83.2459139 mm), mean (83.4002381 mm), and worst (83.4555703 mm).

Convergence rate histories of the final results in Fig. 4.22 display that WOA converged to the best solution faster than other utilized methods. MADE started converging to the final result after 130 iterations. GWO reached the best value in the last iterations whereas SCA converged to its solution from the middle iterations.

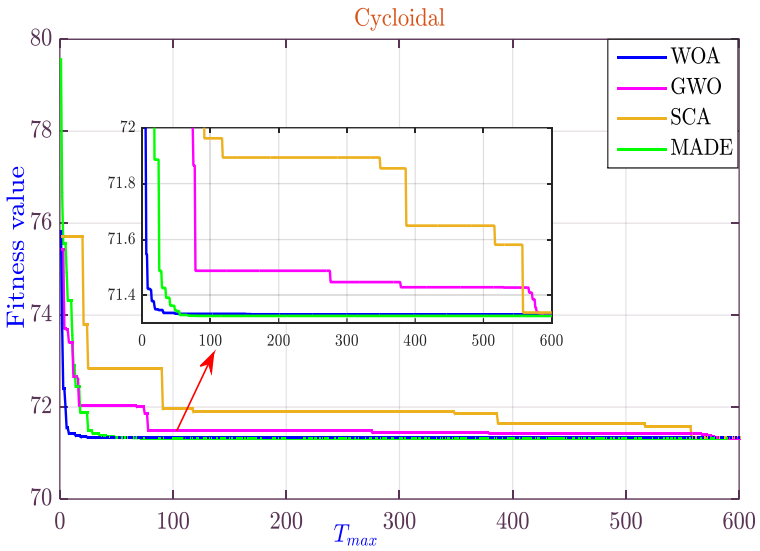

Fig. 4.19 Convergence diagrams of the four algorithms for Case 1.

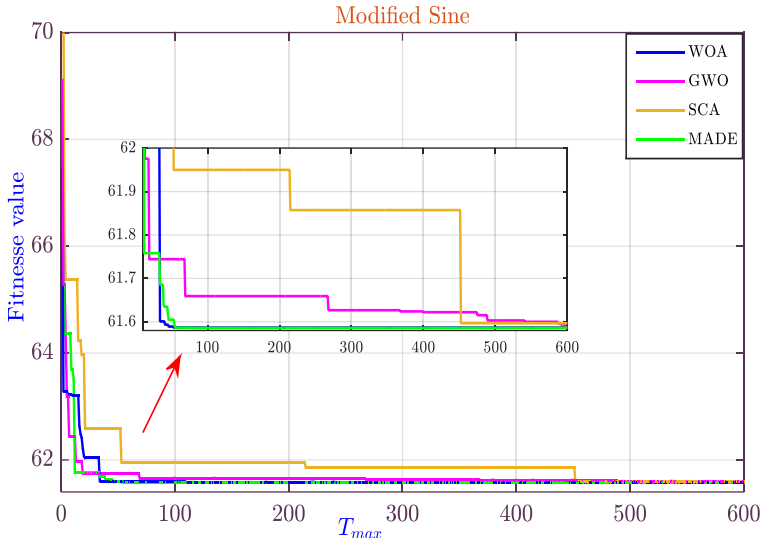

Fig. 4.20 Convergence diagrams of the four algorithms for Case 2.

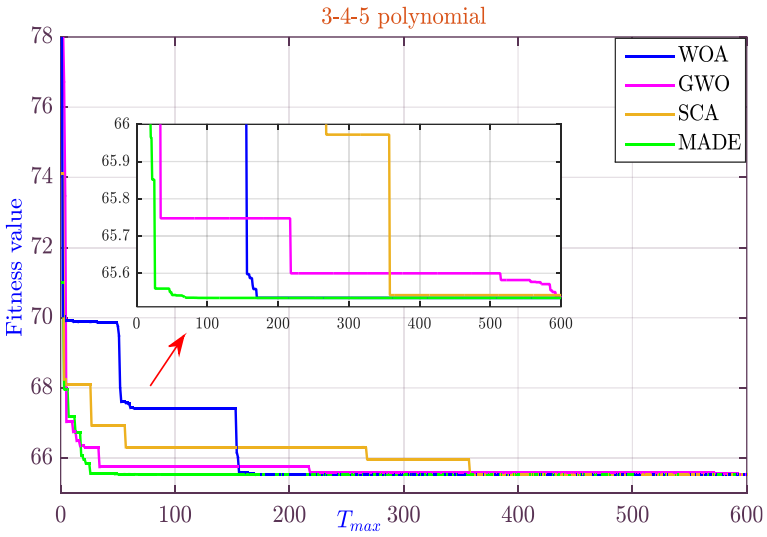

Fig. 4.21 Convergence diagrams of the four algorithms for Case 3.

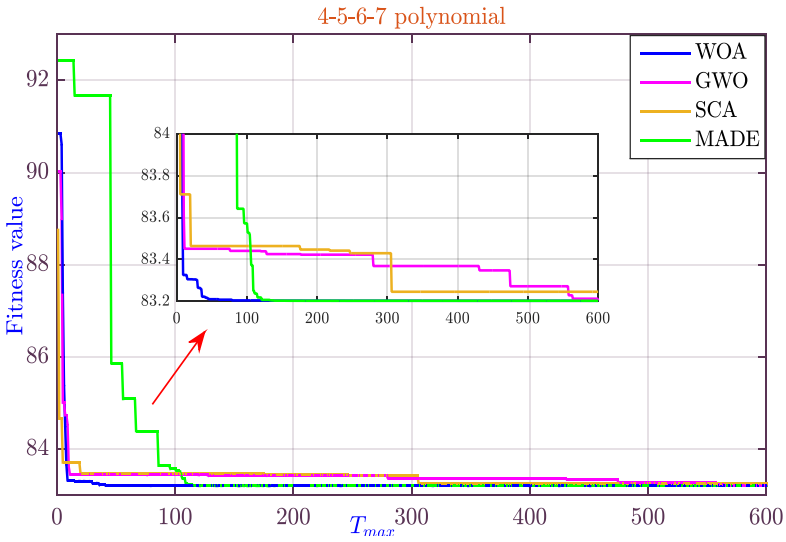

Fig. 4.22 Convergence diagrams of the four algorithms for Case 4.

Table 4.7 Global optimal results of the cam flat-face follower mechanism for the investigated cases.

Variables	**MADE**	**WOA**	**GWO**	**SCA**
		Case 1: Cycloidal		
R_b (mm)	40.769167	40.769167	40.769354	40.773569
L (mm)	30.557749	30.563373	30.558353	30.565275
g_1	1.1100E+01	1.1100E+01	1.1100E+01	1.1101E+01
g_2	2.2058E+00	2.2058E+00	2.2060E+00	2.2102E+00
g_3	3.6787E+01	3.6787E+01	3.6787E+01	3.6787E+01
g_4	1.2434E-14	2.8120E-03	3.0219E-04	3.7634E-03
f (mm)	**71.326916162**	71.3325402684	71.327708255	71.338845205
		Case 2: Modified sine acceleration		
R_b (mm)	34.713430	34.713431	34.714153	34.720352
L (mm)	26.872476	26.873134	26.873112	26.876335
g_1	1.0763E+01	1.0763E+01	1.0763E+01	1.0766E+01
g_2	2.2058E+00	2.2264E+00	2.2272E+00	2.2334E+00
g_3	3.6971E+01	3.6971E+01	3.6971E+01	3.6971E+01
g_4	8.8818E-15	3.2915E-04	3.1777E-04	1.9293E-03
f (mm)	**61.585907403**	61.586565986	61.587265257	61.596688000
		Case 3: 3-4-5 Polynomial		
R_b (mm)	36.885922	36.885922	36.886260	36.892716
L (mm)	28.647889	28.647974	28.648334	28.648570
g_1	1.0623E+01	1.0623E+01	1.0623E+01	1.0626E+01
g_2	2.2168E+00	2.2168E+00	2.2172E+00	2.2236E+00
g_3	3.6861E+01	3.6861E+01	3.6861E+01	3.6861E+01
g_4	0.00	4.2247E-05	2.2224E-04	3.4026E-04
f (mm)	**65.533812169**	**65.533897098**	65.534595180	65.541286470
		Case 4: 4-5-6-7 Polynomial		
R_b (mm)	49.780366	49.780366	49.781949	49.802746
L (mm)	33.422538	33.422559	33.422809	33.443167
g_1	1.2704E+01	1.2704E+01	1.2705E+01	1.2711E+01
g_2	2.1930E+00	2.1930E+00	2.1946E+00	2.2154E+00
g_3	3.6771E+01	3.6771E+01	3.6771E+01	3.6772E+01
g_4	7.1054E-15	1.0601E-05	1.3548E-04	1.0315E-02
f (mm)	**83.202904553**	**83.202926053**	83.204758598	83.245913968

Table 4.8 Statistical results of the four algorithms for the investigated cases.

Algorithm	Best	Mean	Worst	SD
Case 1: Cycloidal				
MADE	**71.326916**	**71.326916**	**71.326916**	**1.450E-14**
WOA	71.332540	71.941615	73.965240	0.7163394
GWO	71.327708	71.333626	71.340716	0.0027433
SCA	71.338845	71.548895	71.748665	0.1121932
Case 2: Modified sine acceleration				
MADE	**61.5859074**	**61.5859074**	**61.5859074**	**7.2519E-15**
WOA	61.5865665	62.0046706	64.3673002	0.57875819
GWO	61.5872653	61.5903237	61.5974044	0.00214746
SCA	61.5966880	61.7183771	61.9174414	0.08449077
Case 3: 3-4-5 Polynomial				
MADE	**65.5338122**	**65.5338122**	**65.5338122**	**4.3512E-14**
WOA	**65.5338971**	65.8581392	67.3068901	0.45465239
GWO	65.5345952	65.5392205	65.5452229	0.00288252
SCA	65.5412865	65.7389642	66.0328109	0.13437887
Case 4: 4-5-6-7 Polynomial				
MADE	**83.2029046**	**83.2029046**	**83.2029046**	**0.00**
WOA	**83.2029261**	83.3265572	83.4953231	0.0957834
GWO	83.2047586	83.2134349	83.2242368	0.0059703
SCA	83.2459139	83.4002381	83.4555703	0.0557051

Now, the results provided by MADE are considered to analyze the motion design. By comparing the solutions obtained in the four cases, the modified sine motion law expresses the best performance based on the lower value of the objective function. The design parameters values recorded by this type of motion are $\{R_b = 34.713430921$ mm, $L = 26.87247648$ mm$\}$, corresponding to $f = 61.585907403$ mm. The constraint violations are [1.0763E+01, 2.2058E+00, 3.6971E+01, 8.8818E-15]. The 3-4-5 polynomial cam profile with the fitness value of 65.533812169 mm performs better than the cycloidal curve with 71.326916162 mm. In contrast, the 4-5-6-7 polynomial cam profile with the fitness value of 83.202904553 mm is the worst motion law in minimizing the size of the cam mechanism.

The modified sine motion law has the lowest amplitude for booth velocity and acceleration (Figs. 4.16 and 4.17), as it provides a good compromise of the motion kinematics. Therefore, it is extensively preferred in the cam design process especially in applications where the cam speed is very high and the follower mass is relatively large

(Norton 2002). These characteristics have demonstrated significantly that the modified sine curve is the appropriate motion law, among the considered types, to optimize the design of the mechanism. Lastly, the evolutions of the pressure angle and curvature radius with the modified sine curve are presented in Figs. 4.23 and 4.24, respectively, to prove the satisfaction of the first two design constraints. The corresponding cam profile is also shown in Fig. 4.25.

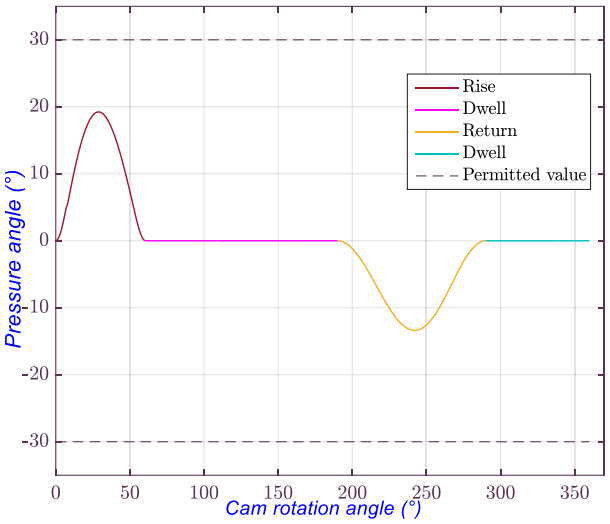

Fig. 4.23 Pressure angle evolution with the modified sine curve.

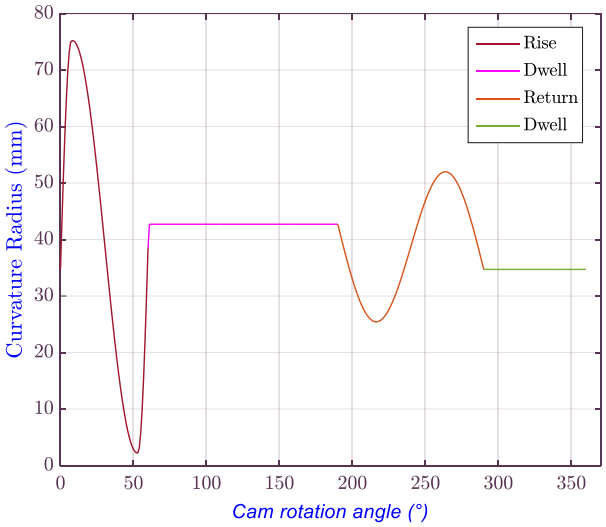

Fig. 4.24 Curvature radius evolution with the modified sine curve.

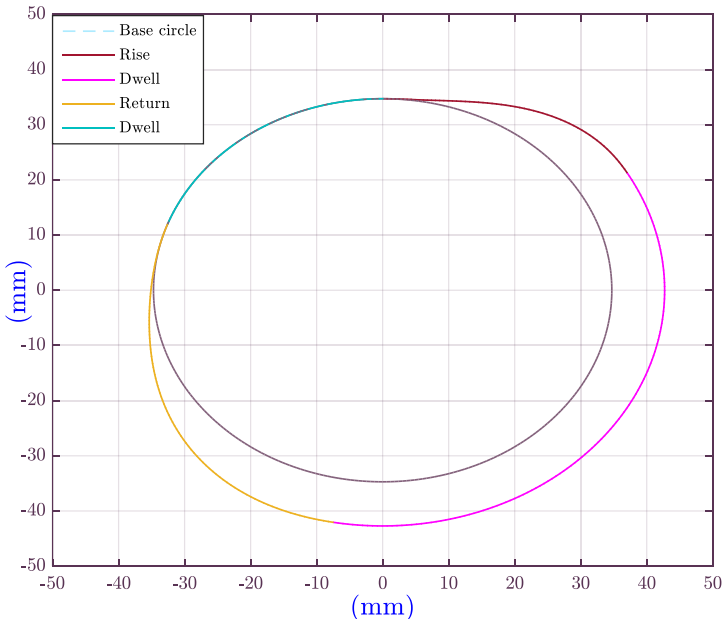

Fig. 4.25 Optimal cam profile obtained with the modified sine curve.

4.5 Conclusion

The present chapter introduces the application of the developed MADE and three recent metaheuristic algorithms (GWO, WOA, and SCA) for a global optimization approach of disc cam mechanisms. In the first problem, a cam mechanism with eccentric roller follower translation has been optimized regarding three objectives: minimum cam size, maximum efficiency, and maximum cam strength resistance. The optimization is subjected to ten constraints and involves six design variables considering the suitable dimensions of the mechanism elements. In order to solve this multi-objective problem, the classical weighted sum method has been adopted where the weighting factors have been chosen in accordance with the importance of each objective. Moreover, instead of providing a single solution, the Pareto optimization approach based on NSGA-II has been employed to give more versatility and flexibility by providing a set of no-dominated solutions. The results found through the design example have showed that the optimum synthesis has been performed by an excellent efficiency and a sufficient durability.

The second problem concerns the optimum design of a cam mechanism with flat-face follower translation in which the effect of four laws of follower motion has been inspected. The design procedure has been established to optimize the size of the mechanism while respecting some relevant constraints related to the cam design process. The follower motion laws considered in study have been cycloidal, modified sine, 3-4-5 polynomial, and 4-5-6-7 polynomial. Based on the final results, the modified sine curve is the best motion law among the four types and can provide a reduction in the objective value of 15.82 %, 06.41 %, and 35.10 % compared with cycloidal, 3-4-5 polynomial and 4-5-6-7 polynomial laws, respectively.

As regards the comparison results of the algorithms applied in solving the cam design optimization problems, it can be deduced that the MADE version is the most effective because of the lowest values for the best solution and standard deviation over all the case studies. WOA is very competitive in solution quality and has showed an evident superiority in terms of convergence speed compared with the other algorithms. However, GWO is better than WOA regarding the values of the mean, worst and standard deviation. On the other hand, the SCA has demonstrated the weakest performance for all cases and can be considered as the worst among the compared algorithms in this study.

Chapter 5

A Novel RBDO Approach

5.1 Introduction

In the majority of cases, practical RBDO problems in mechanical engineering have several computational and modeling challenges; consider multiple conflicting objectives, include various complex constraints on geometry and mechanical resistances, as well as mixed types of design variables (continuous-discrete-integer). This context leaves plenty of room for developing more powerful approaches in the field of RBDO by using accurate optimization algorithms and integrating suitable probabilistic concepts. In the present chapter, an efficient optimization algorithm, hybridizing the developed MADE with the NM local search (Nelder and Mead 1965), is proposed to deal with mechanical RBDO problems.

The RDS concept (Shan and Wang 2008) is firstly employed to convert the RBDO problem into a simple deterministic optimization (SDO) one and the hybrid MADE-NM is then selected as an optimization tool. The efficiency and reliability of the integrated approach, referred as (RDS-MADE-NM), are demonstrated through solving six mechanical problems with different levels of complexities. In addition, an industry case on a specific cylindrical spur gear is studied to verifier the applicability of RDS-MADE-NM to real challenging RBDO problems.

In the remainder of the chapter, the RDS technique is presented in Section 5.2 and followed by the NM algorithm in Section 5.3. The proposed RDS-MADE-NM integrated approach is introduced in Section 5.4 and validated in Section 5.5. A real industry case is investigated in Section 5.6. Finally, some concluding remarks are exposed in Section 5.7.

5.2 Reliable Design Space (RDS) Technique

As mentioned in Chapter 1, the direct solution of RBDO problem (Eq. 1.5) is given by employing two nested optimization loops. The RDS technique has been proposed by Shan and Wang (2008) to remove the inner reliability loops and thus, providing an equivalent deterministic formulation. The main idea is based on the reformulation of the probabilistic constraints defined on the original design space by approximate deterministic ones in the reliable design space. Fig. 5.1 illustrates geometrically the concept of the RDS. For an easy understanding, we assume that an optimization problem contains only one constraint with two variables $X = \{x_1, x_2\}$. When uncertainty is not considered, the feasible design space (FDS) is identified within the global design space by the yellow area and its boundary is determined by the deterministic constraint $(\mathrm{g}\,(x_1, x_1) = 0)$. By considering the uncertainty, the RDS is

separated from the deterministic FDS, as can be seen by the blue area, and its boundary is determined by the probabilistic constraint ($\mathrm{Prob}(\mathrm{g}(d,X) \geq 0) = R^t$).

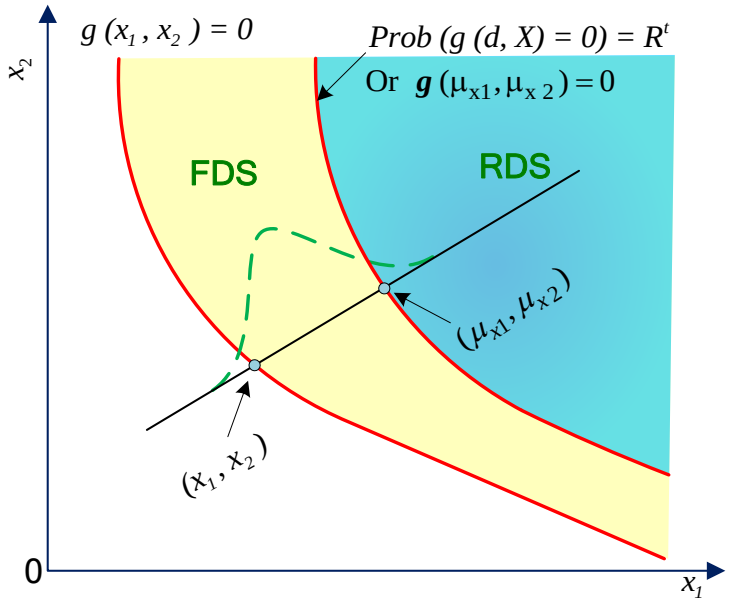

Fig. 5.1 Concept of the reliable design space.

Analytically, the RDS can be denoted by the region of design points whose corresponding inverse MPFPs satisfy the deterministic constraints g_i. In other word, each design point μ_z in the RDS has its inverse MPFP $\boldsymbol{z}$ within the deterministic FDS.

The inverse MPFP $\boldsymbol{z}$ represents the MPFP in the Z space, and its evaluation conventionally requires an iterative procedure during the optimization (Chen et al. 1997; Liang et al. 2008). According to Shan and Wang (2008), the partial derivatives at the current design point μ_z can be employed to approximate the derivatives at its inverse MPFP $\boldsymbol{z}$. Hence, the direct calculation of $\boldsymbol{z}$ at any design point μ_z can be achieved as:

$$\mathbf{z}_j^i = \mu_{zj} - \beta_i^t \sigma_{zj} \alpha_j^i(\mu_z), \qquad i = 1,\ldots,k \text{ and } j = 1,\ldots,Nz \tag{5.1}$$

where μ_z referred as the design point is the mean vector of z, σ_z is the standard deviation vector of z, β^t denotes the target reliability index vector, and $\alpha(\mu_z)$ is the direction cosine:

$$\alpha_j^i(\mu_z) = \frac{\sigma_{zj} \dfrac{\partial g_i(d,\mu_z)}{\partial \mu_{zj}}}{\sqrt{\sum_{q=1}^{Nz} \left(\sigma_{zq} \dfrac{\partial g_i(d,\mu_z)}{\partial \mu_{zq}} \right)^2}} \tag{5.2}$$

Using Eq. 5.1, the reliable design space of the RBDO problem is defined by approximate deterministic constraints $\mathbf{g}_i$ as follows:

$$\mathbf{g}_i(d,\mu_z) = g_i(d,\mathbf{z}^i) = g_i(d,\mu_z - \beta_i^t \times \sigma_z \times \alpha^i(\mu_z)) \geq 0 \tag{5.3}$$

Accordingly, the RBDO problem in Eq.1.5 becomes a SDO problem expressed in the following form:

$$\begin{aligned} &find\ (y = \{d,\mu_x\}) \\ &\min\ f\ (d,\mu_z) \\ &s.t.:\ \mathbf{g}_i\ (d,\mu_z) \geq 0 \qquad i = 1,...,k \\ &y^L \leq y \leq y^U \end{aligned} \tag{5.4}$$

It should be noted that the approximation presented in Eq. 5.1 is only valid for the normal distribution case. For other distributions, the probabilistic transformation (Rosenblatt 1952) is applied to estimate the mean and the standard deviation of the equivalent normal distribution (Haldar and Mahadevan 2000). The pseudocode of the RDS concept is summarized in Algorithm 5.1.

Algorithm 5.1: RDS technique

Input: Number of constraints k, dimension of the random vector Nz, target reliability index vector β^t, mean vector μ_z, and standard deviation vector σ_z.

For $i \coloneqq 1$ to k **do**
  Calculate the partial derivatives of the function $g_i(d,\mu_z)$ with respect to the mean vector μ_z.
  For $j \coloneqq 1$ to Nz **do**
    For each given μ_{zj}, find the corresponding direction cosine $\alpha_j^i(\mu_z)$ using Eq. 5.2.
    Substitute β_i^t,σ_{zj}, and $\alpha_j^i(\mu_z)$ into Eq. 5.1 to obtain the inverse MPFP $\boldsymbol{z}_j^i$.
  End
  For $\boldsymbol{z}^i = \{\boldsymbol{z}_1^i, \boldsymbol{z}_2^i, \dots, \boldsymbol{z}_{Nz}^i\}$, formulate the approximate deterministic constraint $\mathbf{g}_i(d,\mu_z)$ by substituting $\boldsymbol{z}^i$ into the constraint function g_i.
End

Output: The mathematical formulas of approximate deterministic constraints $\mathbf{g}_{i=1,..,k}(d,\mu_z)$.

5.3 Nelder-Mead (NM) Simplex Search Algorithm

The NM simplex search algorithm was originally developed by Nelder and Mead (1965). It is a derivative free method introduced for unconstrained continuous optimization problems. Due to its simple structure and ease of implementation, the NM algorithm has been successfully combined with several metaheuristics to solve different optimization problems in diverse fields (Rajan and Malakar 2015; Liao et al. 2015; Hamid et al. 2016; Moezi et al. 2018; Singh et al. 2018; Xu and Yan 2019; Xu et al. 2019,….).

In this study, the NM technique is used to enhance the local search ability of the MADE algorithm. For each generation and after the mutation and crossover operations, the NM is introduced as local search to replace the worst current solution with the best one. The procedure of the NM method is illustrated in the flowchart presented in Fig. 5.2. According to this figure, the NM contains four operations: reflection, expansion, contraction and shrinkage. It is worth mentioning that the values of the NM control parameters are iteratively updated, during the optimization, according to the method proposed by Xu and Yan (2019).

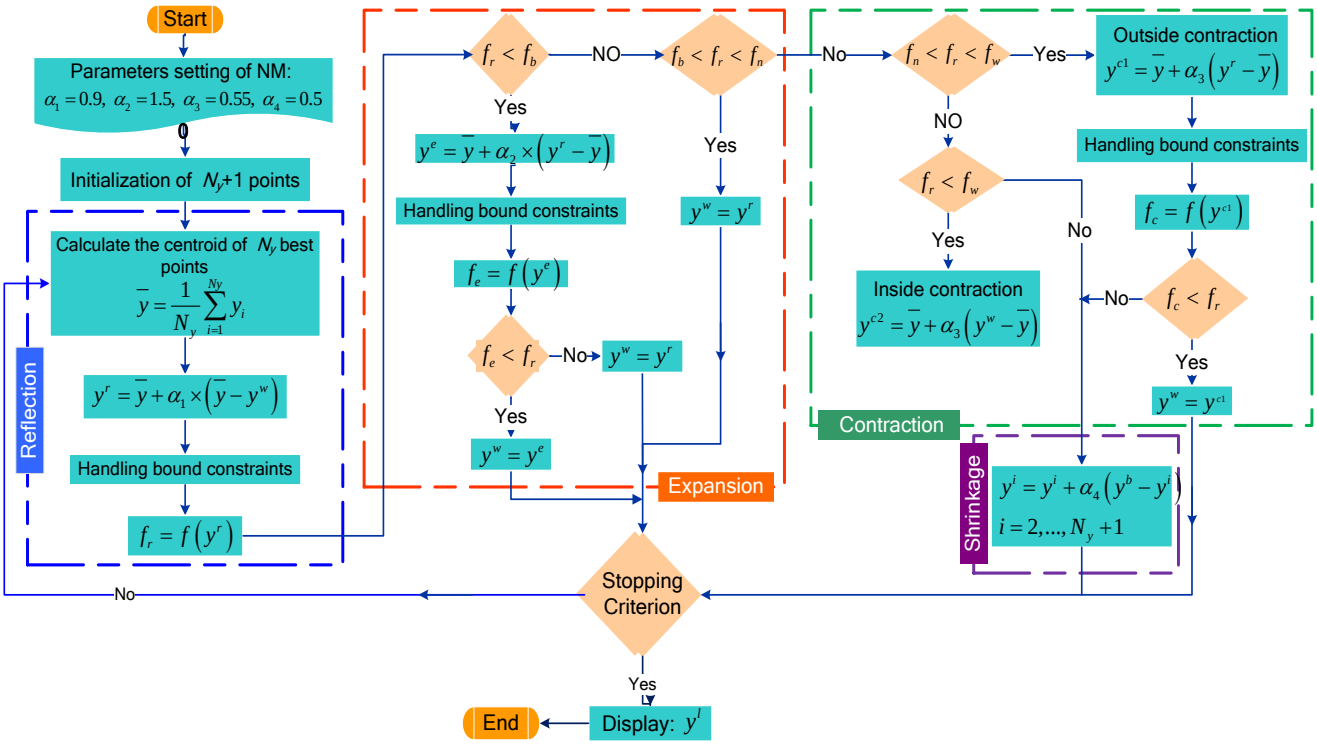

Fig. 5.2 Flowchart of the NM algorithm.

5.4 Proposed RBDO Approach: RDS-MADE-NM

By integrating the RDS concept with the MADE and NM algorithms, a new resolution approach for mechanical RBDO problems is developed, which is addressed to handle continuous, discrete and integer design variables. The proposed approach in this study involves two key steps:

- First, the RBDO problem (Eq. 1.5) is converted into a SDO problem (Eq. 5.4) by applying the RDS strategy.
- Second, the formed optimization problem is solved by introducing a hybrid optimization algorithm, coupling MADE with NM.

In the present approach, the index technique (Onwubolu and Davendra 2009) is adopted to deal with the discrete and integer design variables. The generalized flowchart of the developed RDS-MADE-NM approach is outlined in Fig. 5.3.

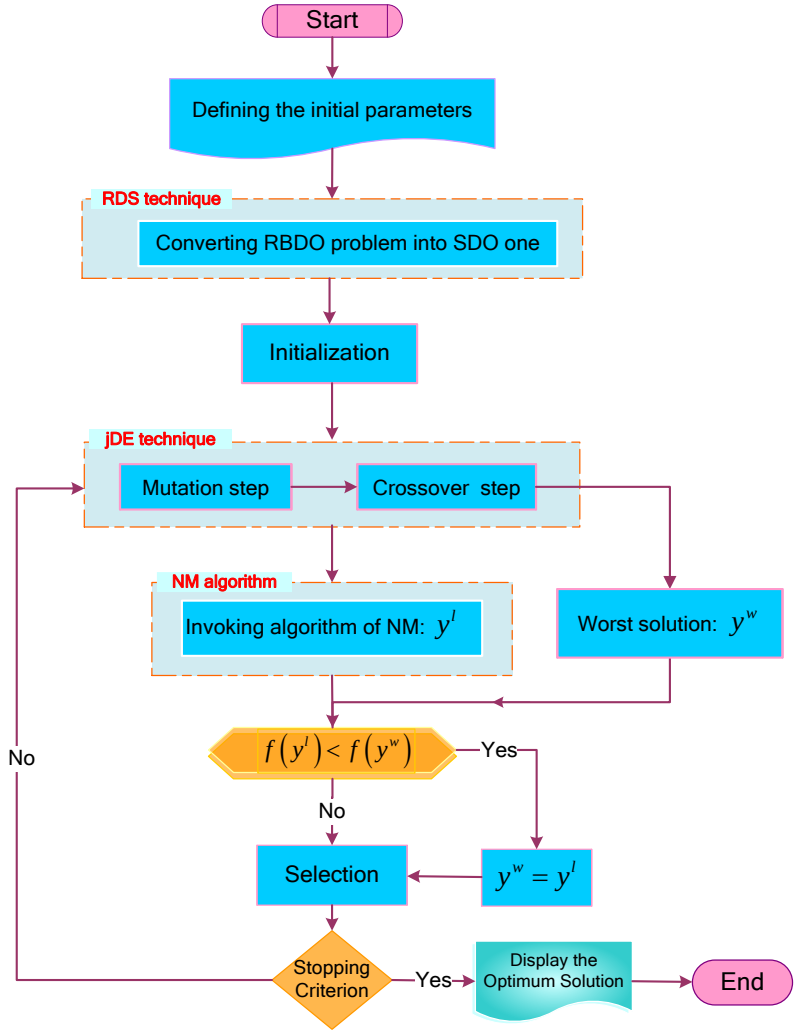

Fig. 5.3 Generalized flowchart of the RDS-MADE-NM integrated approach.

5.5 Evaluation of RDS-MADE-NM

In this section, the performance of the RDS-MADE-NM is shown by solving six nonlinear RBDO problems. The first four mechanical problems chosen from the literature are: the cantilever beam, vehicle side impact, speed reducer, and welded beam. Furthermore, two additional problems of mechanical design are formulated in this study for first time including the multiple disc clutch brake and the cylindrical pressure vessel. The population size and FEs number for each problem are given in Table 5.1. All problems are independently executed 50 times and the obtained results are compared with those available in the literature. For more readability, the better solution is highlighted in bold face.

Table 5.1 *Np* size and FEs number of the RDS-MADE-NM for the RBDO problems.

RBDO problem	***Np***	**FEs**
Cantilever beam	20	15,000
Vehicle side impact	20	35,000
Speed reducer	20	25,000
Welded beam	20	18,000
Multiple disc clutch brake	25	5,000
Pressure vessel	25	25,000

5.5.1 Cantilever Beam

The cantilever beam problem (Fig. 5.4) is widely used in the literature to test the reliability and the efficiency of RBDO methods (Liang et al. 2007; Shan and Wang 2008; Li et al. 2013). The objective is to minimize the beam weight, while two probabilistic constraints are considered. The first is imposed on the stress at the fixed end, which should be less than the yield strength. The second is fixed on the tip displacement, which should be less than the allowable displacement D_0. The problem involves two continuous deterministic design variables: the width d_1 and thickness d_2 of the cross-section. Moreover, four random parameters exist in the probabilistic constraints, supposed to be independent normally distributed where their statistical data are illustrated in Table 5.2. Thus, the RBDO problem is stated as follows:

$$
\begin{aligned}
&find \ \ (d_1, d_2) \\
&\min \ f(d) = d_1 \times d_2 \\
&s.t.: \ \ \mathrm{Prob}\left(g_i(d,p) \geq 0\right) \geq R_i^t, \quad i = 1,2. \\
&g_1 = p_1 - \left(\frac{600}{d_1 {d_2}^2} p_2 + \frac{600}{{d_1}^2 d_2} p_3 \right) \\
&g_2 = D_0 - \frac{4L^3}{p_4 d_1 d_2} \sqrt{\left(\frac{p_2}{{d_2}^2}\right)^2 + \left(\frac{p_3}{{d_1}^2}\right)^2} \\
&0 \leq d_1, d_2 \leq 5 \\
&R_i^t = \Phi(3) = 99.87\%.
\end{aligned}
\tag{5.5}
$$

The beam length L =100 *in* and the allowable displacement D_0= 2.5 *in*.

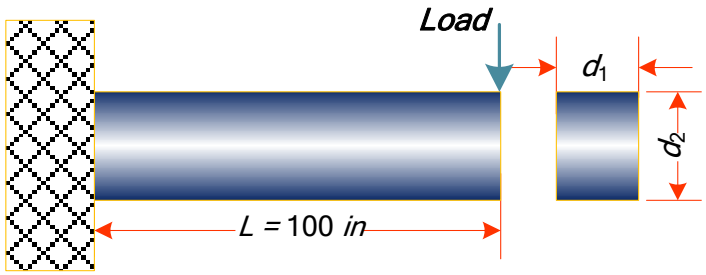

Fig. 5.4 Cantilever beam design.

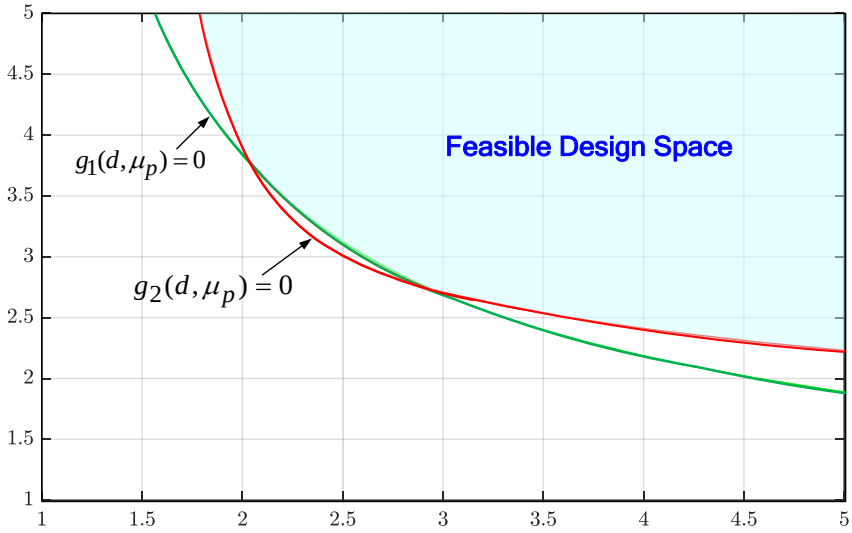

Fig. 5.5 Illustration of the deterministic FDS for the cantilever beam example.

5.5.1.1 Formulating the deterministic optimization problem

The feasible design space of the cantilever beam problem for the deterministic level is presented in Fig. 5.5. To shift the boundaries of the deterministic feasible space to the reliable space, the two probabilistic constraints in Eq. 5.5 are converted into approximate deterministic ones by applying the pseudo-code of the RDS technique (Algorithm 5.1). Algorithm 5.2 presents the procedure of the RDS strategy for the cantilever beam problem. Note that the same procedure is followed for the other problems studied.

Algorithm 5.2: Adopted RDS technique for the cantilever beam problem

Input: $k = 2,\ Nz = 4,\ \beta_t^i = \{3,3\},\ \mu_z = \{40000,1000,500,29\times10^6\},\ \sigma_z = \{2000,100,100,1.45\times10^6\}$.

For $i \coloneqq 1$ to k **do**

The partial derivatives of the function $g_i(d,\mu_z)$ are computed (Appendix A).

For $j \coloneqq 1$ to Nz **do**

The inverse MPFP of the constraint g_i is calculated as follows:

$$\mathbf{z}_j^i = \mu_{zj} - \beta_t^i \sigma_{zj} \frac{\sigma_{zj} \times \dfrac{\partial g_i(d,\mu_z)}{\partial \mu_{zj}}}{\sqrt{\sum_{q=1}^{Nz}\left(\sigma_{zq}\dfrac{\partial g_i(d,\mu_z)}{\partial \mu_{zq}}\right)^2}}$$

End

For $\boldsymbol{z}^i = \{\boldsymbol{z}_1^i, \boldsymbol{z}_2^i, \ldots, \boldsymbol{z}_{Nz}^i\}$, substitute $\boldsymbol{z}^i$ into the constraint function g_i to obtain $\mathbf{g}_i$

End

Output: $\mathbf{g}_1(d,\mu_z) = \mathbf{z}_1^1 - \left(\dfrac{600}{d_1 {d_2}^2}\mathbf{z}_2^1 + \dfrac{600}{{d_1}^2 d_2}\mathbf{z}_3^1\right)$, $\mathbf{g}_2(d,\mu_z) = D_0 - \dfrac{4L^3}{\mathbf{z}_4^2 d_1 d_2}\sqrt{\left(\dfrac{\mathbf{z}_2^2}{{d_2}^2}\right)^2 + \left(\dfrac{\mathbf{z}_3^2}{{d_1}^2}\right)^2}$

After the approximate deterministic constraints have been formed, the reliable design space of the cantilever beam problem is defined, as presented in Fig. 5.6. Thus, the equivalent deterministic optimization problem is established as follows:

$$\begin{aligned}
&\textit{find } (d_1, d_2)\\
&\min f\ (d) = d_1 \times d_2\\
&\textit{s.t.}: \ \mathbf{g}_i(d,\mu_z) \geq 0, \qquad i = 1,2,\\
&\mathbf{g}_1 = \mathbf{z}_1^1 - \left(\frac{600}{d_1 {d_2}^2}\mathbf{z}_2^1 + \frac{600}{{d_1}^2 d_2}\mathbf{z}_3^1\right)\\
&\mathbf{g}_2 = D_0 - \frac{4L^3}{\mathbf{z}_4^2 d_1 d_2}\sqrt{\left(\frac{\mathbf{z}_2^2}{{d_2}^2}\right)^2 + \left(\frac{\mathbf{z}_3^2}{{d_1}^2}\right)^2}\\
&0 \leq d_1, d_2 \leq 5.
\end{aligned} \tag{5.6}$$

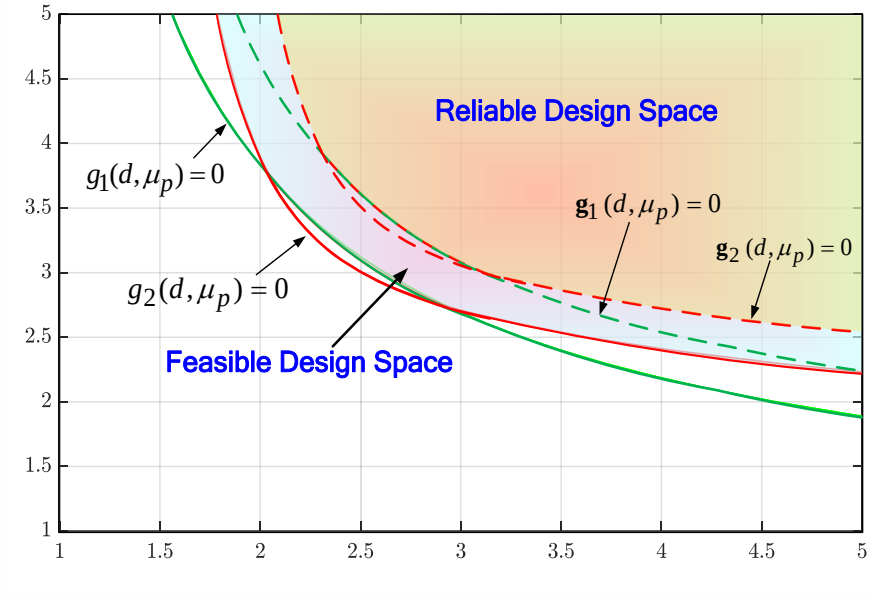

Fig. 5.6 Illustration of the RDS for the cantilever beam example.

5.5.1.2 Results and discussions

This optimization problem has been recently solved using SLDM (Li et al. 2013), IRA-DE (Lobato et al. 2017), Mean anchor (Fenrich and Alonso 2019), and PSO-4M-3M-2M (Liao and Biton 2019). The optimal results of the proposed method and the compared ones are given in Table 5.3. From this table, it is observed that the RDS-MADE-NM can reach the lower value of the objective function of $f(y^*) = 9.520247$ with $y^* = \{2.445990$ mm, 3.892184 mm$\}$. The results given by both IRA-DE and PSO-4M-3M–2M are very competitive compared with those of SLDM and Mean-anchor approach.

Moreover, Table 5.4 represents the statistical results of the proposed method for 50 independent runs. It is clear from the table that RDS-MADE-NM approach is very stable in solving this problem through achieving a small standard deviation of 8.48E-15. Besides, the RDS-MADE-NM needs few iterations to reach the best optimal solution (FEs = 15,000).

Table 5.2 Random parameters of the cantilever beam problem.

Random parameters	$\boldsymbol{\mu}$	$\boldsymbol{\sigma}$
Yield strength p_1 (psi)	40,000	2000
Load lateral p_2 (lb)	1000	100
Load vertical p_3 (lb)	500	100
Young's modulus p_4 (psi)	29×10^6	1.45×10^6

Table 5.3 Comparison of RBDO results for the cantilever beam problem.

Variable	RDS-MADE-NM	PSO-4M-3M-2M	Mean anchor	IRA-DE	SLDM
d_1	2.445990	2.45020	2.6219	2.44881	2.448
d_2	3.892184	3.88050	3.6492	3.88772	3.893
f_{best}	**9.520247**	9.52030	9.5680	9.52026	9.528

Table 5.4 Statistical results of the RDS-MADE-NM for the cantilever beam problem.

Method	Best	Mean	Worst	SD	FEs
RDS-MADE-NM	9.520247	9.520247	9.520247	8.48E-15	15,000

5.5.2 Vehicle Side Impact

This mechanical problem has been modeled for the first time by Gu et al. (2001) using the finite elements analysis, as shown in Fig. 5.7. The objective is to minimize the total vehicle weight while the probabilistic constraints are related to deflections, velocities at different vehicles and dummy locations. The problem has seven continuous random design variables and four random parameters as presented in Table 5.5. All the random quantities follow the normal distribution and are statistically independent. The RBDO problem of the vehicle side impact is expressed as follows:

$$
\begin{aligned}
&find\left(\mu_{x1},\mu_{x2},\mu_{x3},\mu_{x4},\mu_{x5},\mu_{x6},\mu_{x7}\right)\\
&\min f\left(\mu_x\right)=1.98+4.90\mu_{x1}+6.67\mu_{x2}+6.98\mu_{x3}+4.01\mu_{x4}+1.78\mu_{x5}+2.73\mu_{x7}\\
&s.t.:\ \ \mathrm{Prob}(g_i(x,p)\geq 0)\geq R_i^t, \qquad i=1,...,10,\\
&\mu_{xj}{}^{\boldsymbol{L}}\leq\mu_{xj}\leq\mu_{xj}{}^{\boldsymbol{U}}, \qquad j=1,...,7,\\
&R_i^t=\Phi(3)=99.87\%.
\end{aligned}
\tag{5.7}
$$

For more details, the mathematical forms of the probabilistic constraints are provided in Appendix B.1.

Table 5.6 displays the best optimal values of the objective and the design variables for the vehicle side impact problem using different approaches: SLA (Liang et al. 2008), SLDM (Li et al. 2013), AH-SLM (Jiang et al. 2017), and RBDO-dBA (Chakri et al. 2018). Table 5.6 shows obviously that RDS-MADE-NM and RBDO-dBA methods are the most effective in solving the problem by reaching the best fitness value ($f(y^*) = 28.5526$). The SLDM with the value of 28.596 is slightly better than SLA and AH-SLM with values of 28.6977 and 29.5578, respectively. The statistical values of the proposed approach and the RBDO-dBA developed by Chakri et al. (2018) are presented in Table 5.7.

Table 5.7 indicates clearly the robustness of the RDS-MADE-NM compared with the RBDO-dBA through the small standard deviation of 9.00E-13. Moreover, the best, mean and worst solutions provided by the proposed RDS-MADE-NM approach are better than those obtained with the RBDO-dBA. As mentioned in the same table, the RDS-MADE-NM reaches the best value with the lowest FEs, which is about 65% smaller.

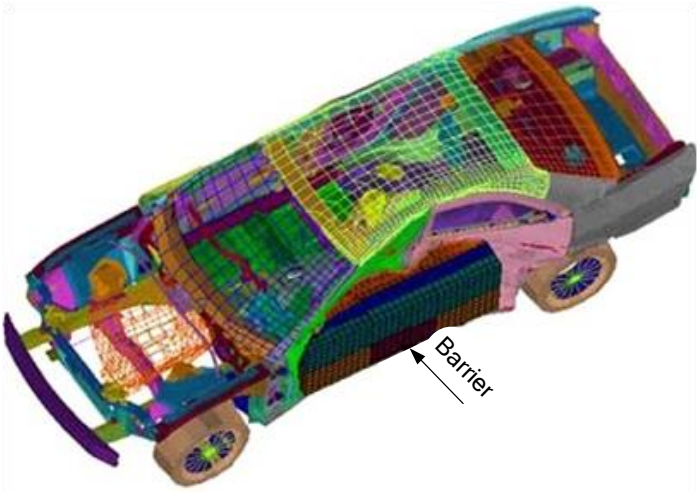

Fig. 5.7 Vehicle side impact design, extracted from (Youn and Choi 2004).

Table 5.5 Random design variables and random parameters of the vehicle side impact problem.

Random design variables	$\mu_{xj}{}^{L}$	$\mu_{xj}{}^{U}$	σ_j
Thickness (mm)			
B-Pillar inner x_1	0.5	1.5	0.03
B-Pillar reinforcement x_2	0.45	1.35	0.03
Floor side inner x_3	0.5	1.5	0.03
Cross members x_4	0.5	1.5	0.03
Door beam x_5	0.875	2.625	0.05
Door belt line reinforcement x_6	0.4	1.2	0.03
Roof rail x_7	0.4	1.2	0.03
Random parameters	μ	σ	
Material of B-Pillar inner p_1	0.345	0.006	
Material of floor side inner p_2	0.192	0.006	
Barrier height (mm) p_3	0.00	10.00	
Barrier hitting position (mm) p_4	0.00	10.00	

Table 5.6 Comparison of RBDO results for the vehicle side impact problem.

Variable	RDS-MADE-NM	RBDO-dBA	AH-SLM	SLDM	SLA
μ_{x1}	0.800849009	0.80084900	0.7872	0.8050	0.81000
μ_{x2}	1.350000000	1.35000000	1.3500	1.3500	1.35000
μ_{x3}	0.713392195	0.71339220	0.6887	0.7170	0.72770
μ_{x4}	1.499999999	1.50000000	1.5000	1.5000	1.50000
μ_{x5}	0.875000000	0.87500000	1.0705	0.8750	0.87500
μ_{x6}	1.200000000	1.20000000	1.2000	1.2200	1.20000
μ_{x7}	0.400000000	0.40000000	0.7284	0.4000	0.40000
f_{best}	**28.55263766**	**28.5526497**	29.5578	28.596	28.6977

Table 5.7 Statistical results for the vehicle side impact problem.

Method	Best	Mean	Worst	SD	FEs
RDS-MADE-NM	**28.5526376**	**28.5526376**	**28.5526376**	**9.00E-13**	**35,000**
RBDO-dBA	28.5526497	28.5526578	28.5527264	1.55E-05	100,000

5.5.3 Speed Reducer

The probabilistic optimization formulation of the speed reducer problem has been proposed in (Yin and Chen 2006). The problem, as described schematically in Fig. 5.8, contains seven continuous design variables. The teeth module d_1 and the number of pinion teeth d_2 are deterministic. The random design variables are: face width x_1, lengths of the shafts (x_2, x_3), and diameters of the shafts (x_4, x_5). There are also fifteen random parameters including the material properties, rotation speed, and engine power. The design problem is subjected to ten probabilistic constraints as well as one deterministic constraint. So, to minimize the system weight, the probabilistic optimization problem can be formulated as follows:

$$find \ \left(d_1, d_2, \mu_{x1}, \mu_{x2}, \mu_{x3}, \mu_{x4}, \mu_{x5}\right)$$

$$\min f\left(d, \mu_x\right) = 0.7854\mu_{x1}d_1^{\,2}\left(3.3333d_2^{\,2} + 14.9334d_2 - 43.0934\right) - 1.5079\mu_{x1}\left(\mu_{x4}^{\,2} + \mu_{x5}^{\,2}\right) + 7.477\left(\mu_{x4}^{\,3} + \mu_{x5}^{\,3}\right) + 0.7854\left(\mu_{x2}\mu_{x4}^{\,2} + \mu_{x3}\mu_{x5}^{\,2}\right)$$

$$s.t.: \begin{cases} \text{Prob}\left(g_i\left(d, x, p\right) \geq 0\right) \geq R_i^t, & i = 1, ..., 10, \\ g_{11}(d) \geq 0, \end{cases} \tag{5.8}$$

$$d_q^{\,L} \leq d_q \leq d_q^{\,U}, \qquad q = 1, 2$$

$$\mu_{xj}^{\,L} \leq \mu_{xj} \leq \mu_{xj}^{\,U}\text{,,} \qquad j = 1, ..., 5$$

$$R_i^t = \Phi\left(1.644\right) = 95\%..$$

The mathematical formulas of the constraints are presented in Appendix B.2. All the random design variables and random parameters are statistically independent with the normal distribution (Table 5.8).

The best optimal results of the RDS-MADE-NM are compared with those of the RBDO-dBA (Chakri et al. 2018), Enhanced SORA (ESORA) and DLA (Yin and Chen 2006). The comparison results are detailed in Table 5.9.The results show that the RDS-MADE-NM can provide new optimal solution for the speed reducer problem, where $f(y^*) = 2856.3662$. The RBDO-dBA approach with best solution of 2856.547 is better than ESORA and DLA with values of 2857.25 and 2878.97, respectively.

The statistical results of the proposed approach and the RBDO-dBA are collected in Table 5.10. The obtained results clearly show that RDS-MADE-NM is better than RBDO-dBA in solving this problem based on the lowest values for the mean (2856.36622), the worst (2856.36622) as well as the standard deviation (9.79E-08). Moreover, the RDS-MADE-NM can reach the best point with the lowest Fes number, which is 50% smaller.

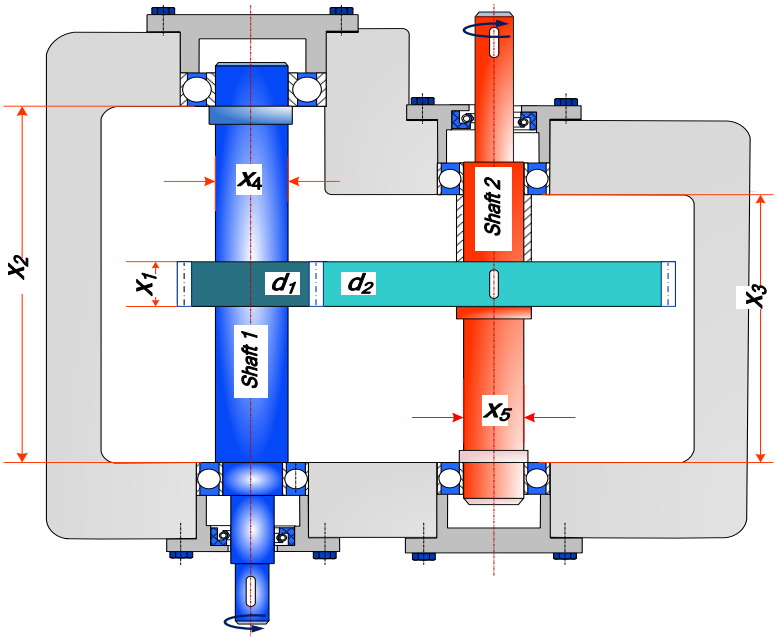

Fig. 5.8 Speed reducer design.

Table 5.8 Characteristics of the speed reducer problem.

Deterministic design variables	d_q^L	d_q^U	
Teeth module (mm) d_1	0.7	0.8	
Pinion teeth number d_2	17	28	
Random design variables (mm)	μ_{xj}^L	μ_{xj}^U	**Covariant**
Face width x_1	2.6	4.2	0.05
Shaft length 1 x_2	7.0	8.3	0.05
Shaft length 2 x_3	7.0	9.3	0.05
Shaft diameter 1 x_4	2.9	3.95	0.02
Shaft diameter 2 x_5	5.0	6.0	0.02
Random parameters	μ	σ	
p_1	27.0	2.7	
p_2	397.5	39.8	
p_3	1.93	0.0965	
p_4	1.93	0.0965	
p_5	1100.0	110.0	
p_6	745.0	74.5	
p_7	1.69×10^7	1.69×10^6	
p_8	0.1	0.005	
p_9	1.58×10^8	1.58×10^7	
p_{10}	850.0	34.0	
p_{11}	5.0	0.25	
p_{12}	12.0	0.6	
p_{13}	1.5	0.75	
p_{14}	1.1	0.11	
p_{15}	1.9	0.19	

Table 5.9 Comparison of RBDO results for the speed reducer problem.

Variable	**RDS-MADE-NM**	**RBDO-dBA**	**ESORA**	**DLA**
d_1	0.700000009	0.700000	0.70000	0.70000
d_2	17.00000000	17.00000	17.0000	17.0000
μ_{x1}	3.859799083	3.860190	3.86180	3.77750
μ_{x2}	7.000000000	7.000000	7.00000	7.00000
μ_{x3}	7.000000000	7.000000	7.00000	7.00000
μ_{x4}	2.932387331	2.932511	2.93260	3.19760
μ_{x5}	5.000000000	5.000000	5.00000	5.00000
f_{best}	**2856.366228**	2856.547	2857.25	2878.97

Table 5.10 Statistical results for the speed reducer problem.

Method	Best	Mean	Worst	SD	FEs
RDS-MADE-NM	**2856.36622**	**2856.36622**	**2856.36622**	**9.79E-08**	**25,000**
RBDO-dBA	2856.547	2856.547	2856.547	9.62E-05	50,000

5.5.4 Welded Beam

The welded beam structure (Roa et al. 2019) (Fig. 5.9) must be designed for the minimum cost using four design variables: welding depth x_1, welding length x_2, beam height x_3, and beam thickness x_4. This problem involves seven parameters and five constraints associated with the geometry, the maximum permissible stress, and the tip deflection. The RBDO formulation of this example has been extensively studied in the literature (Lee and Lee 2005; Cho and Lee 2011; Li at al. 2015) considering that all random design variables are continuous with the normal distribution, and the parameters are all deterministic.

In the present study, we have decided to use the modified formulation proposed by Chakri et al. (2018) where all the random design variables are considered to be discrete; all the parameters are assumed to be random; and mixed types of distribution functions are used. The modified RBDO problem of the welded beam is given by the following equation:

$$
\begin{aligned}
&find \quad \left(\mu_{x1}, \mu_{x2}, \mu_{x3}, \mu_{x4}\right) \\
&\min f\left(\mu_x, \mu_p\right) = c_1 \mu_{x1}^2 \mu_{x2} + c_2 \mu_{x3} \mu_{x4} \left(\mu_{p2} + \mu_{x2}\right) \\
&s.t.: \ \text{Prob.}\left(g_i\left(x, p\right) \geq 0\right) \geq R_i^t, \qquad i = 1, ..., 5 \\
&\mu_{x1}\left(mm\right) \in \left\{3, 4, 5, ..., 50\right\} \\
&\mu_{x2}, \mu_{x3}\left(mm\right) \in \left\{1, 2, 3, ..., 254\right\} \\
&\mu_{x4}\left(mm\right) \in \left\{2, 3, 4, 5, 6, 7, 8, 10, 12, 14, 15, 16, 18, 20, 22, 25\right\} \\
&\sigma_{x1}, \sigma_{x2} = 0.1693, \quad \sigma_{x3}, \sigma_{x4} = 0.0107 \\
&R_i^t = \Phi\left(3\right) = 99.87\%.
\end{aligned}
\tag{5.9}
$$

The mathematical formulation of the probabilistic constraints, for the welded beam problem, is presented in Appendix B.3. The statistical characteristics of the system parameters are taken from (JCSS 2001) and listed in Table 5.11.

The best optimal values of the objective as well as the design variables provided by RDS-MADE-NM and RBDO-dBA methods are presented in Table 5.12. It can be observed from

this table that the proposed approach achieves new best optimal solution for the welded beam problem, considering the case of discrete variables.

Form the statistical analysis given in Table 5.13, the approach proposed in this study outperforms the RBDO-dBA, regarding the values of the best, the mean and the worst solutions. In addition, the introduced approach is more robust in solving this problem with lowest value of the standard deviation of 4.54E-10. From the same table, it can be noticed that the RDS-MADE-NM is capable to provide the optimized results in lesser Fes number (reduction of 64%).

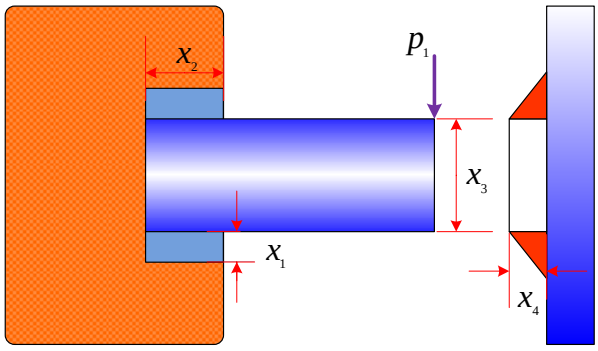

Fig. 5.9 Welded beam design.

Table 5.11 Random parameters of the welded beam problem.

Random parameters	**Distribution**	μ	**Covariant**
Load p_1(N)	Log-normal	26688.0	0.10
Beam length p_2(mm)	Normal	355.6	0.05
Young modulus p_3(Mpa)	Log-normal	206850.0	0.03
Shear modulus p_4(Mpa)	Log-normal	82740.0	0.03
Admissible deflection p_5(mm)	Normal	6.35	0.05
Admissible shear stress p_6(Mpa)	Log-normal	93.77	0.07
Admissible normal stress p_7(Mpa)	Log-normal	206.85	0.07
Weld material cost c_1 ($/mm)	Deterministic	6.74135×10^{-5}	_
Bar stock cost c_2 ($/mm)	Deterministic	2.93585×10^{-6}	_

Table 5.12 Comparison of RBDO results for the welded beam problem.

Variable	**RDS-MADE-NM**	**RBDO-dBA**
μ_{x1}	6.00000	6.00000
μ_{x2}	210.000	233.000
μ_{x3}	219.000	232.000
μ_{x4}	7.00000	7.00000
f_{best}	**2.96502**	3.27626

Table 5.13 Statistical results for the welded beam problem.

Method	Best	Mean	Worst	SD	FEs
RDS-MADE-NM	**2.96502**	**2.96502**	**2.96502**	**4.54E-10**	**18,000**
RBDO-dBA	3.27626	3.30780	3.35368	2.24E-02	50,000

5.5.5 Multiple Disc Clutch Brake

The objective of this problem is to minimize the weight of the multiple disc clutch brake shown in Fig. 5.10, while observing eight design constraints. The optimization problem has been expressed in the deterministic form by Osyczka (2002) and is modified here to be a RBDO problem.

Regarding the RBDO formulation, there are five discrete design variables consisting of four random ones: the inner and the outer radiuses (x_1, x_2), the thickness of discs x_3, and the actuating force x_4. The deterministic variable is the number of friction surfaces d_1. The first three variables are assumed to follow the normal distribution with a covariant of 0.05, while the actuating force variable x_4 follows the lognormal distribution with a covariant of 0.10. There are also nine normally distributed random parameters and their statistical data are described in Table 5.14. All the random variables and random parameters are supposed to be independent. Thus, the RBDO formulation can be expressed as follows:

$$
\begin{aligned}
&\textit{find} \quad \left(d_1, \mu_{x1}, \mu_{x2}, \mu_{x3}, \mu_{x4}\right) \\
&\min f\left(d, \mu_x\right) = \pi c \mu_{x3}\left(\mu_{x2}^2 - \mu_{x1}^2\right) \times \left(d_1 + 1\right) \\
&s.t.: \ \Pr ob.\left(g_i\left(d, x, p\right) \geq 0\right) \geq R_i^t, \qquad i = 1, ..., 8 \\
&d_1 \in \{2,\ 3,\ 4,\ 5,\ 6,\ 7,\ 8,\ 9\} \\
&\mu_{x1} \in \{60,\ 61,\ 62, \ldots, 80\} \\
&\mu_{x2} \in \{90,\ 91, 92, \ldots, 110\} \\
&\mu_{x3} \in \{1,\ 1.5,\ 2,\ 2.5,\ 3\} \\
&\mu_{x4} \hat{I} \{600,\ 610,\ 620, \ldots,\ 1000\} \\
&R_i^t = \Phi(3) = 99.87\%.
\end{aligned}
\tag{5.10}
$$

The mathematical formulation of the probabilistic constraints is detailed in Appendix B.4.

In order to confirm the results of proposed approach for the multiple disc clutch brake and the presser vessel RBDO problems, five additional algorithms are used: the Particle Swarm Optimization (PSO) (Kennedy and Eberhart 1995), the Artificial Bee Colony (ABC) (Karaboga and Basturk 2007), the Bat Algorithm (BA) (Yang 2010), the Krill Herd (KH) (Gandomi and Alavi 2012), and the Interior Search Algorithm (ISA) (Gandomi 2014). It is worth mentioning that the used algorithms are also coupled with the RDS strategy. Concerning the specific parameters of each implemented algorithm, we keep the similar values suggested by the original authors for the two problems. For the statistical comparison, we run each algorithm 50 times.

The optimal results for the multiple disc design problem achieved by the used algorithms are given in Table 5.15. Table 5.16 details the simulated results regarding the values of the best, the mean, the worst solutions, and the standard deviation. According to Table 5.15, all investigated algorithms are able to find the feasible optimal global solution, which is $f(y^*) = 0.73562276$. For the statistical analysis, Table 5.16 clearly shows that the MADE-NM outperforms the other implemented algorithms in terms of the mean and the worst values. Moreover, by achieving the smallest standard deviation of 7.85E-16, the MADE-NM is the most consistent to solve this problem. The mean and the worst solutions given by ABC algorithm are better than the other compared algorithms.

Fig. 5.11 illustrates the convergence plots of the algorithms to the best results. It shows clearly that MADE-NM can converge fast, compared to the other metaheuristics, and take only 10 iterations to find the best solution. PSO and KH can reach the optimal solution at the 19^{th} and 26^{th} iterations, respectively. ISA and BA obtain the best solution almost in the same iteration, while ABC converges to the final value after 96 iterations.

The optimal solution obtained by RDS-MADE-NM is employed to test the reliability of the constraints satisfaction for this example. Table 5.17 presents the values of the eight constraints in the reliable design space, the corresponding reliability indexes and failure probabilities. The probabilistic constraints are estimated here by FORM approximation and Monte Carlo simulation using the Phimeca software. The Monte Carlo simulation is regarded as reference method with 10^6 samples. As it can be observed from Table 5.17, the calculated reliability of each constraint satisfies the imposed level, which validates the solution obtained by developed approach to this RBDO problem. For the fifth and seventh constraints, the symbol ∞ indicates that the reliability index has a high value, meaning that the corresponding probability of failure is very low.

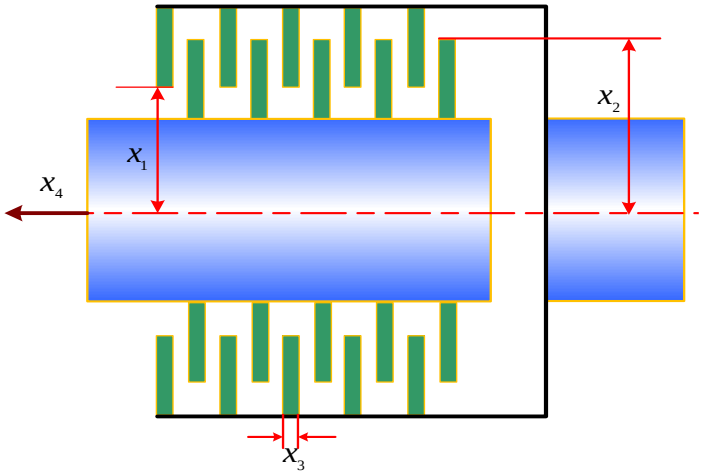

Fig. 5.10 Multiple disc clutch brake design.

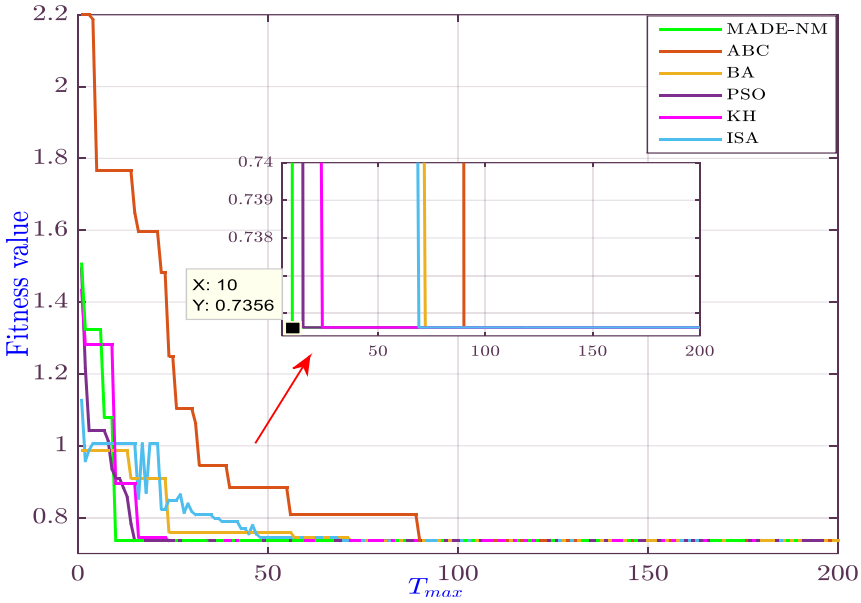

Fig. 5.11 Convergence diagrams for the multiple disc clutch brake RBDO problem.

Table 5.14 Random parameters of the multiple disc clutch brake problem.

Random parameters	$\boldsymbol{\mu}$	**Covariant**
Minimum difference between radii p_1(mm)	20	0.05
Maximum length p_2(mm)	30	0.05
Distance between disc when unloaded p_3(mm)	0.5	0.05
Maximum velocity of slip stick p_4(m/sec)	10	0.05
Maximum allowable pressure on disc p_5(Mpa)	1	0.03
Friction coefficient p_6	0.5	0.03
Disc mass moment of inertia p_7(kg.mm^2)	55	0.15
Frictional resistance torque p_8(N.m)	3	0.15
Static input torque p_9(N.m)	40	0.15
Material density c (kg/mm^3)	78×10^{-7}	_

Table 5.15 Best results obtained by the algorithms for the multiple disc clutch brake RBDO problem.

Variable	MADE-NM	ABC	BA	PSO	KH	ISA
d_1	4.0000000	4.0000000	4.0000000	4.0000000	4.0000000	4.0000000
μ_{x1}	60.000000	60.000000	60.000000	60.000000	62.000000	60.000000
μ_{x2}	98.000000	98.000000	98.000000	98.000000	100.00000	98.000000
μ_{x3}	1.0000000	1.0000000	1.0000000	1.0000000	1.0000000	1.0000000
μ_{x4}	880.00000	1000.0000	1000.0000	950.0000	880.00000	1000.0000
f_{best}	**0.73562276**	**0.73562276**	**0.73562276**	**0.73562276**	**0.73562276**	**0.73562276**

Table 5.16 Statistical results for the multiple disc clutch brake RBDO problem.

Algorithm	Best	Mean	Worst	SD	FEs
MADE-NM	**0.73562276**	**0.73562276**	**0.73562276**	**7.85E-16**	5,000
ABC	**0.73562276**	0.76692962	0.81709997	2.98E-02	5,000
BA	**0.73562276**	1.12175905	2.84055268	4.62E-01	5,000
PSO	**0.73562276**	0.83176636	1.32412098	1.66E-01	5,000
KH	**0.73562276**	0.94456488	1.55260022	2.01E-01	5,000
ISA	**0.73562276**	0.78474924	1.10343415	8.59E-02	5,000

Table 5.17 Constraint value and estimated reliability of the probabilistic constraints for the multiple disc clutch brake problem.

Constraint in the RDS	Value	FORM (abdo-Rackwitz)		$P_{f\,MCS}$
		β	P_f	
$\mathbf{g_1}$	0.5046	3.0865	0.0010	0.00098
$\mathbf{g_2}$	17.9225	5.1974	1.0105E-07	0.0000
$\mathbf{g_3}$	0.8581	6.2652	1.8617E-10	0.0000
$\mathbf{g_4}$	8.3086	7.165	3.8893E-13	0.0000
$\mathbf{g_5}$	8.4649	∞	0.0000	0.0000
$\mathbf{g_6}$	0.0009	3.0252	0.0012	0.0012
$\mathbf{g_7}$	29.3033	∞	0.0000	0.0000
$\mathbf{g_8}$	5.28150	6.8237	4.4363E-12	0.0000

5.5.6 Cylindrical Pressure Vessel

For the cylindrical pressure vessel structure presented in Fig. 5.12, the objective is to optimize the total fabrication cost using four mixed design variables. The thickness of the cylindrical shell x_1 and the thickness of the spherical head x_2 are discrete in multiples of 0.0625, while the inner radius x_3, and the length of the cylindrical segment of the vessel x_4 are continuous. The original design formulation was given by Sandgren (1990) in the deterministic term and then became widely used in the engineering field as a real-world mixed test problem. In the

present research, the probabilistic optimization formulation is investigated to test the effectiveness of the proposed approach in case of mixed design variables. We assume that the four variables are random with the normal distribution and a covariant of 0.05. The RBDO problem is given as follows:

$$
\begin{aligned}
&find\ \left(\mu_{x1},\mu_{x2},\mu_{x3},\mu_{x4}\right)\\
&\min f\left(\mu_x\right)=0.6224\mu_{x1}\mu_{x3}\mu_{x4}+1.7781\mu_{x2}{\mu_{x3}}^2+3.1661{\mu_{x1}}^2\mu_{x4}+19.84{\mu_{x1}}^2\mu_{x3}\\
&s.t.:\ \text{Prob.}\left(g_i\left(x\right)\ge 0\right)\ge R_i^t,\quad i=1,...,4\\
&g_1=x_1-0.0193x_3\\
&g_2=x_2-0.00954x_3\\
&g_3=\pi{x_3}^2x_4+\frac{\left(4\pi{x_3}^3\right)}{3}-1296000\\
&g_4=240-x_4\\
&0.0625\le\mu_{x1},\mu_{x2}\le 6.1875,\quad 10\le\mu_{x3},\mu_{x4}\le 200\\
&R_i^t=\Phi\left(1.645\right)=95\%.
\end{aligned}
\tag{5.11}
$$

Tables 5.18 and 5.19 display the simulated results for the pressure vessel RBDO problem. Table 5.18 obviously demonstrates that only MADE-NM, PSO and ISA are able to get the optimal value of $f(y^*) = 8418.6674\$$ with $y^* = \{1.00\ in,\ 0.500\ in,\ 46.1087\ in,\ 176.1772\ in\}$. From the statistical analysis listed in Table 5.19, the proposed MADE-NM algorithm confirms that is very effective to solve this problem with lowest values of the mean, the worst solutions as well as the standard deviation. Both ABC and KH converge only to the near global solution. However, BA is the worst in dealing with this example with highest values of the best (12585.53$), the mean (28556.45$) and the worst (67892.85$).

As shown in Fig. 5.13, PSO algorithm is relatively faster than the compared algorithms to find the best fabrication cost of the presser vessel structure. The reliability analysis corresponding to the optimal solution obtained by RDS-MADE-NM is also given in Table 5.20. According to this table, the desired reliability is checked for all constraints. The first and third constraints presented in bold are actives, which have the same level of required reliability.

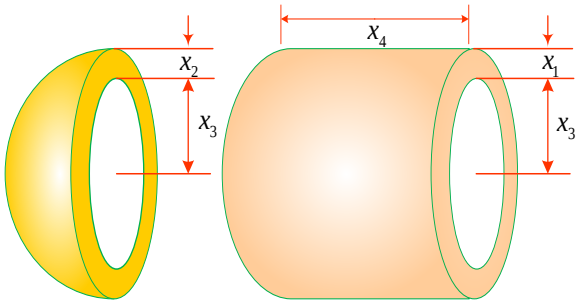

Fig. 5.12 Cylindrical pressure vessel design.

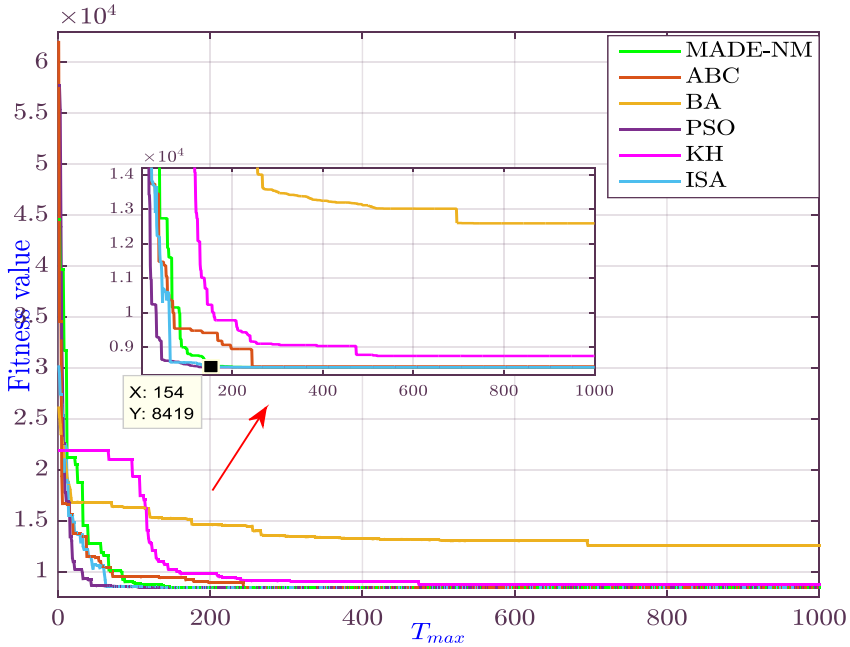

Fig. 5.13 Convergence diagrams for the pressure vessel RBDO problem.

Table 5.18 Best simulated results obtained by the algorithms for the pressure vessel RBDO problem.

Variable	MADE-NM	ABC	BA	PSO	KH	ISA
μ_{x1}	1.0000000	1.0000000	1.81250000	1.0000000	1.0625000	1.0000000
μ_{x2}	0.5000000	0.5000000	0.68750000	0.5000000	0.5625000	0.5000000
μ_{x3}	46.108706	46.029740	64.1257975	46.108706	48.981693	46.108706
μ_{x4}	176.17721	177.68827	40.8397406	176.17721	145.91348	176.17721
f_{best}	**8418.6674**	8450.0475	12585.5311	**8418.6674**	8744.6073	**8418.6674**

Table 5.19 Statistical results for the pressure vessel RBDO problem.

Algorithm	Best	Mean	Worst	SD	FEs
MADE-NM	**8418.66744**	**8418.66744**	**8418.66744**	**6.17E-12**	25,000
ABC	8450.04752	8695.46768	9136.5936	1.60E+02	25,000
BA	12585.5311	28556.4531	67892.8534	1.43E+04	25,000
PSO	**8418.66744**	9775.69268	28441.5616	2.89E+03	25,000
KH	8744.60734	9497.32202	11957.833	6.94E+02	25,000
ISA	**8418.66744**	9419.99224	10742.712	6.01E+02	25,000

Table 5.20 Constraint value and estimated reliability of the probabilistic constraints for the pressure vessel problem.

Constraint in the RDS	Value	FORM (abdo-Rackwitz)		$P_{f\,MCS}$
		β	P_f	
g_1	**0.0000**	**1.6450**	**0.0500**	**0.0497**
g_2	0.0053	1. 8056	0.0355	0.0353
g_3	**0.0000**	**1.6449**	**0.0500**	**0.0501**
g_4	49.3322	3.9763	3.4998E-5	0.00002

5.6 Industry Case Study

A cylindrical spur gear in a large transport machine is taken as a case study. This structure has been investigated by Abderazek et al. (2017) in the deterministic optimization level. The problem is formulated for two objectives, regarding the maximum bending stresses and the specific sliding coefficients. The bending stress is modeled explicitly using FEA (Atanasovska et al. 2010; Atanasovska et al. 2013). In addition, several constraints related to the system performance are considered, such as minimal transverse contact ratio value, thickness of the tooth tip diameter, and tooth interferences. The optimization problem is developed for three mixed design variables including two continuous (the profile shift coefficient x_{p1} and the radius of root curvature ρ_f) and one discrete (the pressure angle α_n).

In this study, the RBDO for this structure is considered to explore the applicability of the proposed approach in real mechanical problems. It is assumed that all the random design variables and parameters are independent with the normal distribution. According to the statistical description proposed by Zhang at al. (2003), the profile shift coefficients (x_{p1}, x_{p2}) have a covariant of 0.033, the radius of root curvature ρ_f, the pressure angle α_n and the normal module m_n have a covariant of 0.005, while the teeth number for the pinion and the wheel (z_1 , z_2) are treated as deterministic. The flowchart in Fig. 5.14 displays the basic steps of the developed RBDO procedure for the problem. The mathematical RBDO model of the cylindrical spur gear is formulated as the following:

$$
\begin{aligned}
&find\left(\mu_{xp1},\mu_{\rho f},\mu_{\alpha n}\right)\\
&\min\begin{cases} f_1=\sigma_{F1}\\ f_2=\gamma_{\max 1}\end{cases}\\
&s.t.:\begin{cases}\Pr ob.\left(g_i\ge 0\right)\ge R_i^t, & i=1,...,5.\\ g_q\ge 0, & q=6,7.\end{cases}\\
&g_1=\varepsilon_\alpha-1.4\\
&g_2=s_{a1}-0.4m_n\\
&g_3=s_{a2}-0.4m_n\\
&g_4=\sqrt{{r_{b2}}^2+\left(a'\sin\alpha_n'\right)^2}-\frac{m_n(z_2+2+2x_{p2})}{2}\\
&g_5=\sqrt{{r_{b1}}^2+\left(a'\sin\alpha_n'\right)^2}-\frac{m_n(z_1+2+2x_{p1})}{2}\\
&g_6=10^{-3}-\left|\sigma_{F1}-\sigma_{F2}\right|\\
&g_7=10^{-6}-\left|\gamma_{\max 1}-\gamma_{\max 2}\right|\\
&-0.5\le\mu_{xp1}\le 0.8,\quad 6\le\mu_{\rho f}\le 8.3,\quad \mu_{\alpha n}\in\{18,\ 19,\ 20,\ 21,\ 22\}\\
&R_i^t=\Phi(3)=99.87\%.
\end{aligned}
\tag{5.12}
$$

where σ_{F1}, σ_{F2} are the maximum bending stresses and γ_{max1}, γ_{max2} are the maximum specific sliding coefficients for the pinion and the wheel, respectively. ε_α is the transverse contact ratio, a' is the distance of the working center, and α_n' is pressure angle at the pitch cylinder. Note that the last two constraints are considered to be deterministic. To provide equally strong teeth on the pinion and the wheel, their maximum bending stresses should be balanced (constraint g_6). Moreover, in order to maximize the wear resistance of the gear pair, the maximum specific sliding coefficients should be equalized at extremes of contact path (as given by the constraint g_7). For more details about the design problem, please refer to (Abderazek et al. 2017).

5.6.1 Simulation Results

For solving this multi-objective RBDO problem, the weighted sum method is applied where the weighting factors for the objectives are chosen as: w_1 = 0.9, w_2 = 0.1. It should be noted that we keep the same parameters tuning of the proposed method (as in the previous section) for this case study, $Np = 20$ and T_{max} = 2500. The best results for the cylindrical spur gear RBDO problem, after 50 runs, are given in Table 5.21. Results show that the proposed RDS-

MADE-NM reaches the optimal solution for all runs, and provides the objective functions values of $f_1(y^*) = 692.3603$ and $f_2(y^*) = 0.9250$, with $y^* = \{0.382792,\ 7.769226$ mm, $22.00\ °\}$.

Accordingly, the achieved results can offer a perfect balancing in the tooth root stresses ($\sigma_{F1} = 692.3603$ MPa, and $\sigma_{F2} = 692.3604$ MPa) and the maximum specific sliding coefficients ($\gamma_{max1} = \gamma_{max2} = 0.9250$) so that the service life of the system is significantly extended. Additionally, the probabilistic constraints at the optimal solution obtained are evaluated using Monte Carlo simulation. The results summarized in Table 5.22 show that the required reliability of each constraint is verified ($P_f = \Phi(-3) \approx 0.0013$). This effectively demonstrates that the proposed approach is capable to solve this real RBDO problem.

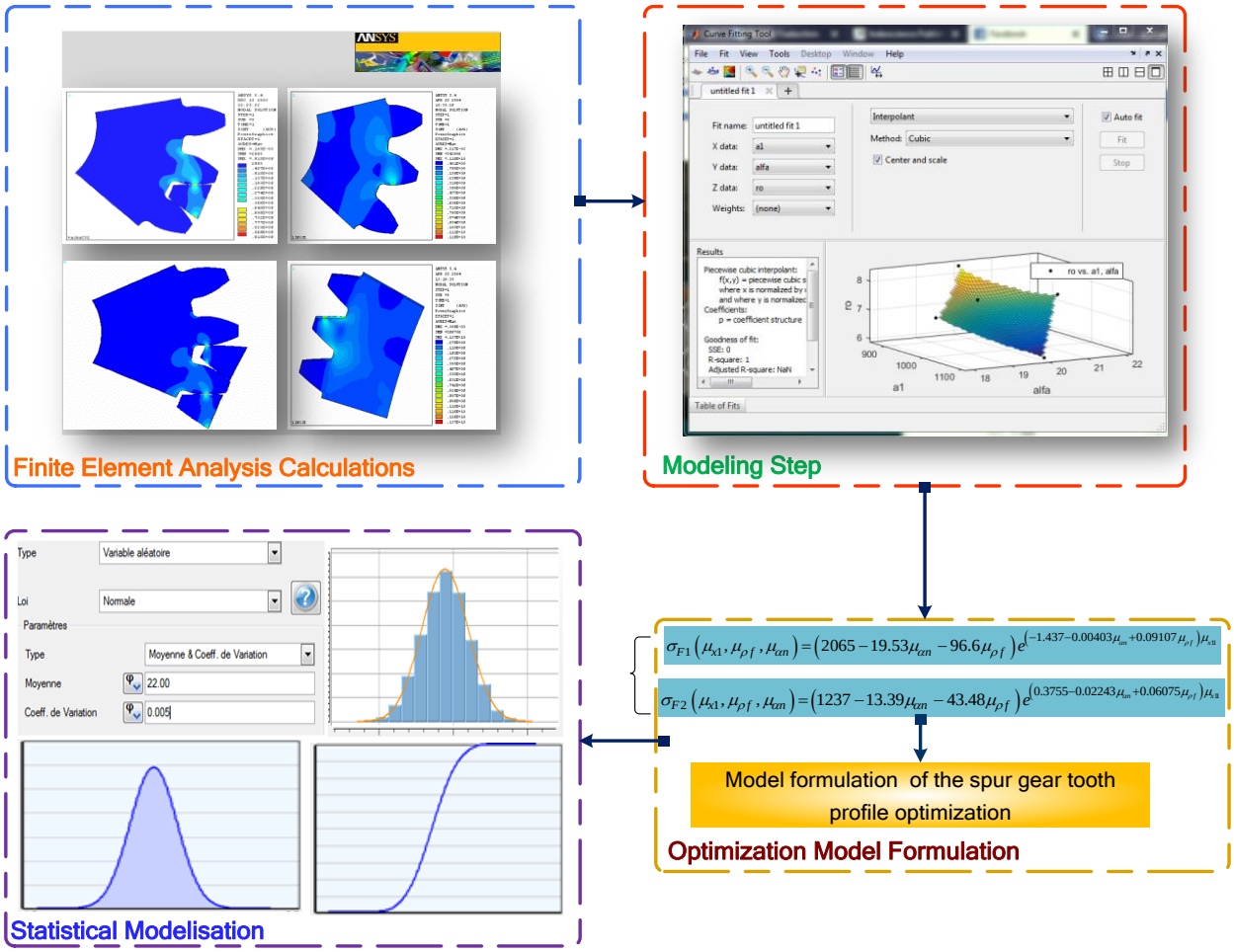

Fig. 5.14 Flowchart of the RBDO procedure for the cylindrical spur gear.

Table 5.21 RBDO results of the cylindrical spur gear problem.

Variable	RDS-MADE-NM
μ_{xp1}	0.382792466550098
μ_{ρ_f} (mm)	7.769226148927356
μ_{α_n} (°)	22.00000000000000
σ_{F1} (*MPa*)	692.3603432173304
σ_{F2} (*MPa*)	692.3604432173306
γ_{max1}	0.925016962706618
γ_{max2}	0.925017962706618
f_{best}	623.2168105918681

Table 5.22 Constraint value and estimated reliability of the probabilistic constraints for the cylindrical spur gear problem.

Constraint in the RDS	Value	$P_{f\,MCS}$
$\mathbf{g_1}$	7.3720E-02	0.0011
$\mathbf{g_2}$	1.6639E+00	0.0002
$\mathbf{g_3}$	7.5690E+00	0.0000
$\mathbf{g_4}$	4.4552E+01	0.0000
$\mathbf{g_5}$	6.2842E+02	0.0000

5.7 Conclusion

Reliability-based design optimization problems are very important in mechanical applications, but their resolution usually involves computational difficulties. In this chapter, a novel RBDO approach called RDS-MADE-NM has been presented for handling the mechanical problems. According to this integrated approach, the RDS concept is initially used to deal with the evaluation of the probabilistic constraints, and then the hybrid MADE-NM algorithm is applied to solve the formed deterministic optimization problem.

The performance of the proposed approach has been evaluated through six mechanical design problems including new RBDO formulations for two systems, the multiple disc clutch brake and pressure vessel. In the first four RBDO problems, the RDS-MADE-NM has been compared with different methods in the literature using double-loop, single-loop, and decoupled strategies. The comparative results have demonstrated obviously the superiority of the developed approach in terms of efficiency and robustness, with the least values of the function evaluations and standard deviation.

For the new RBDO problems, the results obtained by the developed approach have been compared with five metaheuristics implemented using the same probabilistic concept. According to the comparison results, the RDS-MADE-NM is more flexible and consistent to acquire the best solutions. Furthermore, to test the effectiveness of the new approach on complicated limit-state functions and objective functions, the RBDO for a real spur gear mechanism has been studied in this chapter. The found results have really revealed that RDS-MADE-NM is a promising RBDO tool that can be extended to further applications in mechanical engineering.

Conclusions and Future Research

Conclusions

Optimization in the real mechanical applications usually involves highly nonlinear and complex problems with many contradictory design requirements. The primary aim of the designer focuses not only to reduce the manufacturing cost of the structure, but also to improve significantly its performances. However, when taking into account the impact of uncertainties associated with the structural parameters, the reliability of the design becomes an interesting challenge in the optimization process. The present thesis hence attempts to contribute new optimization tools for addressing the complex mechanical design problems, while considering deterministic and reliability based approaches.

Along the course of the thesis, three main contributions have been introduced and discussed. The first contribution lies in the development of an efficient deterministic optimization approach capable of solving the design problems of mechanical engineering with continuous variables. The proposed method called Modified Adaptive Differential Evolution (MADE) is an improved variant of the DE algorithm with two modifications. Particularly, the values of mutation and crossover factors are updated automatically via the self-adaptive mechanism instead of the manual tuning. Meanwhile, the superiority of feasible points technique is used for the selection progress to select the better individuals instead of basic selection.

The effectiveness and applicability of the proposed MADE approach have been verified by optimizing four well-known engineering benchmarks which are the three bar truss, tension spring, welded beam, and hydrostatic thrust bearing. The numerical results obtained have demonstrated that the developed approach is very accurate and robust compared to the existing optimization methods in the literature. Besides, the MADE approach has showed good convergence speed to reach the best solution for the four tested problems.

The second contribution of the thesis presents the application of the developed MADE and three recent metaheuristics, namely, Grey Wolf Optimizer (GWO), Whale Optimization Algorithm (WOA), and Sine-Cosine Algorithm (SCA) for optimizing two cam-follower design problems. The former problem is a multi-objective optimization of a cam mechanism with offset roller follower translation, including the minimum congestion, the maximum performance, and the maximum cam durability. Unlike previous studies where only the main

design parameters of the system are used in the optimization procedure, the optimization model developed in this research considers more geometric parameters and more working conditions to improve the design quality. The second problem is a single-objective optimization of a cam mechanism with radial flat-face follower translation in which the size of the mechanism is minimized. The optimization process established here investigates the influence of the follower motion features on the size minimization of the system.

Several design constraints are observed during the optimization of the two cam mechanisms regarding performance indicators, such as pressure angle and efficiency, resistance indicators, such as radius of curvature and contact stress, as well as geometric restrictions. According to this, the final results obtained for the case studies have provided very useful information and fruitful decisions for the cam synthesis process. Among the four methods employed to solve the optimization problems, our developed MADE has displayed the better performance in terms of the solution quality and robustness whereas the SCA has demonstrated the weakest efficiency in this study.

The last contribution of this dissertation introduces an effective reliability-based optimization approach that is able of handling the mechanical design problems while accounting for the system uncertainties. The new proposed approach is a combination of the Reliable Design Space (RDS) technique and a hybrid optimization algorithm based on the developed MADE and the Nelder-Mead local search (NM). The RDS strategy is initially employed to convert the RBDO problem into a deterministic optimization one, by transforming probabilistic constraints to approximate deterministic constraints, and the hybrid MADE-NM is then used as an optimization tool. Additionally, the index technique is adopted in this approach to deal with the discrete and integer design variables.

The performance of the new integrated approach (RDS-MADE-NM) has been confirmed through solving six mechanical RBDO problems, comprising three examples with continuous variables (cantilever beam, vehicle side impact, and speed reducer), two examples with discrete variables (welded beam, and multiple disc clutch brake), and one with mixed variables (cylindrical pressure vessel). Overall, the simulation results have clearly demonstrated that the proposed approach performs very well with the high robustness and the reasonable computational cost. In particular, the first two examples have verified that RDS-MADE-NM is effective for both weakly and highly dimensional RBDO problems, respectively. By solving the speed reducer design problem, the proposed approach have showed a high capability to handle a mixture of probabilistic and deterministic constraints,

both random and deterministic design variables, as well as with varying variance. The last three examples have proved that RDS-MADE-NM is competent for the discrete and the mixed RBDO problems.

Furthermore, RDS-MADE-NM has been used to solve the RBDO problem of a real spur gear mechanism. The obtained results of the studied case have revealed the efficacy and accuracy of the new approach in solving mechanical engineering problems with computational complexities. This confirms that the RDS-MADE-NM is a promising RBDO approach to deal with real industrial cases. It is important to notice that the RBDO for the multiple disc clutch brake and pressure vessel structures have been formulated in this study for the first time. For both problems, the validity of the new obtained solutions has been checked by FORM approximation and Monte Carlo Simulation. This will allow to use these two examples as benchmarks in RBDO studies in the future.

Future Research

Based on the results obtained in this dissertation, recommendations for future work will be focused on two tasks:

- First, most studies in the field of cam design optimization are based on deterministic approaches without modeling the potential uncertainties, which usually leads to a final design with a high chance of failure. In the near future, the developed RDS-MADE-NM approach will be applied to cam-follower mechanisms in order to compromise between the objectives to be optimized and the design reliability. Moreover, it would be interesting to increase cam performance by using more efficient curves of follower motion, such as the class of spline functions, as well as including additional constraints, such as those associated with the velocity and acceleration limits.
- Second, the probabilistic optimization approach developed in this research has only been applied to mechanical problems with explicit behavior and the random quantities treated have only been assumed to follow Gaussian distributions, i.e., normal, log-normal. Therefore, it seems promising to extend the RDS-MADE-NM to deal with real implicit systems involving finite element and CAD models. In addition, the integration of RDS-MADE-NM into probabilistic transformation techniques for handling random variables with non-Gaussian distributions is also suggested to be further investigated.

Appendix

Annex A

The partial derivatives of the first function $g_1(d,\mu_z)$ with respect to the mean vector μ_z:

$$\frac{\partial g_1(d,\mu_z)}{\partial \mu_{z1}}=1, \qquad \frac{\partial g_1(d,\mu_z)}{\partial \mu_{z2}}=-\frac{600}{d_1 {d_2}^2}, \qquad \frac{\partial g_1(d,\mu_z)}{\partial \mu_{z3}}=-\frac{600}{{d_1}^2 d_2}, \qquad \frac{\partial g_1(d,\mu_z)}{\partial \mu_{z4}}=0.$$

The partial derivatives of the second function $g_2(d,\mu_z)$ with respect to the mean vector μ_z:

$$\frac{\partial g_2(d,\mu_z)}{\partial \mu_{z1}}=0, \qquad \frac{\partial g_2(d,\mu_z)}{\partial \mu_{z2}}=-\frac{4L^3\mu_{z2}}{\mu_{z4} d_1 {d_2}^5\sqrt{\left(\frac{\mu_{z2}}{{d_2}^2}\right)^2+\left(\frac{\mu_{z3}}{{d_1}^2}\right)^2}},$$

$$\frac{\partial g_2(d,\mu_z)}{\partial \mu_{z3}}=-\frac{4L^3\mu_{z3}}{\mu_{z4} {d_1}^5 d_2\sqrt{\left(\frac{\mu_{z2}}{{d_2}^2}\right)^2+\left(\frac{\mu_{z3}}{{d_1}^2}\right)^2}}, \qquad \frac{\partial g_2(d,\mu_z)}{\partial \mu_{z4}}=\frac{4L^3}{(\mu_{z4})^2 d_1 d_2}\sqrt{\left(\frac{\mu_{z2}}{{d_2}^2}\right)^2+\left(\frac{\mu_{z3}}{{d_1}^2}\right)^2}.$$

Annex B

B.1. Vehicle side impact problem

Mathematical formulation of the probabilistic constraints of the vehicle side impact problem:

$$g_1=1-F_{AL}, \quad g_2=32-D_{up}, \quad g_3=32-D_{mid}, \quad g_4=32-D_{law}, \quad g_5=0.32-VC_{up},$$

$$g_6=0.32-VC_{mid}, \quad g_7=0.32-VC_{law}, \quad g_8=4-F_{ps}, \quad g_9=9.9-V_{B-Pillar}, \quad g_{10}=15.69-V_{door}.$$

where

$$F_{AL}=1.16-0.3717x_2x_4-0.00931x_2p_3-0.484x_3p_2+0.01343x_6p_4.$$

$$D_{up}=28.98+3.818x_3-4.2x_1x_2+0.0207x_5p_3+6.63x_6p_2-7.7x_7p_1+0.32p_2p_3.$$

$$D_{mid}=33.86+2.95x_3+0.1792p_3-5.057x_1x_2-11.0x_2p_1-0.0215x_5p_3-9.98x_7p_1+22.0p_1p_2.$$

$$D_{law}=46.36-9.9x_2-12.9x_1p_1+0.1107x_3p_3.$$

$$VC_{up}=0.261-0.0159x_1x_2-0.188x_1p_1-0.019x_2x_7+0.0144x_3x_5+0.0008757x_5p_3+0.08045x_6p_2$$
$$+0.00139p_1p_4+0.00001575p_3p_4.$$

$$VC_{mid}=0.214+0.00817x_5-0.131x_1p_1-0.0704x_1p_2+0.03099x_2x_6-0.018x_2x_7+0.0208x_3p_1$$
$$+0.121x_3p_2-0.00364x_5x_6+0.0007715x_5p_3-0.0005354x_6p_3+0.00121p_1p_4.$$

$$VC_{law} = 0.74 - 0..61x_2 - 0.163x_3 p_1 + 0.001232x_3 p_3 - 0.166x_7 p_2 + 0.227{x_2}^2.$$

$$F_{ps} = 4.72 - 0.5x_4 - 0.19x_2 x_3 - 0.0122x_4 p_3 + 0.009325x_6 p_3 + 0.000191{p_4}^2.$$

$$V_{B-Pillar} = 10.58 - 0.674x_1 x_2 - 1.95x_2 p_1 + 0.02054x_3 p_3 - 0.0198x_4 p_3 + 0.028x_6 p_3.$$

$$V_{door} = 16.45 - 0.489x_3 x_7 - 0.843x_5 x_6 + 0.0432p_2 p_3 - 0.0556p_2 p_4 - 0.000786{p_4}^2.$$

B.2. Speed reducer problem

Mathematical formulas of the constraints of the speed reducer problem:

$$g_1 = 1 - \frac{p_1}{x_1 {d_1}^2 d_2}, \qquad g_2 = 1 - \frac{p_2}{x_1 {d_1}^2 {d_2}^2}, \qquad g_3 = 1 - \frac{p_3 x_2^3}{x_4^4 d_1 d_2}, \qquad g_4 = 1 - \frac{p_4 x_3^3}{x_5^4 d_1 d_2},$$

$$g_5 = 1 - \frac{0.5\sqrt{\left(\frac{p_6 x_2}{d_1 d_2}\right)^2 + p_7}}{p_8 p_5 x_4^3}, \qquad g_6 = 1 - \frac{0.5\sqrt{\left(\frac{p_6 x_3}{d_1 d_2}\right)^2 + p_9}}{p_8 p_{10} x_5^3}, \qquad g_7 = 1 - \frac{0.5 p_{11} d_1}{x_1},$$

$$g_8 = 1 - \frac{x_1}{p_{12} d_1}, \qquad g_9 = 1 - \frac{0.5(p_{13} x_4 + p_{15})}{x_2}, \qquad g_{10} = 1 - \frac{0.5(p_{14} x_5 + p_{15})}{x_3}, \qquad g_{11} = 1 - \frac{d_1 d_2}{80},$$

B.3. Welded beam problem

Mathematical formulas of the probabilistic constraints of the welded beam problem:

$$g_1 = 1 - \frac{\tau(x, p)}{p_6}, \qquad g_2 = 1 - \frac{\sigma(x, p)}{p_7}, \qquad g_3 = 1 - \frac{x_1}{x_4}, \qquad g_4 = 1 - \frac{\delta(x, p)}{p_5}, \qquad g_5 = \frac{P_c(x, p)}{p_1} - 1.$$

where

$$\tau(x, p) = \sqrt{(\tau')^2 + (\tau'')^2 + 2\tau'\tau''\frac{x_2}{2R}}, \qquad \tau' = \frac{p_1}{\sqrt{2}x_1 x_2}, \qquad \tau'' = \frac{MR}{J}, \qquad M = p_1\left(p_2 + \frac{x_2}{2}\right),$$

$$R = \sqrt{\frac{x_2^2 + (x_1 + x_3)^2}{4}}, \quad J = \sqrt{2}x_1 x_2\left(\frac{x_2^2}{12} + \frac{(x_1 + x_3)^2}{4}\right), \quad \sigma(x, p) = \frac{6p_1 p_2}{x_3^2 x_4}, \qquad \delta(x, p) = \frac{4p_1 p_2^3}{p_3 x_3^3 x_4},$$

$$P_c(x, p) = \frac{4.013x_3 x_4^3\sqrt{p_3 p_4}}{6p_2^2}\left(1 - \frac{x_3}{4p_2}\sqrt{\frac{p_3}{p_4}}\right)$$

B.4. Multiple disc clutch brake problem

Mathematical formulation of the probabilistic constraints of the multiple disc clutch brake problem:

$$g_1 = x_2 - x_1 - p_1, \qquad g_2 = p_2 - (d_1 + 1)(x_3 + p_3), \qquad g_3 = p_5 - \frac{x_4}{\pi\left(x_2^2 - x_1^2\right)},$$

$$g_4 = p_4 p_5 - \frac{0.005 x_4 \left(x_2^3 - x_1^3\right)}{54\left(x_2^2 - x_1^2\right)^2}, \qquad g_5 = p_4 - \frac{0.005\pi\left(x_2^3 - x_1^3\right)}{54\left(x_2^2 - x_1^2\right)},$$

$$g_6 = 15 - \frac{25\pi p_7}{3(M + p_8)}, \qquad g_7 = M - 1.5 p_9, \qquad g_8 = \frac{25\pi p_7}{3(M + p_8)}.$$

where

$$M = 0.002 p_6 x_4 d_1 \frac{x_2^3 - x_1^3}{3(x_2^2 - x_1^2)}$$

Bibliography

Abderazek, H., Ferhat, D., Atanasovska, I., & Boualem, K. (2015). A differential evolution algorithm for tooth profile optimization with respect to balancing specific sliding coefficients of involute cylindrical spur and helical gears. *Advances in Mechanical Engineering, 7*(9), 1687814015605008.

Abderazek, H., Ferhat, D., & Ivana, A. (2017). Adaptive mixed differential evolution algorithm for bi-objective tooth profile spur gear optimization. *The International Journal of Advanced Manufacturing Technology, 90*(5-8), 2063-2073.

Abderazek, H., Yildiz, A. R., & Mirjalili, S. (2020). Comparison of recent optimization algorithms for design optimization of a cam-follower mechanism. *Knowledge-Based Systems, 191*, 105237.

Angeles, J., & López-Cajún, C. S. (2012). *Optimization of cam mechanisms* (Vol. 9): Springer Science & Business Media.

António, C. C. (2001). A hierarchical genetic algorithm for reliability based design of geometrically non-linear composite structures. *Composite Structures, 54*(1), 37-47.

Aoues, Y., & Chateauneuf, A. (2010). Benchmark study of numerical methods for reliability-based design optimization. *Structural and Multidisciplinary Optimization, 41*(2), 277-294.

Arora, J. S. (1990). Computational design optimization: a review and future directions. *Structural Safety, 7*(2-4), 131-148.

Arora, J. S. (2004). *Introduction to optimum design*: Elsevier.

Arthur, G., George, N., & Sridhar, K. (2001). Mechanism design analysis and synthesis volume I: Prentice-Hall, Upper Saddle River, NJ.

Askari, Q., Younas, I., & Saeed, M. (2020). Political Optimizer: A novel socio-inspired meta-heuristic for global optimization. *Knowledge-Based Systems*, 105709.

Atanasovska, I., Mitrovic, R., & Momcilovic, D. (2013). *Explicit parametric method for optimal spur gear tooth profile definition.* Paper presented at the Advanced Materials Research.

Atanasovska, I., Mitrović, R., Momčilović, D., & Subic, A. (2010). Analysis of the nominal load effects on gear load capacity using the finite-element method. *Proceedings of the*

Institution of Mechanical Engineers, Part C: Journal of Mechanical Engineering Science, 224(11), 2539-2548.

Au, S.-K., & Beck, J. L. (2001). Estimation of small failure probabilities in high dimensions by subset simulation. *Probabilistic engineering mechanics, 16*(4), 263-277.

Bekdaş, G., Nigdeli, S. M., Kayabekir, A. E., & Yang, X.-S. (2019). Optimization in civil engineering and metaheuristic algorithms: A review of state-of-the-art developments *Computational intelligence, optimization and inverse problems with applications in engineering* (pp. 111-137): Springer.

Belegundu, A., & Rajan, S. (1988). A shape optimization approach based on natural design variables and shape functions. *Computer Methods in Applied Mechanics and Engineering, 66*(1), 87-106.

Berzak, N. (1982). Optimization of Cam-follower systems with kinematic and dynamic constraints.

Beyer, H.-G., & Schwefel, H.-P. (2002). Evolution strategies–A comprehensive introduction. *Natural computing, 1*(1), 3-52.

Birattari, M., Paquete, L., Stützle, T., & Varrentrapp, K. (2001). Classification of metaheuristics and design of experiments for the analysis of components. *Teknik Rapor, AIDA-01-05*.

Biswas, P. P., Suganthan, P. N., Mallipeddi, R., & Amaratunga, G. A. (2018). Optimal power flow solutions using differential evolution algorithm integrated with effective constraint handling techniques. *Engineering Applications of Artificial Intelligence, 68*, 81-100.

BoussaïD, I., Lepagnot, J., & Siarry, P. (2013). A survey on optimization metaheuristics. *Information sciences, 237*, 82-117.

Bouzakis, K., Mitsi, S., & Tsiafis, J. (1997). Computer-aided optimum design and NC milling of planar cam mechanisms. *International Journal of Machine Tools and Manufacture, 37*(8), 1131-1142.

Breitung, K. (1984). Asymptotic approximations for multinormal integrals. *Journal of Engineering Mechanics, 110*(3), 357-366.

Brest, J., Greiner, S., Boskovic, B., Mernik, M., & Zumer, V. (2006). Self-adapting control parameters in differential evolution: A comparative study on numerical benchmark problems. *IEEE transactions on evolutionary computation, 10*(6), 646-657.

Buhl, T., Pedersen, C. B., & Sigmund, O. (2000). Stiffness design of geometrically nonlinear structures using topology optimization. *Structural and Multidisciplinary Optimization, 19*(2), 93-104.

Carter, A. D. S. (1997). *Mechanical reliability and design*: Macmillan International Higher Education.

Cavazzuti, M. (2012). *Optimization methods: from theory to design scientific and technological aspects in mechanics*: Springer Science & Business Media.

Chakri, A., Yang, X.-S., Khelif, R., & Benouaret, M. (2018). Reliability-based design optimization using the directional bat algorithm. *Neural Computing and Applications, 30*(8), 2381-2402.

Champasak, P., Panagant, N., Pholdee, N., Bureerat, S., & Yildiz, A. R. (2020). Self-adaptive many-objective meta-heuristic based on decomposition for many-objective conceptual design of a fixed wing unmanned aerial vehicle. *Aerospace Science and Technology, 100*, 105783.

Chan, Y. W., & Sim, S. K. (1998). Optimum cam design using the Monte Carlo optimization technique. *Journal of Engineering Design, 9*(1), 29-45.

Chang, W. (1996). Repetitive control of a high-speed cam-follower system, *Ph. D. Dissertation, Lehigh University*.

Chen, F. (1973). Kinematic synthesis of cam profiles for prescribed acceleration by a finite integration method.

Chen, F. Y. (1969). An algorithm for computing the contour of a slow speed cam. *Journal of Mechanisms, 4*(2), 171-175.

Chen, F. Y. (1972). A refined algorithm for finite-difference synthesis of cam profiles. *Mechanism and Machine Theory, 7*(4), 453-460.

Chen, F. Y. (1982). *Mechanics and design of cam mechanisms*: Pergamon Pr.

Chen, J., Tang, Y., Ge, R., An, Q., & Guo, X. (2013). Reliability design optimization of composite structures based on PSO together with FEA. *Chinese Journal of Aeronautics, 26*(2), 343-349.

Chen, X., Hasselman, T., Neill, D., Chen, X., Hasselman, T., & Neill, D. (1997). *Reliability based structural design optimization for practical applications.* Paper presented at the 38th Structures, structural dynamics, and materials conference.

Chen, Z., Qiu, H., Gao, L., Su, L., & Li, P. (2013). An adaptive decoupling approach for reliability-based design optimization. *Computers & structures, 117*, 58-66.

Cheng, G., Xu, L., & Jiang, L. (2006). A sequential approximate programming strategy for reliability-based structural optimization. *Computers & structures, 84*(21), 1353-1367.

Cheng, W.-T. (2002). Synthesis of universal motion curves in generalized model. *J. Mech. Des., 124*(2), 284-293.

Chew, M., & Chuang, C. (1995). Minimizing residual vibrations in high-speed cam-follower systems over a range of speeds.

Chew, M., Freudenstein, F., & Longman, R. (1983). Application of optimal control theory to the synthesis of high-speed cam-follower systems. Part 1: Optimality criterion.

Cho, T. M., & Lee, B. C. (2011). Reliability-based design optimization using convex linearization and sequential optimization and reliability assessment method. *Structural Safety, 33*(1), 42-50.

Civicioglu, P., & Besdok, E. (2013). A conceptual comparison of the Cuckoo-search, particle swarm optimization, differential evolution and artificial bee colony algorithms. *Artificial intelligence review, 39*(4), 315-346.

Coello, C. A. C. (2000). Treating constraints as objectives for single-objective evolutionary optimization. *Engineering Optimization+ A35, 32*(3), 275-308.

Coello, C. A. C. (2002). Theoretical and numerical constraint-handling techniques used with evolutionary algorithms: a survey of the state of the art. *Computer Methods in Applied Mechanics and Engineering, 191*(11-12), 1245-1287.

Cracks, S. F. (1992). Mechanical Engineering Publications Limited: London.

Cuevas, E., & Cienfuegos, M. (2014). A new algorithm inspired in the behavior of the social-spider for constrained optimization. *Expert Systems with Applications, 41*(2), 412-425.

Das, S., & Suganthan, P. N. (2010). Differential evolution: A survey of the state-of-the-art. *IEEE transactions on evolutionary computation, 15*(1), 4-31.

Deb, K. (2000). An efficient constraint handling method for genetic algorithms. *Computer Methods in Applied Mechanics and Engineering, 186*(2-4), 311-338.

Deb, K. (2001). *Multi-objective optimization using evolutionary algorithms* (Vol. 16): John Wiley & Sons.

Deb, K. (2012). *Optimization for engineering design: Algorithms and examples*: PHI Learning Pvt. Ltd.

Deb, K., Gupta, S., Daum, D., Branke, J., Mall, A. K., & Padmanabhan, D. (2009). Reliability-based optimization using evolutionary algorithms. *IEEE transactions on evolutionary computation, 13*(5), 1054-1074.

Deb, K., Pratap, A., Agarwal, S., & Meyarivan, T. (2002). A fast and elitist multiobjective genetic algorithm: NSGA-II. *IEEE transactions on evolutionary computation, 6*(2), 182-197.

Dhande, S., Bhadoria, B., & Chakraborty, J. (1975). A unified approach to the analytical design of three-dimensional cam mechanisms.

Ding, D., Shen, K., Chen, X., Chen, H., Chen, J., Fan, T., . . . Li, Y. (2018). Multi-level architecture optimization of MOF-templated Co-based nanoparticles embedded in hollow N-doped carbon polyhedra for efficient OER and ORR. *ACS Catalysis, 8*(9), 7879-7888.

Diwekar, U. (2008). *Introduction to applied optimization* (Vol. 22): Springer Science & Business Media.

Djeddou, F., Smata, L., & Ferhat, H. (2018). Optimization and a reliability analysis of a cam-roller follower mechanism. *Journal of Advanced Mechanical Design, Systems, and Manufacturing, 12*(7), JAMDSM0121-JAMDSM0121.

Dorigo, M., Birattari, M., & Stutzle, T. (2006). Ant colony optimization. *IEEE computational intelligence magazine, 1*(4), 28-39.

Dragoi, E. N., & Curteanu, S. (2016). The use of differential evolution algorithm for solving chemical engineering problems. *Reviews in Chemical Engineering, 32*(2), 149-180.

Du, X., & Chen, W. (2001). A most probable point-based method for efficient uncertainty analysis. *Journal of Design and Manufacturing automation, 4*(1), 47-66.

Du, X., & Chen, W. (2004). Sequential optimization and reliability assessment method for efficient probabilistic design. *J. Mech. Des., 126*(2), 225-233.

Dudley, W. M. (1948). *New methods in valve cam design* (0148-7191). Retrieved from

Enevoldsen, I., & Sørensen, J. D. (1994). Reliability-based optimization in structural engineering. *Structural Safety, 15*(3), 169-196.

Eskandar, H., Sadollah, A., Bahreininejad, A., & Hamdi, M. (2012). Water cycle algorithm–A novel metaheuristic optimization method for solving constrained engineering optimization problems. *Computers & structures, 110*, 151-166.

Fabien, B., Longman, R., & Freudenstein, F. (1994). The design of high-speed dwell-rise-dwell cams using linear quadratic optimal control theory.

Fan, H.-Y., & Lampinen, J. (2003). A trigonometric mutation operation to differential evolution. *Journal of global optimization, 27*(1), 105-129.

Fenrich, R. W., & Alonso, J. J. (2019). *Sequential Reliability-Based Design Optimization via Anchored Decomposition*. Paper presented at the AIAA Scitech 2019 Forum.

Fletcher, R., & Reeves, C. M. (1964). Function minimization by conjugate gradients. *The computer journal, 7*(2), 149-154.

Flocker, F. W. (2009). Addressing cam wear and follower jump in single-dwell cam-follower systems with an adjustable modified trapezoidal acceleration cam profile. *Journal of engineering for gas turbines and power, 131*(3).

Flores, P. (2013). A computational approach for cam size optimization of disc cam-follower mechanisms with translating roller followers. *Journal of Mechanisms and Robotics, 5*(4).

Fogel, L. J., Owens, A. J., & Walsh, M. J. (1966). Adaption of evolutionary programming to the prediction of solar flares.

Gandomi, A. H. (2014). Interior search algorithm (ISA): a novel approach for global optimization. *ISA transactions, 53*(4), 1168-1183.

Gandomi, A. H., & Alavi, A. H. (2012). Krill herd: a new bio-inspired optimization algorithm. *Communications in nonlinear science and numerical simulation, 17*(12), 4831-4845.

Gass, S., & Saaty, T. (1955). The computational algorithm for the parametric objective function. *Naval research logistics quarterly, 2*(1-2), 39-45.

Gasser, M., & Schuëller, G. (1998). Some basic principles of reliability-based optimization (RBO) of structures and mechanical components. Stochastic programming methods and technical applications (pp. 80-103): Springer.

Geem, Z. W., Kim, J. H., & Loganathan, G. V. (2001). A new heuristic optimization algorithm: harmony search. *simulation, 76*(2), 60-68.

Gong, W., Cai, Z., & Liang, D. (2014). Engineering optimization by means of an improved constrained differential evolution. *Computer Methods in Applied Mechanics and Engineering, 268*, 884-904.

González-Palacios, M. A., & Angeles, J. (2012). *Cam synthesis* (Vol. 26): Springer Science & Business Media.

Gu, L., Yang, R., Tho, C.-H., Makowskit, M., Faruquet, O., & Y. Li, Y. L. (2001). Optimisation and robustness for crashworthiness of side impact. *International journal of vehicle design, 26*(4), 348-360.

H Bravo, R., & W Flocker, F. (2011). Optimizing cam profiles using the particle swarm technique. *Journal of Mechanical Design, 133*(9).

Haftka, R. T., & Gürdal, Z. (2012). *Elements of structural optimization* (Vol. 11): Springer Science & Business Media.

Haimes, Y. (1971). On a bicriterion formulation of the problems of integrated system identification and system optimization. *IEEE transactions on systems, man, and cybernetics, 1*(3), 296-297.

Haldar, A., & Mahadevan, S. (2000). *Probability, reliability, and statistical methods in engineering design*: J. Wiley & Sons, Incorporated.

Halicioglu, R., Dulger, L. C., & Bozdana, A. T. (2017). Modeling, design, and implementation of a servo press for metal-forming application. *The International Journal of Advanced Manufacturing Technology, 91*(5-8), 2689-2700.

Halicioglu, R., Dulger, L. C., & Bozdana, A. T. (2018). Improvement of metal forming quality by motion design. *Robotics and Computer-Integrated Manufacturing, 51*, 112-120.

Hamid, N. F. A., Rahim, N. A., & Selvaraj, J. (2016). Solar cell parameters identification using hybrid Nelder-Mead and modified particle swarm optimization. *Journal of Renewable and Sustainable Energy, 8*(1), 015502.

Hamza, F., Abderazek, H., Lakhdar, S., Ferhat, D., & Yıldız, A. R. (2018). Optimum design of cam-roller follower mechanism using a new evolutionary algorithm. *The International Journal of Advanced Manufacturing Technology, 99*(5-8), 1267-1282.

Hasofer, A. M., & Lind, N. C. (1974). Exact and invariant second-moment code format. *Journal of the Engineering Mechanics division, 100*(1), 111-121.

Hertz, H. (1881). On the contact of elastic solids. *Z. Reine Angew. Mathematik, 92*, 156-171.

Ho-Huu, V., Le-Duc, T., Le-Anh, L., Vo-Duy, T., & Nguyen-Thoi, T. (2018). A global single-loop deterministic approach for reliability-based design optimization of truss structures with continuous and discrete design variables. *Engineering Optimization, 50*(12), 2071-2090.

Ho-Huu, V., Nguyen-Thoi, T., Nguyen-Thoi, M., & Le-Anh, L. (2015). An improved constrained differential evolution using discrete variables (D-ICDE) for layout optimization of truss structures. *Expert Systems with Applications, 42*(20), 7057-7069.

Ho-Huu, V., Nguyen-Thoi, T., Truong-Khac, T., Le-Anh, L., & Vo-Duy, T. (2018). An improved differential evolution based on roulette wheel selection for shape and size optimization of truss structures with frequency constraints. *Neural Computing and Applications, 29*(1), 167-185.

Ho-Huu, V., Vo-Duy, T., Luu-Van, T., Le-Anh, L., & Nguyen-Thoi, T. (2016). Optimal design of truss structures with frequency constraints using improved differential evolution algorithm based on an adaptive mutation scheme. Automation in construction, 68, 81-94.

Holland, J. (1975). adaptation in natural and artificial systems, university of michigan press, ann arbor,". *Cité page, 100*.

Hu, H., & Li, G. (2014). Granular risk-based design optimization. *IEEE Transactions on Fuzzy Systems, 23*(2), 340-353.

Huang, Z., Jiang, C., Zhou, Y., Luo, Z., & Zhang, Z. (2016). An incremental shifting vector approach for reliability-based design optimization. *Structural and Multidisciplinary Optimization, 53*(3), 523-543.

Hwang, W.-M., & Yu, C. (2005). Optimal synthesis of the adjustable knock-out cam-follower mechanism of a bolt former. *Proceedings of the Institution of Mechanical Engineers, Part C: Journal of Mechanical Engineering Science, 219*(8), 767-774.

Jaimes, A. L., Martınez, S. Z., & Coello, C. A. C. (2009). An introduction to multiobjective optimization techniques. *Optimization in Polymer Processing*, 29-57.

Jamkhande, A., Tikar, S., Ramdasi, S., & Marathe, N. (2012). *Design of high speed engine's cam profile using B-spline functions for controlled dynamics* (0148-7191). Retrieved from

Jana, R., & Bhattacharjee, P. (2017). A multi-objective genetic algorithm for design optimisation of simple and double harmonic motion cams. *International Journal of Design Engineering, 7*(2), 77-91.

JCSS, J. (2001). Probabilistic Model Code: Joint Committee on Structural Safety. *JCSS, Japan*.

Jia, G., Wang, Y., Cai, Z., & Jin, Y. (2013). An improved (μ+ λ)-constrained differential evolution for constrained optimization. *Information sciences, 222*, 302-322.

Jiang, C., Qiu, H., Gao, L., Cai, X., & Li, P. (2017). An adaptive hybrid single-loop method for reliability-based design optimization using iterative control strategy. *Structural and Multidisciplinary Optimization, 56*(6), 1271-1286.

Jiang, L. L., Maskell, D. L., & Patra, J. C. (2013). Parameter estimation of solar cells and modules using an improved adaptive differential evolution algorithm. *Applied Energy, 112*, 185-193.

Juárez-Castillo, E., Acosta-Mesa, H.-G., & Mezura-Montes, E. (2019). Adaptive boundary constraint-handling scheme for constrained optimization. *Soft Computing, 23*(17), 8247-8280.

Kanzaki, K., & Itao, K. (1972). Polydyne cam mechanisms for typehead positioning.

Kaplan, H. (2014). Mathematical modeling and simulation of high-speed cam mechanisms to minimize residual vibrations. *Proceedings of the Institution of Mechanical Engineers, Part C: Journal of Mechanical Engineering Science, 228*(13), 2402-2415.

Kapucu, S., DAS, M. T., & Kiliç, A. (2010). Cam motion tuning of shedding mechanism for vibration reduction of heald frame. *Gazi University Journal of Science, 23*(2), 227-232.

Karaboga, D., & Basturk, B. (2007). A powerful and efficient algorithm for numerical function optimization: artificial bee colony (ABC) algorithm. *Journal of global optimization, 39*(3), 459-471.

Kaveh, A., & Farhoudi, N. (2013). A new optimization method: Dolphin echolocation. *Advances in Engineering Software, 59*, 53-70.

Kaveh, A., & Khayatazad, M. (2012). A new meta-heuristic method: ray optimization. *Computers & structures, 112*, 283-294.

Kawaji, S., & Kogiso, N. (2013). *Convergence improvement of reliability-based multiobjective optimization using hybrid MOPSO.* Paper presented at the 10th world congress on structural and multidisciplinary optimization, Orlando.

Kennedy, J., & Eberhart, R. (1995). *Particle swarm optimization.* Paper presented at the Proceedings of ICNN'95-International Conference on Neural Networks.

Kim, J., Ahn, K., & Kim, S. (2002). Optimal synthesis of a spring-actuated cam mechanism using a cubic spline. *Proceedings of the Institution of Mechanical Engineers, Part C: Journal of Mechanical Engineering Science, 216*(9), 875-883.

Kirjner-Neto, C., Polak, E., & Der Kiureghian, A. (1998). An outer approximations approach to reliability-based optimal design of structures. *Journal of optimization theory and applications, 98*(1), 1-16.

Kirkpatrick, S., Gelatt, C. D., & Vecchi, M. P. (1983). Optimization by simulated annealing. *Science, 220*(4598), 671-680.

Kirsch, U. (1989). Optimal topologies of structures.

Koza, J. R. (1994). Genetic programming II: Automatic discovery of reusable subprograms. *Cambridge, MA, USA, 13*(8), 32.

Kramer, O. (2010). A review of constraint-handling techniques for evolution strategies. *Applied Computational Intelligence and Soft Computing, 2010*.

Kukkonen, S., & Lampinen, J. (2006). *Constrained real-parameter optimization with generalized differential evolution*. Paper presented at the 2006 IEEE International Conference on Evolutionary Computation.

Kusano, I., Baldomir, A., Jurado, J. Á., & Hernández, S. (2014). Reliability based design optimization of long-span bridges considering flutter. Journal of Wind Engineering and Industrial Aerodynamics, 135, 149-162.

Kuster, J., & Mize, J. (1973). Box's Complex Algorithm in Optimization Techniques with Fortran.

Kwakernaak, H., & Smit, J. (1968). Minimum vibration cam profiles. *Journal of Mechanical Engineering Science, 10*(3), 219-227.

Lee, J.-O., Yang, Y.-S., & Ruy, W.-S. (2002). A comparative study on reliability-index and target-performance-based probabilistic structural design optimization. *Computers & structures, 80*(3-4), 257-269.

Lee, J. J., & Lee, B. C. (2005). Efficient evaluation of probabilistic constraints using an envelope function. *Engineering Optimization, 37*(2), 185-200.

Li, F., Wu, T., Badiru, A., Hu, M., & Soni, S. (2013). A single-loop deterministic method for reliability-based design optimization. *Engineering Optimization, 45*(4), 435-458.

Li, F., Wu, T., Hu, M., & Dong, J. (2010). An accurate penalty-based approach for reliability-based design optimization. *Research in Engineering Design, 21*(2), 87-98.

Li, G., & Hu, H. (2014). Risk design optimization using many-objective evolutionary algorithm with application to performance-based wind engineering of tall buildings. *Structural Safety, 48*, 1-14.

Li, G., Meng, Z., & Hu, H. (2015). An adaptive hybrid approach for reliability-based design optimization. *Structural and Multidisciplinary Optimization, 51*(5), 1051-1065.

Liang, J., Mourelatos, Z. P., & Nikolaidis, E. (2007). A single-loop approach for system reliability-based design optimization.

Liang, J., Mourelatos, Z. P., & Tu, J. (2008). A single-loop method for reliability-based design optimisation. *International Journal of Product Development, 5*(1-2), 76-92.

Liao, K.-W., & Biton, N. I. D. (2019). A heuristic moment-based framework for optimization design under uncertainty. *Engineering with Computers*, 1-14.

Liao, K.-W., & Ivan, G. (2014). A single loop reliability-based design optimization using EPM and MPP-based PSO. *Latin American Journal of Solids and Structures, 11*(5), 826-847.

Liao, S.-H., Hsieh, J.-G., Chang, J.-Y., & Lin, C.-T. (2015). Training neural networks via simplified hybrid algorithm mixing Nelder–Mead and particle swarm optimization methods. *Soft Computing, 19*(3), 679-689.

Libertiny, G. Z. (1997). Safe design without safety factors. *American Society of Mechanical Engineers (Paper), Dallas, TX, USA*.

Lieu, Q. X., Do, D. T., & Lee, J. (2018). An adaptive hybrid evolutionary firefly algorithm for shape and size optimization of truss structures with frequency constraints. *Computers & structures, 195*, 99-112.

LIN, A. C., CHANG, H., & WANG, H.-P. (1988). Computerized design and manufacturing of plate cams. *The International Journal Of Production Research, 26*(8), 1395-1430.

Lobato, F., Steffen Jr, V., & Neto, A. S. (2012). Estimation of space-dependent single scattering albedo in a radiative transfer problem using differential evolution. *Inverse Problems in Science and Engineering, 20*(7), 1043-1055.

Lobato, F. S., Gonçalves, M. S., Jahn, B., Cavalini, A. A., & Steffen, V. (2017). Reliability-based optimization using differential evolution and inverse reliability analysis for engineering system design. *Journal of optimization theory and applications, 174*(3), 894-926.

Loprencipe, G. C.-D. D.-G., & Ranzo, A. (2001). Spline Curves for Geometric Modelling of Highway Design.

Madsen, H. O., Krenk, S., & Lind, N. C. (2006). *Methods of structural safety*: Courier Corporation.

Masmoudi, M., Guillaume, P., & Broudiscou, C. (1995). Application of automatic differentiation to optimal shape design *Advances in structural optimization* (pp. 413-446): Springer.

Masood, S. (1999). A CAD/CAM system for high performance precision drum cams. *The International Journal of Advanced Manufacturing Technology, 15*(1), 32-37.

Mastinu, G., Gobbi, M., & Miano, C. (2007). Optimal design of complex mechanical systems: with applications to vehicle engineering: Springer Science & Business Media.

Mathakari, S., Gardoni, P., Agarwal, P., Raich, A., & Haukaas, T. (2007). Reliability-based optimal design of electrical transmission towers using multi-objective genetic algorithms. *Computer-Aided Civil and Infrastructure Engineering, 22*(4), 282-292.

Melchers, R. E. (1999). Structural Reliability Analysis and Prediction–John Wiley & Sons. *New York, NY*.

Mezura-Montes, E. (2009). Constraint-Handling in Evolutionary Optimization: UNIV NAC LA PLATA, FAC INFORMATICA 50 Y 115, 1ER PISO, LA PLATA, 1900, ARGENTINA.

Meng, Z., Li, G., Wang, X., Sait, S. M., & Yıldız, A. R. A. (2020). Comparative Study of Metaheuristic Algorithms for Reliability-Based Design Optimization Problems. DOI: 10.1007/s11831-020-09443-z

Mezura-Montes, E., & Coello, C. A. C. (2011). Constraint-handling in nature-inspired numerical optimization: past, present and future. *Swarm and Evolutionary Computation, 1*(4), 173-194.

Mezura-Montes, E., Coello Coello, C., Velázquez-Reyes, J., & Muñoz-Dávila, L. (2007). Multiple trial vectors in differential evolution for engineering design. *Engineering Optimization, 39*(5), 567-589.

Mirjalili, S. (2016). SCA: a sine cosine algorithm for solving optimization problems. *Knowledge-Based Systems, 96*, 120-133.

Mirjalili, S., & Lewis, A. (2016). The whale optimization algorithm. *Advances in Engineering Software, 95*, 51-67.

Mirjalili, S., Mirjalili, S. M., & Lewis, A. (2014). Grey wolf optimizer. *Advances in Engineering Software, 69*, 46-61.

Moezi, S. A., Zakeri, E., & Zare, A. (2018). Structural single and multiple crack detection in cantilever beams using a hybrid Cuckoo-Nelder-Mead optimization method. *Mechanical Systems and Signal Processing, 99*, 805-831.

Mohamed, A. W. (2018). A novel differential evolution algorithm for solving constrained engineering optimization problems. *Journal of Intelligent Manufacturing, 29*(3), 659-692.

Mohamed, A. W., & Sabry, H. Z. (2012). Constrained optimization based on modified differential evolution algorithm. *Information sciences, 194*, 171-208.

Moise, V., Ene, M., Tabara, I., & Dugăeşescu, I. (2011). *Determination of the minimum size of the disk cam with translating flat-face follower.* Paper presented at the Proceedings of 13th World congress in mechanism and machine science, Guanajuato, México.

Mooney, C. Z. (1997). *Monte carlo simulation* (Vol. 116): Sage publications.

Muro, C., Escobedo, R., Spector, L., & Coppinger, R. (2011). Wolf-pack (Canis lupus) hunting strategies emerge from simple rules in computational simulations. *Behavioural processes, 88*(3), 192-197.

Nelder, J. A., & Mead, R. (1965). A simplex method for function minimization. *The computer journal, 7*(4), 308-313.

Nguyen, T. T. N. (2018). *Motion Design of Cam Mechanisms by Using Non-Uniform Rational B-Spline, Ph. D. Dissertation, RWTH Aachen university*.

Nikolaidis, E., & Burdisso, R. (1988). Reliability based optimization: a safety index approach. *Computers & structures, 28*(6), 781-788.

Nobakhti, A., & Wang, H. (2006). *A Self-adaptive differential evolution with application on the ALSTOM gasifier.* Paper presented at the 2006 American Control Conference.

Norton, R. L. (2002). *Cam design and manufacturing handbook*: Industrial Press Inc.

Norton, R. L. (2004). *Design of machinery: an introduction to the synthesis and analysis of mechanisms and machines*: Boston: McGraw-Hill Higher Education.

Nowacki, H. (1973). Optimization in pre-contract ship design.

Onwubiko, C. O. (2000). *Introduction to engineering design optimization*: Prentice Hall.

Onwubolu, G. C., & Davendra, D. (2009). *Differential evolution: A handbook for global permutation-based combinatorial optimization* (Vol. 175): Springer Science & Business Media.

Osyczka, A. (2002). Evolutionary algorithms for single and multicriteria design optimization.

Ouyang, T., Wang, P., Huang, H., Zhang, N., & Chen, N. (2017). Mathematical modeling and optimization of cam mechanism in delivery system of an offset press. *Mechanism and Machine Theory, 110*, 100-114.

Pallaschke, D., & Recht, P. (1985). On the Steepest-Descent Method for a Class of Quasi-Differentiable Optimization Problems *Nondifferentiable Optimization: Motivations and Applications* (pp. 252-263): Springer.

Pan, W.-T. (2012). A new fruit fly optimization algorithm: taking the financial distress model as an example. *Knowledge-Based Systems, 26*, 69-74.

Papadrakakis, M., & Lagaros, N. D. (2002). Reliability-based structural optimization using neural networks and Monte Carlo simulation. *Computer Methods in Applied Mechanics and Engineering, 191*(32), 3491-3507.

Papalambros, P. (1995). Optimal design of mechanical engineering systems.

Pareto, V. (1964). *Cours d'économie politique* (Vol. 1): Librairie Droz.

Pareto, V. (1971). Manual of political economy.

Parkinson, A. R., Balling, R., & Hedengren, J. D. (2013). Optimization methods for engineering design. *Brigham Young University, 5*, 11.

Pedrammehr, S., Danaei, B., Abdi, H., Masouleh, M. T., & Nahavandi, S. (2018). Dynamic analysis of Hexarot: axis-symmetric parallel manipulator. *Robotica, 36*(2), 225-240.

Phadke, M. S. (1995). *Quality engineering using robust design*: Prentice Hall PTR.

Phan, M., Longman, R. W., & Juang, J.-N. (1989). *Indirect repetitive control for linear discrete multivariable systems.* Paper presented at the Proceedings of the 27th Annual Allerton Conference on Communication, Control, and Computing.

Phat, L. T., Long, N. N. P., Son, N. H., & Vinh, H. H. (2020). Global optimization of laminated composite beams using an improved differential evolution algorithm. Journal of Science and Technology in Civil Engineering (STCE)-NUCE, 14(1), 54-64.

Powell, M. J. (1964). An efficient method for finding the minimum of a function of several variables without calculating derivatives. *The computer journal, 7*(2), 155-162.

Pridgen, B., & Singhose, W. (2010). *Comparison of Polynomial Cam Profiles and Input Shaping For Vibration Reduction.* Paper presented at the The 17th International Congress in Sound and Vibration, Cairo.

Qiu, H., Lin, C.-J., Li, Z.-Y., Ozaki, H., Wang, J., & Yue, Y. (2005). A universal optimal approach to cam curve design and its applications. *Mechanism and Machine Theory, 40*(6), 669-692.

Rackwitz, R., & Flessler, B. (1978). Structural reliability under combined random load sequences. *Computers & structures, 9*(5), 489-494.

Rajan, A., & Malakar, T. (2015). Optimal reactive power dispatch using hybrid Nelder–Mead simplex based firefly algorithm. *International Journal of Electrical Power & Energy Systems, 66*, 9-24.

Ramezani, F., & Lotfi, S. (2013). Social-based algorithm (SBA). *Applied Soft Computing, 13*(5), 2837-2856.

Rao, R. V., & Savsani, V. J. (2012). Mechanical design optimization using advanced optimization techniques: Springer Science & Business Media.

Rao, R. V., Savsani, V. J., & Vakharia, D. (2011). Teaching–learning-based optimization: a novel method for constrained mechanical design optimization problems. *Computer-Aided Design, 43*(3), 303-315.

Rao, S. S. (2019). *Engineering optimization: theory and practice*: John Wiley & Sons.

Rashedi, E., Nezamabadi-Pour, H., & Saryazdi, S. (2009). GSA: a gravitational search algorithm. *Information sciences, 179*(13), 2232-2248.

Ravindran, A., Reklaitis, G. V., & Ragsdell, K. M. (2006). *Engineering optimization: methods and applications*: John Wiley & Sons.

Redjechta, A., Djeddou, F., & Ferhat, H. (2019). Deterministic Optimization and Reliability Analysis of a Cam Mechanism with Translating Flat-Face Follower.

Rosen, E. M. (1966). A review of quasi-Newton methods in nonlinear equation solving and unconstrained optimization. *Communications of the ACM, 9*(7), 475.

Rosenblatt, M. (1952). Remarks on a multivariate transformation. *The annals of mathematical statistics, 23*(3), 470-472.

Rothbart, H. A., & Klipp, D. L. (2004). Cam design handbook. *J. Mech. Des., 126*(2), 375-375.

Royset, J. O., Der Kiureghian, A., & Polak, E. (2001). Reliability-based optimal structural design by the decoupling approach. *Reliability Engineering & System Safety, 73*(3), 213-221.

Sadek, K., & Daadbin, A. (1990). Improved cam profiles for high-speed machinery using polynomial curve fitting. *Proceedings of the Institution of Mechanical Engineers, Part E: Journal of Process Mechanical Engineering, 204*(2), 127-132.

Sadollah, A., Bahreininejad, A., Eskandar, H., & Hamdi, M. (2013). Mine blast algorithm: A new population based algorithm for solving constrained engineering optimization problems. *Applied Soft Computing, 13*(5), 2592-2612.

Sahu, L. K., Gupta, O. P., & Sahu, M. (2016). Design of cam profile using higher order B-spline. *Int J Innocative Sci Eng Technol, 13*, 327-335.

Sandgren, E. (1990). Nonlinear integer and discrete programming in mechanical design optimization.

Saremi, S., Mirjalili, S., & Lewis, A. (2017). Grasshopper optimisation algorithm: theory and application. *Advances in Engineering Software, 105*, 30-47.

Sateesh, N., Rao, C., & Janardhan Reddy, T. (2009). Optimisation of cam-follower motion using B-splines. *International Journal of Computer Integrated Manufacturing, 22*(6), 515-523.

Schaffer, J. (1984). Multiple objective optimization with vector evaluated. *Genetic Algorithms, Ph. D. Dissertation, Vanderbilt University*.

Schumaker, L. (2007). *Spline functions: basic theory*: Cambridge University Press.

Semenov, M. A., & Terkel, D. A. (2003). Analysis of convergence of an evolutionary algorithm with self-adaptation using a stochastic Lyapunov function. *Evolutionary Computation, 11*(4), 363-379.

Shakoor, M. M. (2006). Fatigue life investigation for cams with translating roller-follower and translating flat-face follower systems, *Ph. D. Dissertation, Iowa State university*.

Shalaa, A., & Likaja, R. (2013). Analytical Method for Synthesis of Cam Mechanism. *International Journal of Current Engineering and Technology, 3*(2).

Shan, S., & Wang, G. G. (2008). Reliable design space and complete single-loop reliability-based design optimization. *Reliability Engineering & System Safety, 93*(8), 1218-1230.

Simon, D. (2008). Biogeography-based optimization. *IEEE transactions on evolutionary computation, 12*(6), 702-713.

Singh, P. R., Abd Elaziz, M., & Xiong, S. (2018). Modified Spider Monkey Optimization based on Nelder–Mead method for global optimization. *Expert Systems with Applications, 110*, 264-289.

Smith, M. (2001). *Mechanisms and machine theory*: Higher Education Press.

Starkey, R. (2005). *Off-design performance characterization of a variable geometry scramjet.* Paper presented at the 41st AIAA/ASME/SAE/ASEE Joint Propulsion Conference & Exhibit.

Stoddart, D. A. (1953). *Polydyne cam design*: Penton Publishing Company.

Storn, R., & Price, K. (1995). Differential evolution–a simple and efficient adaptive scheme for global optimization over continuous spaces: technical report TR-95-012. *International Computer Science, Berkeley, California*.

Sun, G., Tian, J., Liu, T., Yan, X., & Huang, X. (2018). Crashworthiness optimization of automotive parts with tailor rolled blank. *Engineering Structures, 169*, 201-215.

Talbi, E.-G. (2009). *Metaheuristics: from design to implementation* (Vol. 74): John Wiley & Sons.

Tamboli, K., Singh, T., Sheth, S., & Patel, T. (2016). Dynamic Analysis of High Speed Cam Follower System using MATLAB.

Tan, Z., Fan, W., Li, H., De, G., Ma, J., Yang, S., . . . Tan, Q. (2020). Dispatching optimization model of gas-electricity virtual power plant considering uncertainty based on robust stochastic optimization theory. *Journal of Cleaner Production, 247*, 119106.

Terauchi, Y., & El-Shakery, S. A. (1983). A computer-aided method for optimum design of plate cam size avoiding undercutting and separation phenomena—I Design procedure and cycloidal cam design results. *Mechanism and Machine Theory, 18*(2), 157-163.

Tolson, B. A., Maier, H. R., Simpson, A. R., & Lence, B. J. (2004). Genetic algorithms for reliability-based optimization of water distribution systems. *Journal of Water Resources Planning and Management, 130*(1), 63-72.

Torrealba, R. R., & Udelman, S. B. (2016). Design of cam shape for maximum stiffness variability on a novel compliant actuator using differential evolution. *Mechanism and Machine Theory, 95*, 114-124.

Tsay, D., & Huey Jr, C. (1988). Cam motion synthesis using spline functions.

Tsiafis, I., Mitsi, S., Bouzakis, K., & Papadimitriou, A. (2013). Optimal design of a cam mechanism with translating flat-face follower using genetic algorithm. *Tribology in industry, 35*(4), 255-260.

Tsiafis, I., Paraskevopoulou, R., & Bouzakis, K. (2009). Selection of optimal design parameters for a cam mechanism using multi-objective genetic algorithm. *Annals of the "Constantin Brancusi" University of Targu Jiu, Engineering series*(2), 57-66.

Tsompanakis, Y., Lagaros, N. D., & Papadrakakis, M. (2008). *Structural Design Optimization Considering Uncertainties: Structures & Infrastructures Book, Vol. 1, Series, Series Editor: Dan M. Frangopol*: CRC Press.

Tu, J., Choi, K. K., & Park, Y. H. (1999). A new study on reliability-based design optimization.

Tu, Y., Ren, P., Deng, D., & Bao, X. (2018). Structural and electronic optimization of graphene encapsulating binary metal for highly efficient water oxidation. *Nano Energy, 52*, 494-500.

Uicker, J. J., Pennock, G. R., Shigley, J. E., & Mccarthy, J. M. (2003). *Theory of machines and mechanisms* (Vol. 3): Oxford University Press New York.

Ulucenk, Ç. (2009). Implementation of reliability based design optimization techniques for aerospace structures, *Ph. D. Dissertation, Istanbul technical university*.

Varaee, H., & Ghasemi, M. R. (2017). Engineering optimization based on ideal gas molecular movement algorithm. *Engineering with Computers, 33*(1), 71-93.

Venter, G. (2010). Review of optimization techniques. *Encyclopedia of aerospace engineering*.

Vitaliy, F. (2006). Differential evolution–in search of solutions: Springer, New York.

Wang, H., Hu, Z., Sun, Y., Su, Q., & Xia, X. (2019). A novel modified BSA inspired by species evolution rule and simulated annealing principle for constrained engineering optimization problems. *Neural Computing and Applications, 31*(8), 4157-4184.

Wang, H., & Lin, A. (1989). Camex: An expert system for selecting cam-follower design parameters. *The International Journal of Advanced Manufacturing Technology, 4*(1), 46-71.

Wang, L., & Li, L.-p. (2010). An effective differential evolution with level comparison for constrained engineering design. *Structural and Multidisciplinary Optimization, 41*(6), 947-963.

Wang, Y., Cai, Z., & Zhang, Q. (2011). Differential evolution with composite trial vector generation strategies and control parameters. *IEEE transactions on evolutionary computation, 15*(1), 55-66.

Wehrens, R., & Buydens, L. M. (2006). Classical and nonclassical optimization methods. *Encyclopedia of Analytical Chemistry: Applications, Theory and Instrumentation*.

Wilson, C. E., & Sadler, J. P. (2013). *Kinematics and Dynamics of Machinery: Pearson New International Edition*: Pearson Higher Ed.

Wong, K. P., & Dong, Z. Y. (2005). *Differential evolution, an alternative approach to evolutionary algorithm.* Paper presented at the Proceedings of the 13th International Conference on, Intelligent Systems Application to Power Systems.

Wu, Y.-T. (1994). Computational methods for efficient structural reliability and reliability sensitivity analysis. *AIAA journal, 32*(8), 1717-1723.

Wu, Z. (2020). Postbuckling analysis and optimization of laminated composite plates with applications in aerospace *Polymer Composites in the Aerospace Industry* (pp. 123-146): Elsevier.

Xiao, H., & Zu, J. W. (2009). Cam profile optimization for a new cam drive. *Journal of Mechanical Science and Technology, 23*(10), 2592-2602.

Xiao, H., & Zu, J. W. (2010). Evolutionary multi-objective optimisation of cam profile for a new cam drive engine. *International journal of vehicle design, 53*(3), 198-219.

Xu, B., Chen, X., & Tao, L. (2018). Differential evolution with adaptive trial vector generation strategy and cluster-replacement-based feasibility rule for constrained optimization. *Information sciences, 435*, 240-262.

Xu, J., & Yan, F. (2019). Hybrid Nelder–Mead algorithm and dragonfly algorithm for function optimization and the training of a multilayer perceptron. *Arabian Journal for Science and Engineering, 44*(4), 3473-3487.

Xu, S., Wang, Y., & Wang, Z. (2019). Parameter estimation of proton exchange membrane fuel cells using eagle strategy based on JAYA algorithm and Nelder-Mead simplex method. *Energy, 173*, 457-467.

Xuan, G. T., Shao, Y. Y., & Lü, Z. Q. (2012). *Reduction of residual vibrations in high-speed cam mechanisms using non-uniform rational B-splines.* Paper presented at the Advanced Materials Research.

Yang, I.-T., & Hsieh, Y.-H. (2011). Reliability-based design optimization with discrete design variables and non-smooth performance functions: AB-PSO algorithm. *Automation in construction, 20*(5), 610-619.

Yang, I.-T., & Hsieh, Y.-H. (2013). Reliability-based design optimization with cooperation between support vector machine and particle swarm optimization. *Engineering with Computers, 29*(2), 151-163.

Yang, J., Tan, J., Zeng, L., & Liu, S. (2014). Design and analysis of cam lifting curve in applying to transient and heavy load. *Mechanics, 20*(3), 299-304.

Yang, R., & Gu, L. (2004). Experience with approximate reliability-based optimization methods. *Structural and Multidisciplinary Optimization, 26*(1-2), 152-159.

Yang, X.-S. (2010). A new metaheuristic bat-inspired algorithm *Nature inspired cooperative strategies for optimization (NICSO 2010)* (pp. 65-74): Springer.

Yi, W., Li, X., Gao, L., Zhou, Y., & Huang, J. (2016). ε constrained differential evolution with pre-estimated comparison using gradient-based approximation for constrained optimization problems. *Expert Systems with Applications, 44*, 37-49.

Yildiz, A. R. (2013a). Hybrid Taguchi-differential evolution algorithm for optimization of multi-pass turning operations. *Applied Soft Computing, 13*(3), 1433-1439.

Yildiz, A. R. (2013b). A new hybrid differential evolution algorithm for the selection of optimal machining parameters in milling operations. *Applied Soft Computing, 13*(3), 1561-1566.

Yildiz, A. R., Abderazek, H., & Mirjalili, S. (2019). A comparative study of recent non-traditional methods for mechanical design optimization. *Archives of Computational Methods in Engineering*, 1-18.

Yıldız, B. S., & Yıldız, A. R. (2019). The Harris hawks optimization algorithm, salp swarm algorithm, grasshopper optimization algorithm and dragonfly algorithm for structural design optimization of vehicle components. *Materials Testing, 61*(8), 744-748.

Yin, X., & Chen, W. (2006). Enhanced sequential optimization and reliability assessment method for probabilistic optimization with varying design variance. *Structures and Infrastructure Engineering, 2*(3-4), 261-275.

Yoon, K., & Rao, S. (1993). Cam motion synthesis using cubic splines.

Youn, B. D., & Choi, K. K. (2004). A new response surface methodology for reliability-based design optimization. *Computers & structures, 82*(2-3), 241-256.

Youn, B. D., Choi, K. K., & Du, L. (2005). Enriched Performance Measure Approach for Reliability-Based Design Optimization. *AIAA journal, 43*(4), 874-884.

Youn, B. D., Choi, K. K., & Park, Y. H. (2003). Hybrid analysis method for reliability-based design optimization. *J. Mech. Des., 125*(2), 221-232.

Yu, H. (2011). Reliability-based design optimization of structures: methodologies and applications to vibration control, *Ph. D. Dissertation, Ecole centrale de Lyon*.

Yu, Q., & Lee, H. (1998). Size optimization of cam mechanisms with translating roller followers. *Proceedings of the Institution of Mechanical Engineers, Part C: Journal of Mechanical Engineering Science, 212*(5), 381-386.

Yu, X., Chang, K.-H., & Choi, K. K. (1998). Probabilistic structural durability prediction. *AIAA journal, 36*(4), 628-637.

Zeid, I. (1991). *CAD/CAM theory and practice*: McGraw-Hill Higher Education.

Zhang, M., Luo, W., & Wang, X. (2008). Differential evolution with dynamic stochastic selection for constrained optimization. *Information sciences, 178*(15), 3043-3074.

Zhang, Y., Liu, Q., & Wen, B. (2003). Practical reliability-based design of gear pairs. *Mechanism and Machine Theory, 38*(12), 1363-1370.

Zhi, L., Zhansheng, L., & Yigong, L. (2005). Dynamic simulation of distribution cam mechanism in internal combustion engine based on ant colony algorithm [J]. *Transactions of The Chinese Society of Agricultural Engineering, 6*.

Zhou, A., Qu, B.-Y., Li, H., Zhao, S.-Z., Suganthan, P. N., & Zhang, Q. (2011). Multiobjective evolutionary algorithms: A survey of the state of the art. *Swarm and Evolutionary Computation, 1*(1), 32-49.

Zigo, M. (1967). A general numerical procedure for the calculation of cam profiles from arbitrarily specified acceleration curves. *Journal of Mechanisms, 2*(4), 407-414.

List of Publications

Publications in Peer-Reviewed Journals

1. **Ferhat H**, Hammoudi A, Smata L, Djeddou F, Yıldız AR (2018) Optimum design of cam-roller follower mechanism using a new evolutionary algorithm. Int J Adv Manuf Techno 99(5–8): 1267–1282. https://doi.org/10.1007/s00170-018-2543-3
2. Djeddou F, Smata L, **Ferhat H** (2018) Optimization and a reliability analysis of a cam-roller follower mechanism. J Adv Mech Des Syst 12(7): JAMDSM0121. https://doi.org/10.1299/jamdsm.2018jamdsm0121
3. Redjechta A, Djeddou F, **Ferhat H** (2019) Deterministic optimization and reliability analysis of a cam mechanism with translating flat-face follower. Univers. J. Mech. Eng 7(6): 318-324. doi: 10.13189/ujme.2019.070602
4. **Ferhat H**, Djeddou F, Hammoudi A, Dahane M (2020) A new efficient hybrid approach for reliability-based design optimization problems. Eng Comput**.** https://doi.org/10.1007/s00366-020-01187-5
5. Hammoudi A, **Ferhat H**, Yıldız BS, Yıldız AR, Sait SM (2020) A comparative investigation of recent metaheuristics for optimal design of mechanical design problems. Engineering Optimization and Part C: J. Mech. Eng. Sci, **under minor revision.**

Publications in Peer-Reviewed International Conferences

1. **Ferhat H**, Djeddou F, Hammoudi A, Rezki I (2018) Mesure de sensibilité et analyse fiabiliste d'un mécanisme à came. International Conference on Industrials Metrology and Maintenance ICIMM 2018 (28–29) October, Setif, Algeria.
2. Hammoudi A, **Ferhat H**, Djeddou F (2018) Sensitivity measurement and reliability based design of a cylindrical spur gear. International Conference on Industrials Metrology and Maintenance ICIMM 2018 (28–29) October, Setif, Algeria.
3. **Ferhat H**, Djeddou F, Hammoudi A (2018) Optimisation déterministe et analyse fiabiliste d'un mécanisme à came terminé par un plateau. International Conference on Advanced Mechanics and Renewable Energies ICAMRE 2018 (28–29) November, Boumerdes, Algeria.

4. Hammoudi A, **Ferhat H** (2018) Engineering design optimization using adaptive mixed differential evolution algorithm. International Conference on Advanced Mechanics and Renewable Energies ICAMRE 2018 (28–29) November, Boumerdes, Algeria.
5. Rezki I, Djeddou F, Hammouda A, **Ferhat H** (2018) Optimal design of mechanical element using metaheuristic algorithm. International Conference on Advanced Mechanics and Renewable Energies ICAMRE 2018 (28–29) November, Boumerdes, Algeria.
6. **Ferhat H**, Djeddou F, Hammoudi A, Rezki I (2019) Optimization and reliability approaches of a cam mechanism. International Symposium on Technology & Sustainable Industry Development ISTSID'2019 (24–26) February, EL OUED, Algeria.
7. Rezki I, Djeddou F, **Ferhat H** (2019) Optimal design of multiple disc clutch brake using hybrid metaheuristic algorithm. International Symposium on Technology & Sustainable Industry Development ISTSID'2019 (24–26) February, EL OUED, Algeria.
8. **Ferhat H**, Djeddou F, Hammoudi A, Rezki I (2019) Optimal synthesis of a disc cam mechanism with translating flat-face follower using various follower motion laws. International Conference on Mechanics and Materials ICMM 2019 (11–12) November, Setif, Algeria.
9. Harrag A, **Ferhat H**, Hammoudi A (2019) Multi-objective Optimization of a Cam-Roller Follower Mechanism Based on NSGA-II. International Conference on Mechanics and Materials ICMM 2019 (11–12) November, Setif, Algeria.
10. Hammoudi A, **Ferhat H**, Harrag A (2019) Recent swarm intelligence approaches for mechanical design systems. International Conference on Mechanics and Materials ICMM 2019 (11–12) November, Setif, Algeria.

Abstract

This dissertation essentially introduces the methodology for deterministic and reliability based design optimization of complex mechanical systems. The present research passes through three consecutive stages. Firstly, an effective deterministic optimization approach is developed. The proposed approach (MADE) is a new version of the DE algorithm with two improvements. Secondly, the developed MADE is applied to optimize two cam design problems. Overall, the final results obtained provide very suitable decisions for cam mechanism syntheses. Lastly, the developed MADE is adjusted to deal with Reliability-Based Design Optimization (RBDO). In this way, a novel optimization approach is proposed to handle the mechanical design problems under the impact of uncertainties. The simulation results on six mechanical problems and an industry case of cylindrical spur gear demonstrate that the developed approach is a promising tool with extensive applicability.

Keywords: *Mechanical design, Deterministic optimization, Reliability-based design optimization, Differential evolution algorithm, Cam mechanism, Roller follower, Flat-face follower.*

Résumé

Cette thèse introduit essentiellement la méthodologie d'optimisation déterministe et fiabiliste pour la conception des systèmes mécaniques complexes. La présente recherche passe par trois volets consécutifs. Dans le premier volet, une approche d'optimisation déterministe effective est développée. La méthode proposée (MADE) est une nouvelle version de l'algorithme à évolution différentielle (DE) avec deux améliorations. Dans le deuxième volet, la MADE est appliquée pour optimiser deux problèmes de conception des mécanismes à came-tige. Les résultats obtenus offrent des décisions très utiles pour la synthèse des mécanismes à came. Dans le dernier volet de la thèse, la MADE est ajustée pour traiter la formulation d'optimisation basée sur la fiabilité (RBDO), Dans ce contexte, une nouvelle approche d'optimisation est proposée pour résoudre les problèmes de conception mécanique sous l'impact des incertitudes. Les résultats de simulation sur six problèmes mécaniques et un cas pratique d'un train d'engrenage cylindrique démontrent que l'approche développée est un outil prometteur pour des applications étendues.

Mots clés: *Conception mécanique, Optimisation déterministe, Optimisation fiabiliste, Algorithme à évolution différentielle, Mécanisme à came, Tige-galet, Tige-plateau.*